This electronic thesis or dissertation has been downloaded from Explore Bristol Research, http://research-information.bristol.ac.uk

Author:
Etheridge, Alice R

Title:
Characterising the molecular pharmacology of ligand-dependent and -independent activity of the platelet P2Y12 receptor

This electronic thesis or dissertation has been downloaded from Explore Bristol Research, http://research-information.bristol.ac.uk

Author:
Etheridge, Alice R

Title:
Characterising the molecular pharmacology of ligand-dependent and -independent activity of the platelet P2Y12 receptor

Characterising the molecular pharmacology of ligand-dependent and -independent activity of the platelet P2Y12 receptor

Alice Etheridge

A dissertation submitted to the University of Bristol in accordance with the requirements for award of the degree of Research Masters in the Faculty of Life Sciences. Submitted to the School of Physiology, Pharmacology and Neuroscience

September 2023

Word Count: 22,580

Abstract

Acute coronary syndrome (ACS) arises from a reduction in blood flow to the heart, leading to severe cardiovascular events, including myocardial infarction. Atherosclerotic plaque formation drives arterial occlusions seen in ACS, and is linked to dysregulated platelet response in the vasculature. Thus, using anti-platelet therapies, and more specifically targeting the platelet P2Y12 receptor (P2Y12R), is the gold-standard clinical treatment for ACS patients. Recent studies have demonstrated that P2Y12R exhibits constitutive activity (CA), and hence anti-P2Y12R blockers, such as ticagrelor, have been re-defined as inverse agonists. Following this discovery, our understanding of P2Y12R activity remains ill-defined. Therefore, this thesis explores both the molecular structure of P2Y12R, and the influence of the membrane environment upon receptor activation.

Focusing on *in vitro* assessment of receptor activation using bioluminescence resonance energy transfer (BRET) assays, this work explores the effects of missense mutations in key residues identified in P2Y12R on ligand-dependent activity and CA. This work revealed that transfection level-dependent increases in P2Y12R surface expression increase CA. Among the different mutant receptor constructs there was a significant increase in agonist-dependent activity at the Y105A and D294N mutants was observed, whilst the patient-derived R265P mutation demonstrated a global reduction in ligand-dependent activity. Further, Y209, a key residue within the NPxxY motif of P2Y12R, was identified as being important for CA.

Study examining the relationship between the membrane microenvironment and P2Y12R activity was also undertaken. Changes in membrane cholesterol significantly affected P2Y12R activity with Si cholesterol-dependent increases in P2Y12R CA were observed using BRET. In platelets meanwhile there was a global reduction in platelet aggregation response upon changing cholesterol levels.

This thesis therefore presents an in vitro characterisation of ligand-dependent and independent activity in key P2Y12R mutations, and begins to explore the effects of manipulating the cholesterol plasma membrane environment on receptor activity, and global platelet function. Exploring two factors affecting the molecular mechanisms of P2Y12R helps to further our understanding of P2Y12R and subsequently improves our understanding of anti-P2Y12R therapies in the treatment of ACS.

Author's Declaration

I declare that the work in this dissertation was carried out in accordance with the requirements of the University's Regulations and Code of Practice for Research Degree Programmes and that it has not been submitted for any other academic award. Except where indicated by specific reference in the text, the work is the candidate's own work. Work done in collaboration with, or with the assistance of, others, is indicated as such. Any views expressed in the dissertation are those of the author.

Signed: Alice Etheridge   DATE: 01/09/2023

Acknowledgements

Firstly, I must to thank Stuart Mundell and Lawrence Hutchinson. My last interaction with a pipette had been in the second year of my undergraduate degree, and with their guidance and help I think I can work one pretty well now. Alongside the rest of the Bristol Platelet Group, who have been so wonderfully helpful, encouraging and true friends, they have inspired me to pursue a PhD. Hopefully I will end up on the keys/violin playing some 80s tunes with them in the future.

Secondly, I must thank my family and friends for their support. My siblings have been a welcome distraction from working hard with their perpetual silliness, and my mum for her support and endless cups of tea. Sophie and Gus, my dear friends who were both avid supporters of my work and a sounding board for the frustrations often faced when conducting research for the first time. And to Jonny, both my rock and my joy.

Contents

List of Figures

List of Tables

Abbreviations

β_2AR	β_2 Adrenoreceptor
AC	Adenylyl Cyclase
Act-Met	Active Metabolite
ACS	Acute Coronary Syndrome
ADP	Adenosine Diphosphate
ANOVA	Analysis of Variance
ATP	Adenosine Triphosphate
BRET	Bioluminescence Resonance Energy Transfer
BSA	Bovine Serum Albumin
cAMP	Cyclic Adenosine Monophosphate
COX	Cyclooxygenase
CWxP	Cysteine-Tryptophan-Proline
D294N	Aspartate-294 to Asparagine Mutation
D70A	Aspartate-70 to Alanine Mutation
DAPT	Dual-Antiplatelet Therapy
D-Gluc	D-Glucose Anhydrase
DMEM	Dulbecco's Modified Eagle Medium
DNA	Deoxyribonucleic Acid
D/NPxxY	Aspartate/Asparagine-Proline-Tyrosine
DRY	Aspartate-Arginine-Tyrosine
EC50	Half Maximal Effective Concentration
ELISA	Enzyme-Linked Immunosorbent Assay
Emax	Maximum Effect of Drug
ERK	Extracellular-Regulated Protein Kinase
F249W	Phenylalanine-249 to Tryptophan Mutation
FCS	Foetal Bovine Serum
FITC	Fluorescein isothiocyanate
GFP	Green Fluorescent Protein
GPCR	G Protein-Coupled Receptor
GP	Glycoprotein

G protein	Guanine Protein
HA	Hemagglutinin
HEK	Human Embryonic Kidney
HEK293T	Human Embryonic Kidney Cells Expressing SV40 T-antigen
HT	HEPEs-Tyrode's
IgG	Immunoglobulin G
Imax	Maximal Inhibitory Effect
LTA	Light Transmission Aggregometry
MAb	Monoclonal Antibody
MAPK	Mitogen-Activated Protein Kinase
MβCD	Methyl-β-Cyclodextrin
MFI	Median Fluorescence Intensity
MM	Master Mix
mOPR	Mu Opioid Receptor
Na	Sodium
NaOH	Sodium Hydroxide
NSAIDs	Non-Steroidal Anti-Inflammatory Drugs
NIF	Asparagine-Isoleucine-Phenylalanine
Opti-MEM	Opti- Minimum Essential Media
PAR	Protease Activated Receptor
PBS	Phosphor-Buffered Saline
pcDNA	Profilerating Cell Deoxyribonucleic Acid
PE	Phycoerythrin
PFA	Paraformaldehyde
PGE1	Prostaglandin E1
pVASP	Phosphorylated-Vasodilator Stimulated Phosphoprotein
PI3K	Phophoinositide-3-kinase
PIF	Proline-Isoleucine-Phenylalanine
PKA	Protein Kinase A
PLATO	Platelet Inhibition and Patient Outcomes
PPP	Platelet Poor Plasma

PRP	Platelet Rich Plasma
P2Y12R	Purinergic P2Y12 Receptor
R	Inactive receptor state
R*	Active receptor state
R122C	Arginine-122 to Cysteine Mutation
R265P	Arginine-265 to Proline Mutation
RLucII	*Renilla* Luciferase II
RPM	Revolutions Per Minute
SEM	Standard Error of the Mean
TBS	Tris-Buffered Saline
Tic	Ticagrelor
TIRF	Total Internal Reflection Fluorescence
TM	Transmembrane
V234T	Valine-234 to Threonine Mutation
V238A	Valine-238 to Alanine Mutation
VASP	Vasodilator Stimulated Phosphoprotein
WT	Wildtype
2MesADP	2-Methylthioadenosine 5'-Diphosphate
Y105A	Tyrosine-105 to Alanine Mutation
Y105C	Tyrosine-105 to Cysteine Mutation
Y209A	Tyrosine-209 to Alanine Mutation
5-HT_{1B}	Serotonergic 1_B Receptor

Chapter 1: Introduction

1.1 Role of platelets in the vasculature

Platelets are small, anucleate cells found within the vasculature, that have an essential role in the regulation of haemostasis upon vascular injury. Platelets express a diverse repertoire of cell surface receptors and adhesion molecules, mediating complex crosstalk between platelets and other blood and vascular cells. This serves to coordinate haemostatic mechanisms, predominantly the maintenance of regular blood flow and vascular integrity [1]. Upon vascular damage, pro-thrombotic factors such as collagen are exposed on the subendothelial extracellular matrix, promoting rapid platelet adhesion to the site of injury [2]. Following adhesion to the blood vessel wall, activated platelets release soluble agonists, alongside other pro-coagulant molecules, into the extracellular environment via secretory vesicles called granules [3]. Platelets contain a wide variety of soluble agonists including adenosine diphosphate (ADP). Granular release furthers platelet activation and subsequent platelet aggregation. This is a feedforward mechanism that rapidly ensures the formation of a platelet plug at the site of injury to prevent further vascular damage. This process is tightly controlled by platelet adhesion and signalling receptors, however dysregulation of haemostatic processes can lead to pathological thrombosis [4]. The feedforward amplification of initial platelet activation is primarily mediated through receptors belonging to the G-protein coupled receptor (GPCR) family, expressed at the platelet surface, such as the ADP P2Y12 receptor. This amplification is critical in ensuring rapid platelet recruitment and further activation [5].

1.2 The platelet P2Y12 receptor

The platelet P2Y12 receptor (P2Y12R) is a key mediator in a feedforward mechanism, after initial platelet adhesion to a site of injury, to ensure rapid aggregation and stabilisation of thrombi [6]. The P2Y12R is a purinergic receptor belonging to the diverse class A family of GPCRs, including the P2Y1 receptor on also found on platelets, that is critical for thrombus formation [7]. The structure of the P2Y12R is similar to other class A GPCRs, composed of seven distinct transmembrane (TM) domains that span the platelet plasma membrane and form a ligand binding pocket. The P2Y12R associates intracellularly with heterotrimeric guanine binding proteins, or G proteins [8]. Upon ligand binding, conformational changes within the TM helices stabilise the receptor in distinct states. For example, binding of the endogenous agonist ADP to P2Y12R stabilises an active receptor conformation, resulting in the disassociation of the inhibitory G_i protein coupled to the receptor. The G_i protein signalling pathways and their involvement in platelet activation is outlined in *figure 1.*

Pharmacological inhibition or genetic knockout of the platelet P2Y12R has demonstrated the importance of P2Y12R in the platelet aggregation response, both *in vivo* and *in vitro.* In P2Y1-

deficient mice a complete absence of platelet aggregation has been observed when platelets stimulated with low concentrations of ADP, whereas partial aggregation can be observed at higher concentrations [9]. This has been attributed to P2Y1-independent signalling through the P2Y12R, highlighting its role in the amplification of platelet response to pro-coagulant agents. In *P2Y12R -/-* there is a loss of sustained platelet aggregation and a significantly prolonged bleeding time [10, 11]. Stimulating the G_i pathway using adrenaline restored platelet responses, highlighting the importance of the G_i signalling pathway in haemostasis. Pharmacological inhibition of the P2Y12R in human platelets ablates ADP-induced aggregation [12]. The importance of P2Y12R in platelet aggregation coupled with its relatively high expression in platelets versus other cell types, makes the receptor an attractive target for anti-platelet therapies in the treatment of cardiovascular diseases, where platelet response becomes dysregulated.
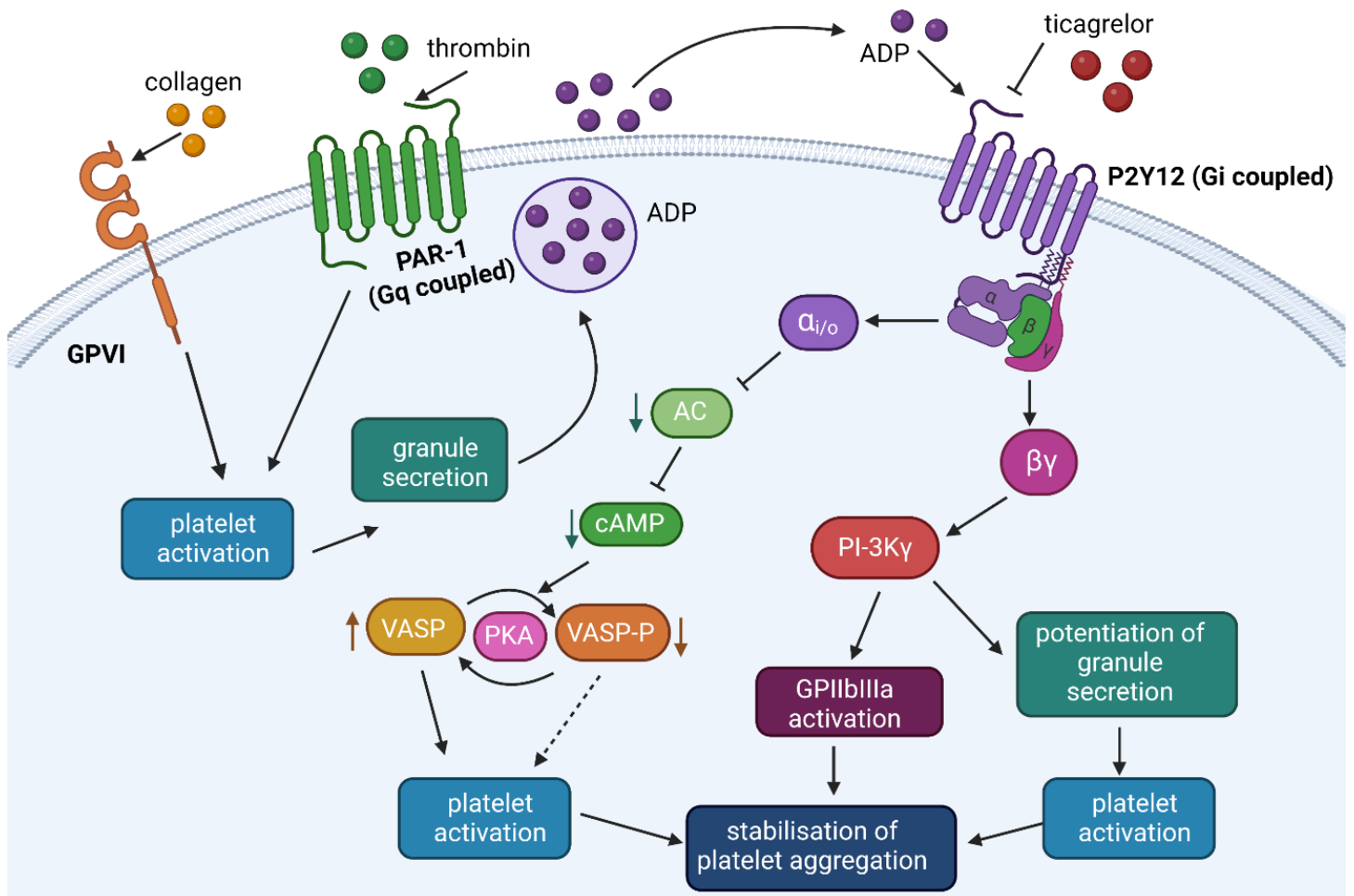
Figure 1 Schematic outlining platelet receptor signalling pathways involved in platelet activation and aggregation. Glycoprotein (GP) VI, protease activated receptor (PAR)-1, and P2Y12 receptor (P2Y12R) have important roles in platelet adhesion, secretion and aggregation, involved in haemostasis and pathological thrombus formation. Adenosine diphosphate (ADP) is the endogenous ligand for the P2Y12R, which is secreted by neighbouring activated platelets upon collagen exposure in damaged vasculature [13]. Upon ADP binding, the P2Y12R undergoes conformational change, resulting in dissociation of the coupled G_i protein heterotrimer. The $G\alpha_i$ subunit inhibits adenylyl cyclase (AC) which decreases cyclic adenosine monophosphate (cAMP) production. Reduced cAMP results in attenuation of protein kinase A (PKA) activation, which is important in the phosphorylation of vasodilator-stimulated phosphoprotein (VASP). Non-phosphorylated VASP is able to activate integrins involved in further platelet activation. The $G\beta\gamma$ dimer is involved in the activation of two phophoinositide-3-kinase (PI3K) phosphorylation pathways. Activation of the mitogen-activated protein kinase (MAPK) and extracellular-regulated protein kinase (ERK) pathways, alongside upregulation of integrin $\alpha IIb\beta 3$ results in further platelet aggregation [14]. Therefore, activation of P2Y12R by ADP results in feed-forward amplification of the platelet response to other soluble agonists, contributing to rapid haemostasis via stabilisation of platelet aggregation. *Created in BioRender.com*

1.3 Anti-platelet treatments

In a pathological environment, injury to vascular endothelia may occur as a result of an atherosclerotic plaque rupture event. Platelets then aggregate at the site and form a thrombus, promoting clot formation and subsequent arterial occlusion. Significant arterial occlusion can result in myocardial infarction [1]. Uncontrolled thrombosis is also implicated in diseases such as acute coronary syndrome (ACS). Cardiovascular diseases associated with unwanted thrombosis are successfully targeted using ligands that attenuate platelet function. Efficacious treatments predominantly target the P2Y12R, acting as antagonists to reduce platelet aggregation responses. The gold-standard treatment for ACS patients is the dual-antiplatelet therapy (DAPT), comprised of a P2Y12R antagonist such as clopidogrel. Used in combination with aspirin, clopidogrel as part of a DAPT approach has been shown to significantly reduce adverse cardiovascular events and risk of stroke [15] and manage patients with thrombotic conditions [16].

1.3.1 Thienopyridines

Interestingly, drugs such as ticlopidine, the predecessor to clopidogrel, were first identified for the treatment of patients with high thrombosis risk, without any link to anti-platelet effects in 1978 [17]. The involvement of platelet aggregation in cardiovascular events was disputed between cardiologists at the time. It was only when P2Y12R was cloned in 2001 [18] that it was found to be the specific receptor targeted by drugs such as ticlopidine and clopidogrel. These compounds are thienopyridines, a class of pro drugs that are converted into their active metabolites upon hepatic metabolism [19]. This mechanism of action was not fully recognised until 2011, more than 30 years following the discovery of ticlopidine [20]. Clopidogrel has an improved safety profile compared to ticlopidine [21] and has remained the cornerstone of management of thrombosis within DAPT. However, there are some limitations in thienopyridines and their treatment of ACS. These include a slow onset of action and a high variability in response between patients [22]. Between 5-44% of patients that receive clopidogrel treatment will continue to suffer adverse cardiac events, such as stent thrombosis, and are been termed 'clopidogrel-resistant' [23]. Thus, development of antiplatelet treatments have since focused on patients that respond poorly to clopidogrel. Prasugrel, a third generation thienopyridine, has demonstrated significant increase in potency when compared to clopidogrel, and has been particularly successful in clopidogrel non-responsive patients [24]. However, over time the risk of arterial thrombosis significantly increases with thienopyridine treatment [25].

1.3.2 Ticagrelor

Compounds that are structurally-distinct from thienopyridines have since been developed as potent antiplatelet drugs. Ticagrelor is a synthetic analogue of the endogenous competitive inhibitor, adenosine triphosphate (ATP) but exhibits high selectivity for P2Y12R [26, 27]. Approved for use in patients with ACS in 2010 [28], ticagrelor is a non-competitive antagonist of P2Y12R and is reported to bind reversibly to the receptor. Ticagrelor has demonstrated a greater inhibition of platelet aggregation when compared to clopidogrel [29, 30] and demonstrates a non-inferior adverse risk of bleeding. Ticagrelor does not require metabolic activation and therefore demonstrates a significantly increased onset of action with reduction in inter-patient variability when compared to clopidogrel [30]. Limitations of ticagrelor use however include an increased rate of non-operative related bleeding in patients following treatment [31].

Whilst treatment has progressed significantly in recent years, there are still shortcomings in management of ACS in patients. Understanding the structural basis of P2Y12R, and the mechanism of action of antagonists such as ticagrelor, is essential for improving treatment for ACS patients.

1.4 P2Y12R: a structurally distinct GPCR

The structure of P2Y12R remained poorly understood until its crystal structure, both agonist and antagonist-bound, was resolved by Zhang et al. in 2014 [32, 33]. These seminal papers revealed striking differences in receptor structure that distinguished P2Y12R from other GPCRs of the class A family. In particular, when P2Y12R was complexed with AZD1283, a reversible antagonist, the conformation of helix V was straight. This is unlike other class A GPCRs, which produce bent conformations upon ligand binding [33]. Another significant finding of the antagonist-bound P2Y12R structure is the loss of the disulphide bridge between helix III and extracellular loop 2. This bridge is highly conserved across all GPCRs, thus its absence indicates a possible increase in dynamism within this receptor region.

1.4.1 P2Y12R conformational changes

Unlike other GPCRs, molecular modelling by Zhang et al., P2Y12R demonstrated its most significant conformational changes within the extracellular domains of the receptor upon ligand binding [32, 33]. Most interestingly, the extracellular domains were differentially changed dependent on whether a nucleotide, such as (2MesADP) or non-nucleotide (AZD1283) ligand were bound to the receptor. Orientation of bound ligands were different within P2Y12R, revealing that the binding pockets for non-nucleotide and nucleotide ligands were only partially overlapped.

1.5 Constitutive activity of GPCRs

Costa and Hertz in 1989 proposed the idea that GPCRs exist in an equilibrium between an active and inactive state [34] dependent on the presence or absence of ligand. In early receptor theory, full agonist binding to its receptor results in a shift of this equilibrium, and stabilises the active GPCR conformation. Antagonists binding to a GPCR has no effect on the equilibrium between the active and inactive state of the receptor, however it blocks the ligand effect [35].

However, it was discovered that some GPCRs can exist in a basally-active state. These receptors are able to spontaneously transition from an inactive to an active state in the absence of agonist. This has been termed as constitutive activity. This was first observed in β_2ARs [36] by Cerione et al. in 1984. A basal level of GTPase activity was recorded in the absence of agonist upon co-transfection of the β_2AR with $G\alpha_s$ protein. The degree of constitutive activity varies across different GPCR types. A more constitutively active receptor will have a greater proportion of the receptor population in a basally-active state, compared to inactive. Constitutive GPCR activity has been observed in pathological environments such as in hyperthyroidism *in vivo* [37] and can be observed when GPCRs are overexpressed within cell lines *in vitro* [38].

1.5.1 Mechanism of constitutive activity

The mechanism by which GPCRs exhibit constitutive activity is widely thought to be linked to structural changes within the TM regions of the receptor, although this precise mechanism has not been identified [39]. The shift from an inactive receptor conformation to an active one appears to involve changes in the orientation of TM III and VI, thought to result in position change of intracellular loop 3. This is thought to then 'uncover' amino acid residues involved in G protein coupling and subsequent activation [40]. Since its first discovery, an increasing number of GPCRs have been found to demonstrate ligand-independent activity.

1.5.2 Constitutive Activity at P2Y12R

The P2Y12R expressed on platelets was first identified to exhibit agonist-independent levels of activity by Aungraheeta et al. [41] in 2016. P2Y12R-transfected 1321N1 cells exhibited significant increase in cAMP levels, indicating agonist-independent P2Y12R activity that was subsequently reversed by ticagrelor. An increase in phospho-VASP was also observed upon ticagrelor treatment. This phenomenon was further demonstrated in 2019 by Garcia et al. [42]. Using a human embryonic kidney (HEK)293T cell system in which P2Y12R was overexpressed, these studies have re-defined our understanding of P2Y12R function and pharmacology in platelets. Changes in platelet function in pathological environments may affect, or be affected by basal levels of P2Y12R activity, and re-

frames the way in which anti-platelet treatments are thought to act at the receptor. Constitutive activity also changes how we assess pharmacological parameters of ligands acting at the receptor.

1.5.3 Regulatory motifs found in the P2Y12R

There are several motifs in class A GPCRs that are key to activation. Intriguingly a number of these are different in the P2Y12R. The PIF motif, comprised of proline, isoleucine and phenylalanine, is uniquely altered in P2Y12R [43]. These residues are found on transmembrane domains (TMs) 3,5,6 respectively [44]. This motif is important in other GPCRs, such as the β_2 adrenoreceptor (β_2AR), serving as an important connection between the agonist binding pocket to the conformational reconfiguration of the receptor into an active state [45]. In the P2Y12R however, this proline residue is altered to an asparagine, creating a 'NIF' motif. Proline acts as a hinge and swivel point, and so its loss results in the straightening of the α helix of TM 5 [46]. This may indicate that the change in receptor rotation around this point may favour a more active-associated state [46]. Other motifs of note include: the aspartate-arginine-tyrosine (DRY) motif; the aspartate/asparagine-proline-tyrosine (D/NPxxY) motif and the cysteine-tryptophan-proline (CWxP) motif. All named motifs are involved in various aspects of receptor activation. The sodium (Na) binding pocket is also an important region highly conserved across GPCRs, to which Na^+ binds and produces negative allosteric effects [47].The DRY motif is also highly conserved, and is hypothesised to be critical in maintaining an inactive receptor conformation. The arginine residue serves to form an 'ionic lock' with TM6 [48, 49]. The P2Y12R lacks this distinct arginine and may be unable to form this lock [32, 33]. This decreases receptor stability in its inactive form and may contribute to the high degree of P2Y12R constitutive activity.

1.5.4 Linking receptor expression with constitutive activity

Changes to structural motifs in the P2Y12R may offer an explanation for the high degree of constitutive activity seen at this receptor. Another factor to be considered is that changes in the degree of receptor expression in a cell system may contribute to increased basal activity levels. Other GPCRs, such as the β2AR have demonstrated significant increases in basal cAMP levels in an expression-dependent manner [50]. In addition, receptors that may not display constitutive activity at a physiological level of expression can exhibit spontaneous activation upon extreme increases in transfected receptor levels. This was demonstrated by the calcitonin receptor [51] in 1997. Work within the host laboratory has seen changes to the degree of constitutive P2Y12R activity with increasing the amount of P2Y12R DNA transfected into a HEK293 cell line. Therefore it is apt to quantify how changes in receptor levels influence both constitutive P2Y12R activity and cell surface expression.

1.5.5 Linking receptor expression with patient pathology

A number of recent studies have indicated that P2Y12R expression in human platelets is affected by patient pathology [52, 53] and age [54]. Clinical trials using P2Y12R blockers for the prevention of coronary events demonstrate a significant benefit reduction in elderly patients, as well as residual platelet hyperreactivity following treatment, in comparison to younger cohorts [55, 56]. Aging is also associated with a distinctive platelet phenotype of increased basal activation, ADP hyperreactivity and greater P2Y12R surface density [54]. Notably in patients with either type 2 diabetes mellitus (Type2-DM), or with ACS [52] there are also reported increases in P2Y12R surface expression. This poses an important question: does upregulation of P2Y12R surface expression influence the degree of agonist-independent P2Y12R activity in ACS patient platelets, and does this in turn contribute to platelet hyperreactivity?

1.6 Inverse agonism

Neutral antagonists are classified by their ability to prevent agonist binding to receptors, whilst exerting no effect on the shift of equilibrium between active (R*) and inactive (R) receptor states. Since the discovery of constitutively-active GPCRS, some antagonists have now been demonstrated to not only compete for agonist binding sites, but also reduce the receptor's ability to exist in a basally-active conformation. These molecules have been reclassified as 'inverse agonists' due to their negative effect on the receptor's intrinsic activity [40]. Inverse agonists induce conformational changes in the receptor to stabilise the inactive, R state. This reduces constitutive activity of the receptors, shifting the equilibrium to favour R over R* in the receptor population. It is believed that around 85% of known GPCR antagonists in reality may act as inverse agonists [57].

1.6.1 Ticagrelor: an inverse agonist

Until recently, the anti-platelet drug ticagrelor was considered a potent neutral antagonist of P2Y12R, exhibiting superior efficacy and reduction in cardiovascular death when compared to other antiplatelet treatments such as clopidogrel [58]. The Aungraheeta et al. study in 2016 [41] first proposed that ticagrelor is instead acting as an inverse agonist at the platelet P2Y12R, promoting receptor inactivation and reducing basal levels of P2Y12R activity. The inverse agonist mechanism of ticagrelor may offer advantages over classical antagonists used in anti-platelet treatments. This may also explain the superiority of ticagrelor over drugs such as clopidogrel in the prevention of cardiovascular death and thrombotic events, as highlighted in the PLATelet inhibition and patient Outcomes (PLATO) study of 2009 [59]. In a pathological vascular environment, such as in patients with ACS, reducing constitutive activity of P2Y12R may be advantageous over simply blocking ADP acting at the receptor, consequently ameliorating long-term outcomes for patients. The Garcia et al. study utilised a BRET assay to explore possible biased inverse agonism between ticagrelor and

cangrelor, another nucleoside analogue similar to ticagrelor. This study, using an elegant probe system, found that cangrelor stabilised an inactive P2Y12R conformation distinct from that induced by ticagrelor [42]. This was further consolidated in patient platelets, and offers an interesting avenue into possible downstream signalling pathway modulation, to limit adverse effects of platelet inhibition in the clinic.

1.7 P2Y12R Mutations

The crystal structure of P2Y12R sets it apart from other class A GPCRs, and helps to offer an explanation for its distinctively high degree of constitutive activity and inverse agonism. The relationship between amino acid residues within the receptor structure, and function of P2Y12R has been explored through mutational studies. Patient-derived missense mutations that hold clinical relevance have been pharmacologically investigated, alongside generated mutants for academic purposes, to study the relatively unique structure of P2Y12R.

1.7.1 Mutations in the P2Y12R

A robust way to study the relationship between P2Y12R structure and its function in platelets is to study natural receptor variants within the human population. Although there are few naturally-occurring mutations, those identified within P2Y12R are associated with decreased receptor expression, internalisation and trafficking, or loss of receptor function[60, 61]. The first patient with a congenital defect in P2Y12R expression or function was identified in 1992 [60]. This patient's platelet responses to ADP were significantly attenuated, presenting as a lifelong issue of extended bleeding times. Abnormal ligand binding was observed by Remijn et al. upon a substitution mutation of a proline residue with a threonine at position 258 in a patient presenting with an adverse bleeding risk [62]. This substitution is found at the front of the extracellular loop 3, which has been shown to be important in ligand-induced conformational changes of TM6 [32].

An arginine-265 mutation to proline (R265P) mutation was assessed by Mundell et al. in 2017 [63] and concluded that R265P, found in extracellular loop 3, resulted in loss of ADP-stimulated platelet response. This study also highlighted that formation of P2Y12R homodimers is essential in both downstream signalling and trafficking of P2Y12R. Another clinically-derived mutation investigated in was an arginine-122 mutation to cysteine (R122C). R122C is part of the DRY motif outlined above, which regulates receptor activity. Whereas R265P mutation showed no changes in P2Y12R expression on both cell surface and total expression, R122C resulted in reduced cell surface expression in a study by Patel et al. in 2014 [64]. This mutation also saw a reduced P2Y12R function in platelets upon ADP stimulation. Thus, patient studies are instrumental in validating proposed functions of structural motifs within P2Y12R.

Several mutational studies have been conducted in order to identify additional residues important for receptor function and expression. Measurement of P2Y12R activity in transfected 12321N cells by Hoffman et al. in 2000 [65] demonstrated the importance of arginine-256 in TM6 for agonist recognition, and both tyrosine-259 and lysine-280 residues in receptor function. A study by Mao et al. in 2010 [66] further explored the proposed role of R256 and other residues in TM6, and found that both R256 and R265 were important for antagonist recognition, displaying increased sensitivity to the P2Y12R antagonist AR-C69931MX. Since the determination of P2Y12R's crystal structure, computational techniques have since been employed to characterise more extensive libraries of P2Y12R variants. Molecular dynamic simulations have been applied to various mutants, focusing on ligand binding and effects on GPCR oligomerisation [67, 68].

Work within the Mundell group has also recently highlighted potentially exciting regions of the P2Y12R that may regulate receptor activity and ligand binding. Together, clinically derived mutations and novel variants identified through computational analysis set the foundation for the mutants this body of work will investigate *in vitro*. A summary of each mutant residue, its location and proposed function are highlighted in the table below:

Table 1. Summary of investigated P2Y12R mutants

P2Y12 Receptor Mutation	Location	(Proposed) Role	Patient or Molecular Modelling-Derived
P2Y12-D70A	Na$^+$ binding pocket	Enhanced antagonist binding (negative allosteric effects)	Modelling [69]
P2Y12-Y105A	TM3 (orthosteric cavity)	Antagonist binding	Modelling [32, 33]
P2Y12-Y105C	TM3 (orthosteric cavity) DRY motif?	Antagonist binding	Modelling [32, 33]
P2Y12-R122C	DRY Motif	Maintaining high constitutive activity	Patient [64]
P2Y12-Y209A	D/NPxxY motif	Receptor activation	Modelling [69]
P2Y12-V234T	TM6	Maintaining high constitutive activity	Modelling [33]
P2Y12-V238A	TM6	Maintaining high constitutive activity	Modelling [32, 33, 69]
P2Y12-F249W	CWxP motif	Switch between active and inactive state	Modelling [69]
P2Y12-R265P	Extracellular loop 3	Ligand binding and receptor activation	Patient [63, 70]
P2Y12-D294N	D/NPxxY motif	Receptor activation	Modelling [32]

1.8 Role of Lipid Rafts in GPCR Signalling

The plasma membrane environment plays a critical role in GPCR signal transduction and receptor trafficking. First described in 1982 by Karnovsky et al., the plasma membrane is a highly organised bilayer, forming specialised lipid domains [71]. Receptors, including GPCRs, have been found to preferentially localise to plasma membrane regions known as lipid rafts [72]. Lipid rafts are enriched with lipids and cholesterol, the interactions of which drive the formation of highly-ordered membrane microdomains. Proteins such as caveolins and tetraspanins enable recruitment of signalling molecules such as G proteins, phosphatases and secondary downstream messengers, providing a platform to facilitate receptor-signalling complexes [73]. This platform enhances G protein signalling specificity by preventing cross-talk with other weaker, G protein mediated signals [74]. Facilitation of these interactions by lipid rafts makes them crucial for GPCR signalling and trafficking.

Lipid rafts demonstrate greater rigidity and stability when compared to the fluidity of the surrounding phospholipid bilayer [75, 76]. This rigidity is orchestrated by cholesterol acting as 'spacers' [75] that anchor scaffold proteins such as flotillins [77]. Lipid rafts are enriched with glycosphingolipids. These are insoluble in non-ionic detergents, and can therefore be isolated and identified experimentally using gradient centrifugation [78]. This technique has been utilised in platelets, demonstrating localisation of integrin signalling complexes to lipid rafts, and how this is required for platelet activation and adhesion [79, 80]. A study by Quinton et al. revealed that lipid rafts are critical for P2Y12R signalling through $G\alpha_i$ [81] and subsequent platelet activation. This study demonstrated localisation of Gα into lipid rafts, and an attenuation of platelet activation upon cholesterol depletion

1.8.1 Ticagrelor effects on lipid rafts and GPCR signalling

It has been demonstrated that lipid raft integrity is required for P2Y12R agonist-mediated signalling pathways. Studies then looked at the effect of antagonists on lipid rafts in platelets. A study by Savi et al. demonstrated the effect of clopidogrel on P2Y12R in lipid rafts [82]. Oligomeric assembly of P2Y12R was observed in untreated platelets localised to lipid raft microdomains, indicating that P2Y12R exists in functional homo-oligomers in platelets. Upon addition of the clopidogrel active metabolite (Act-met), oligomeric P2Y12R was undetected and there was a compensatory increase in dimers and monomers, and these receptors were partitioned out of the lipid rafts. The potent anti-aggregating effects of clopidogrel were thus attributed to its ability to disrupt both assembly and localisation of P2Y12R oligomers at the cell surface, preventing P2Y12R from binding to endogenous ligands such as ADP. From this, a study by Rabani et al. [83] looked at the effects of ADP and ticagrelor stimulation on cholesterol levels and its distribution, and the localisation of platelet P2Y1R

and P2Y12R to lipid rafts. Both ADP and ticagrelor seemed to increase presence of P2Y12R and P2Y1R in lipid raft domains, and re-distributed cholesterol outside of raft fractions compared to control. Therefore, there appears to be an interesting interplay between the effects of lipid rafts on enhancing receptor activation, and possible ligand-induced effects on the lipid rafts themselves in the plasma membrane.

1.9 Thesis Aims

This thesis aims to further develop understanding of how both intrinsic receptor structure and external plasma membrane factors influence both ligand-dependent and independent activity of P2Y12R. To better characterise these effects, this thesis is divided into three main aims:

1. Characterising the effects of changing receptor expression on ligand-dependent and independent activity of P2Y12R

2. Characterising the effects of missense mutations in key residues of P2Y12R and its effect on ligand-dependent and independent activity

3. Investigate effects of manipulating the plasma membrane cholesterol environment on P2Y12R activity in HEK293 cell work and platelets

Chapter 2: Materials and Methods

2.1 Materials
Cell Culture and Transfection

HEK293 cells (ATCC reference: CRL-1573), and HEK293 cells expressing the SV40 T-antigen (HEK293T) (ATCC reference: CRL-3216)

 DMEM with phenol red (Gibco reference: 11995065) supplemented with 5% Penicillin-Streptomycin antibiotic (Gibco reference: 15140122) and 10% FBS (Gibco reference: A5256701) termed as 'complete DMEM'

Clear DMEM (Gibco reference: A1443001)

Opti-MEM media (Gibco reference: 31985070)

Lipofectamine 2000 (Invitrogen reference: 11668019)

100mm culture dishes (Corning reference: CLS430167)

60mm culture dishes (Corning reference: 430166)

T75 culture flasks (thermo-scientific reference: 130189).

Ligands

Ticagrelor, (Bio-techne reference: 6864/10)

Adenosine 5'diphosphate (ADP, Thermofisher reference: J60672)

U46619 (Tocris reference: 1932)

DAMGO (Sigma-Aldrich reference: E7384)

Plasmid Construction

pcDNA3.1-Gα_i-RlucII, pcDNA3.1-Gβ and pcDNA3.1-Gγ-GFP, were all gifted by Dr Michel Bouvier, University of Montreal

The pcDNA3-HA-rMOPR construct was gifted by Professor Eamonn Kelly, University of Bristol

All mutant receptors were made in house by Dr Sukhvinder Bancroft, University of Bristol [69]

BRET

Coelenterazine 400a: (Biotum reference: 10124)

ELISA:

Bovine serum albumin (BSA) (Sigma reference: 9048-46-8)

Primary monoclonal anti-FLAG (M2) raised in rabbit (Sigma-Aldrich reference: F2555)

Secondary anti-mouse IgG alkaline phosphatase (Sigma-Aldrich reference: A9316)

Alkaline phosphatase diethanolamine substrate (Thermofisher reference: 34064)

Alkaline phosphatase tablets: (Thermofisher reference:34047

NaOH made in house

Cholesterol Manipulation

Methyl-β-cyclodextrin (Sigma-Aldrich: 128446-36-6)

Cholesterol Water-Soluble (Sigma-Aldrich: C4951)

VASP/P2Y12 PLT Kit (Biocytex reference: 7014)

PFA and TBS made in-house

2.2 Cell Culture

Human embryonic kidney (HEK)-293/HEK293T cells were maintained in T75 culture flasks in Dulbecco's Modified Eagle Medium (DMEM) containing phenol red, and supplemented with 10% foetal bovine serum (FBS), 100U/mL penicillin and 100ug/mL streptomycin, referred to as 'complete DMEM'. Cells were incubated at 37°C in 95% air and 5% CO_2, humidified atmosphere. For cell passaging, flasks/dishes were allowed to reach 90% confluency before being washed with phosphor buffered saline (PBS) and incubated at 37°C with x10 trypsin-EDTA to lift cells. The trypsin response was then saturated by adding complete DMEM in a volume ratio of at least 3:1 to the trypsin added and cells were resuspended in fresh complete DMEM. The cell suspension was then split into sterile flasks, dishes or plates according to experimental needs and left to incubate at 37°C. Media was replaced on flasks and dishes when a colour change to orange-yellow was observed. All medias used in cell culture were pre-incubated to 37°C before use.

2.3 Cell Transfection

Cells were grown to a 60-80% confluency in 100mm or 60mm dishes. Dishes were transiently transfected with varying amounts of proliferating cell deoxyribonucleic acid (pcDNA) or different receptor deoxyribonucleic acid (DNA) including: FLAG-tagged receptors (P2Y12, P2Y1 and P2Y12R mutants); haemagglutinin (HA)-tagged μ opioid receptor (MOPR); and mutant P2Y12R DNA. These receptor constructs were transfected with or without RLucII-Gα, Gβ and GFP-Gγ protein constructs dependent on subsequent assays. Receptor DNA+G protein construct complexes were incubated with lipofectamine 2000 for 20 minutes at room temperature as per manufacture's guidance. Complete DMEM was aspirated from cell dishes and washed with phosphor-buffered saline (PBS) before addition of Opti-MEM. Cells were incubated in the DNA/lipofectamine complexes for minimum 6 hours in opti-MEM before media was replaced with complete DMEM. Cells were assayed 48 hours post-transfection. The tables below present all transfections completed for experimental work.

Table 2. Measurement of G protein activity in pcDNA control, P2Y12R, P2Y1R and MOPR

Tube	Amount (total 5µg per condition)
1 (pcDNA 1µg)	4µg master mix (MM) + 1µg pcDNA
2 (P2Y12 1µg)	4µg MM + 1µg flag-P2Y12 DNA
3 (P2Y1 1µg)	4µg MM + 1µg flag-P2Y1
4 (MOPR 1µg)	4µg MM + 1ug HA-MOPR

Table 3. Measurement of G protein activity with decreasing amounts of P2Y12R DNA

Tube	Amount (total 6µg per condition)
1 (pcDNA)	4µg master mix (MM) + 2µg pcDNA
2 (P2Y12 2µg)	4µg MM + 2µg flag-P2Y12 DNA
3 (P2Y12 1µg)	4µg MM + 1µg pcDNA + 1µg flag-P2Y12
4 (P2Y12 0.5µg)	4µg MM + 1.5µg pcDNA + 0.5µg flag-P2Y12
5 (P2Y12 0.25µg)	4µg MM + 1.75µg pcDNA 0.25µg flag-P2Y12
6 (P2Y1 0.125µg)	4µg MM + 1.875µg pcDNA + 0.125 µg flag-P2Y12

Table 4. Measurement of G protein activity of 0.8µg P2Y12R mutant DNA (Y105A, Y105C, R122C)

Tube	Amount (total 2.4µg per condition)
1 (pcDNA 0.8µg)	1.6µg master mix (MM) + 0.8µg pcDNA
2 (wildtype P2Y12 0.8µg)	1.6µg MM + 0.8µg WT flag-P2Y12
3 (P2Y12-Y105A 0.8µg)	1.6µg MM + 0.8µg flag-P2Y12-Y105A
4 (P2Y12-Y105C 0.8µg)	1.6µg MM + 0.8µg flag-P2Y12-Y105C
5 (P2Y12-R122C 0.8µg)	1.6µg MM + 0.8µg HA-P2Y12-R122C

Table 5. Measurement of G protein activity of 0.4µg P2Y12R mutant DNA (Y105A, Y105C, R122C)

Tube	Amount (total 2µg per condition)
1 (pcDNA 0.4µg)	1.6µg master mix (MM) + 0.4µg pcDNA
2 (wildtype P2Y12 0.4µg)	1.6µg MM + 0.4µg WT flag-P2Y12
3 (P2Y12-Y105A 0.4µg)	1.6µg MM + 0.4µg flag-P2Y12-Y105A
4 (P2Y12-Y105C 0.4µg)	1.6µg MM + 0.4µg flag-P2Y12-Y105C
5 (P2Y12-R122C 0.4µg)	1.6µg MM + 0.4µg HA-P2Y12-R122C

Table 6. Measurement of G protein activity of 0.2µg P2Y12R mutant DNA (Y105A, Y105C, R122C)

Tube	Amount (total 1.8µg per condition)
1 (pcDNA 0.2µg)	1.6µg master mix (MM) + 0.2µg pcDNA
2 (wildtype P2Y12 0.2µg)	1.6µg MM + 0.2µg WT flag-P2Y12
3 (P2Y12-Y105A 0.2µg)	1.6µg MM + 0.2µg flag-P2Y12-Y105A
# 4 (P2Y12-Y105C 0.2µg)	1.6µg MM + 0.2µg flag-P2Y12-Y105C
5 (P2Y12-R122C 0.2µg)	1.6µg MM + 0.2µg HA-P2Y12-R122C

Table 7. Measurement of G protein activity of 0.1µg P2Y12R mutant DNA (Y105A, Y105C, R122C)

Tube	Amount (total 1.7µg per condition)
1 (pcDNA)	1.6µg master mix (MM) + 0.1µg pcDNA
2 (wildtype P2Y12 0.1µg)	1.6µg MM + 0.1µg WT flag-P2Y12
3 (P2Y12-Y105A 0.1µg)	1.6µg MM + 0.1µg flag-P2Y12-Y105A
4 (P2Y12-Y105C 0.1µg)	1.6µg MM + 0.1µg flag-P2Y12-Y105C
5 (P2Y12-R122C 0.1µg)	1.6µg MM + 0.1µg HA-P2Y12-R122C

Table 8. Measurement of G protein activity in further investigated P2Y12R mutants (D294N, R265P)

Tube	Amount (total 1.8µg per condition)
1 (pcDNA 0.2µg)	1.6µg master mix (MM) + 0.2µg pcDNA
2 (wildtype P2Y12 0.2µg)	1.6µg MM + 0.2µg WT flag-P2Y12
3 (P2Y12-D294N 0.2µg)	1.6µg MM + 0.2µg flag-P2Y12-D294N
4 (P2Y12-R265P 0.2µg)	1.6µg MM + 0.2µg flag-P2Y12-R265P

Table 9. Measurement of G protein activity of P2Y12R mutants (F249W, Y209A,V234T)

Tube	Amount (total 1.8µg per condition)
1 (pcDNA 0.2µg)	1.6µg master mix (MM) + 0.2µg pcDNA
2 (wildtype P2Y12 0.2µg)	1.6µg MM + 0.2µg WT flag-P2Y12
3 (P2Y12-F249W 0.2µg)	1.6µg MM + 0.2µg flag-P2Y12-F249W
4 (P2Y12-Y209A 0.2µg)	1.6µg MM + 0.2µg flag-P2Y12-Y209A
5 (P2Y12-V234T 0.2µg)	1.6µg MM + 0.2µg flag-P2Y12-V234T

Table 10. Measurement of G protein activity of P2Y12R mutants (V238A,D70A)

Tube	Amount (total 1.8µg per condition)
1 (pcDNA 0.2µg)	1.6µg master mix (MM) + 0.2µg pcDNA
2 (wildtype P2Y12 0.2µg)	1.6µg MM + 0.2µg WT flag-P2Y12
3 (P2Y12-V238A 0.2µg)	1.6µg MM + 0.2µg flag-P2Y12-V238A
4 (P2Y12-D70A 0.2µg)	1.6µg MM + 0.2µg flag-P2Y12-D70A

Table 11. Measurement of ligand-dependent G protein activity upon changes in membrane cholesterol

Tube	Amount (total 6µg per condition)
1 (pcDNA 2µg)	4µg master mix (MM) + 2µg pcDNA
2-4 (P2Y12 2µg)	4µg MM + 2µg WT flag-P2Y12

Cells were seeded onto 60mm dishes 24 hours post-transfection and allowed to rest in complete DMEM overnight. On experimental day, cells were washed and serum-starved in serum-free DMEM for 3 hours, hereby referred to as 'clear DMEM'. Cells were then incubated at 37°C and were left untreated, or incubated with either 5mM methyl-β-cyclodextrin (MβCD) to deplete membrane cholesterol, or 0.732mM water-soluble cholesterol to enrich membrane cholesterol for 1 hour. Cells were plated onto a white 96-well plate in clear DMEM and allowed to rest for 1 hour. Cells were then assayed using BRET as described below.

2.4 Measurement of G protein activation by bioluminescence resonance energy transfer

HEK293/HEK293T cells were co-transfected with pcDNA or various receptor construct DNA as described above. 48 hours post-transfection, HEK293/HEK293T cells were seeded onto white 96-well plates in clear DMEM for analysis by bioluminescence resonance energy transfer (BRET). Cells were allowed to rest at 37°C for 1-2 hours before experimentation. Plates were loaded into the CLARIOstar plate reader and were incubated for 10 minutes in the presence or absence of 0.001-10µM ADP, or 0.001-10µM ticagrelor in a 1:10 serial dilution, diluted using clear DMEM. The coelenterazine substrate was then added to a final concentration of 10µM and the RLucII (515nm) and GFP (410nm) emission was measured in intervals of 1,5 and 8 seconds. Values for each ligand concentration and untreated wells at both emissions were averaged. The BRET ratio was calculated: RLucII/GFP. ΔBRET

ratio was used to determine change in BRET ratio from experimental baseline and demonstrates ligand-dependent effects: ΔBRET ratio was plotted in a concentration-response curve.

ΔBRET ratio = ligand-treated cell BRET ratio − untreated cell BRET ratio

At least three technical replicates were produced per N for each BRET assay and averaged. Data was analysed and pharmacological parameters were derived using curve fitting analyses (Stimulation or Inhibition curves with three parameters) on GraphPad Prism 9. Each N was curve-fitted individually and collated for statistical analysis.

2.5 Quantification of P2Y12R cell surface expression by ELISA

Surface expression of P2Y12 receptor was assessed using alkaline phosphatase enzyme-linked immunosorbent assays (ELISAs). HEK293 cells were transiently transfected with 5µg, 2µg or 1µg of FLAG-tagged P2Y12R, or with pcDNA and incubated at 37°C in complete DMEM for minimum 18 hours, before being seeded onto 24-well and 48-well tissue culture plates pre-treated with 0.1mg/ml of poly-D lysine. Plated cells were allowed to rest overnight before experimentation. Absorbance values were measured using an LT-4500 Labtech plate reader. On experimental day, plated cells were incubated at 37°C in clear DMEM for 1 hour before fixing with 3.7% paraformaldehyde (PFA). Cells were washed three times using 3.7% tris-buffered saline (TBS) before a 45-minute treatment with 1% bovine serum albumin (BSA), a non-specific protein blocker. Cells were then incubated at room temperature for 1 hour on a rocker with a primary antibody (anti-FLAG M2 antibody, diluted in clear DMEM 1:2000). Cells were then washed again, and blocked with BSA for 15 minutes. Addition of the secondary antibody (anti-mouse alkaline phosphatase antibody, diluted in clear DMEM 1:1000) for 1 hour at room temperature on a rocker. The cells were then washed again, and incubated at 37°C in the alkaline phosphatase developing solution for 10-30min. Once a deep yellow colour had developed, the reaction was terminated upon transfer of 50µl of each well solution, to a 96-well transparent microplate containing 50µl of 0.4M sodium hydroxide (NaOH). The 96-well plate samples were then measured at an absorbance of 405nm on an LT-4500 plate reader. An average of the pcDNA wells was used to determine background readings. Changes in surface receptor expression was determined by subtracting background and normalising to pcDNA average. At least three technical replicates were produced per N of this experiment and averaged. Data was analysed using GraphPad Prism 9.

2.6 Blood work and ethics

Study approved by NHS Health Research Authority (IRAS: 283543). Human blood was drawn from drug-free, healthy volunteers. Volunteers gave written, informed consent in accordance with the

Declaration of Helsinki. Blood was collected in vacutainer with 3.2% trisodium citrate to prevent coagulation before use as whole blood, or platelet isolation.

2.7 Platelet isolation

2.7.1 Platelet rich plasma (PRP) isolation

Whole human blood was collected from healthy donors. Whole blood was centrifuged at 1000 revolutions per minute (rpm) for 17 minutes to separate the PRP supernatant from other blood components. PRP was then collected in a 15ml falcon tube, and platelets were rested for at least 30 minutes in a 30°C water bath before experimentation.

2.7.2 Platelet poor plasma (PPP) isolation

Once PRP was prepared, any residual PRP and possible white blood cell layer left in the separated whole blood was collected. This was centrifuged at 1700rpm for 10 minutes to separate residual blood components from PPP. PPP was removed from centrifuged sample and rested in a water bath at 30°C for at least 30 minutes before experimentation.

2.8 Light Transmission Aggregometry (LTA)

Platelet aggregation was measured using LTA, performed on the CHRONO-LOG Model 700 aggregometer. 250µl of PRP was dispensed into glass aggregometry cuvettes and incubated for at least 2 minutes at 37°C within the heating slots of the aggregometer. A reference cuvette containing 500µl of PPP +1:10 dilution of vehicle was loaded into the reference well. Experimental cuvettes were then placed simultaneously into the channel wells with a stirring magnet set at 1200 rpm. All channels were calibrated to baseline before the addition of 2.5µl ligand treatment. Aggregation traces were then recorded for up to 5 minutes until response plateau. LTA traces were exported and data was trimmed appropriately in GraphPad Prism 9. Area under each curve was analysed as a quantification of aggregation.

2.8.1 Effects of manipulating membrane cholesterol levels on platelet aggregation response

PRP was isolated and rested for 30 minutes before treatment with either cholesterol or MβCD. Final concentrations of 0.732mM ('high'), 0.366mM ('medium') and 0.183mM ('low') of water-soluble cholesterol was prepared in 150mM NaCl solution to enrich cholesterol in PRP. 5mM, 1.5mM and 0.5mM of MβCD (final concentration) was also prepared in 150mM NaCl solution to deplete cholesterol levels. PRP was then incubated with different cholesterol treatments alongside untreated PRP (with NaCl vehicle) for 1 hr in a water bath at 30°C. ADP at a final concentration of 10µM, 5µM and 2.5µM was then prepared. Thromboxane receptor agonist U46619 at final concentrations of 5µM, 2.5µM and 1µM was also assayed.

2.9 Quantification of phospho-vasodilator-stimulated phosphoprotein (VASP) by flow cytometry

Using whole blood, the degree of phosphorylated-VASP (pVASP) production was determined using a standardised flow cytometry assay from BioCytex, measured using a BD Accuri C6 Plus Flow Cytometer.

2.9.1 Treatment of citrated whole-blood with MβCD

MβCD was made up in 10mM HEPEs-Tyrode's (HT) supplemented with 5.5mM D-glucose anhydrase (D-Gluc) at x10 concentration required. Whole blood was then treated with a 1:10 dilution of each MβCD treatment to produce final concentrations of 5mM MβCD, 1.5mM MβCD and 0.5mM MβCD, and a 1:10 dilution of HT + D-Gluc. Whole blood was incubated with each treatment rolling at room temperature at 6rpm for 45 minutes.

2.9.2 BioCytex assay for pVASP production

Each MβCD-treated whole blood sample and control sample were incubated with prostaglandin E1 (PGE1), or with PGE1+10µM ADP for 10 minutes before fixing with PFA for 5 minutes. Cells were then incubated for 5 minutes with a permeabilising agent and immunolabelled using either anti phospho-VASP mouse monoclonal antibody (MAb), or a negative isotypic MAb control. All cells were then incubated with staining reagent, anti-mouse polyclonal immunoglobulin G (IgG)- Fluorescein isothiocyanate (FITC) antibody, anti CD61-phycoerythrin (PE) platelet counter stain and a permeabilization agent for 5 minutes. All cells were then diluted 1:10 with diluent for 20 minutes before cytometric analysis. Samples were gated for 10,000 platelet events, and median fluorescence intensity (MFI) for phospho-VASP was recorded in the presence of PGE1 alone, or with PGE1+10µM ADP, alongside unstimulated platelets and a negative isotypic control. Percentage of ADP-mediated inhibition of phospho-VASP production was then calculated.

2.10 Data Analyses

All data was exported into GraphPad Prism version 9 (GraphPad Software Inc., San Diego, California, USA). Data was presented as mean ± standard error of the mean (SEM) although individual Ns are visible in graphs. One-way ANOVAs and two-way ANOVAs were employed and corrected using post-hoc Dunnett's test for multiple comparisons. Where normality of data failed, Kruskal-Walls non-parametric tests were utilised where appropriate, as outlined in each figure.

Chapter 3: Results

3.1: Changes in receptor expression affect ligand dependent and independent activity of P2Y12R

3.1. Introduction

The constitutive activity of P2Y12R is well documented [41], although the mechanisms by which this basal activity is maintained are not well understood. The use of the BRET system to measure G protein activation for GPCRs is well-established, and the principals of this assay are outlined in *figure 2*. This technique can accurately monitor ligand-receptor interactions without disrupting the cytosolic environment [84]. Overexpression of P2Y12 in HEK293 cells is known to result in basal receptor activity as shown by Aungraheeta et al. [41]. However changes in P2Y12R expression and its ability to influence the degree of constitutive activity and ligand-dependent activity in the cell system has not been fully characterised. Work within the Mundell group (host laboratory) has observed that the degree of P2Y12R constitutive activity may be influenced by changes in receptor expression.

In initial studies, we aimed to characterise how the changes in P2Y12R expression in HEK293 cells by increasing amounts of P2Y12R DNA transfected affected both ligand dependent and independent activity of the P2Y12R in the BRET system. We hypothesised that an increase in receptor expression would result in an increased degree of constitutive activity. A higher degree of constitutive activity would be indicative of a greater proportion of the P2Y12R population existing in an active state, and so the degree of inverse agonism that can be produced would be significantly increased, as a greater proportion of receptor can be returned to an inactive conformation from an active one. An accompanying decrease in ADP response may also be observed, as an increased population of active receptors will 'mask' ADP agonism resulting in a reduction of ADP's maximum effect (Emax).
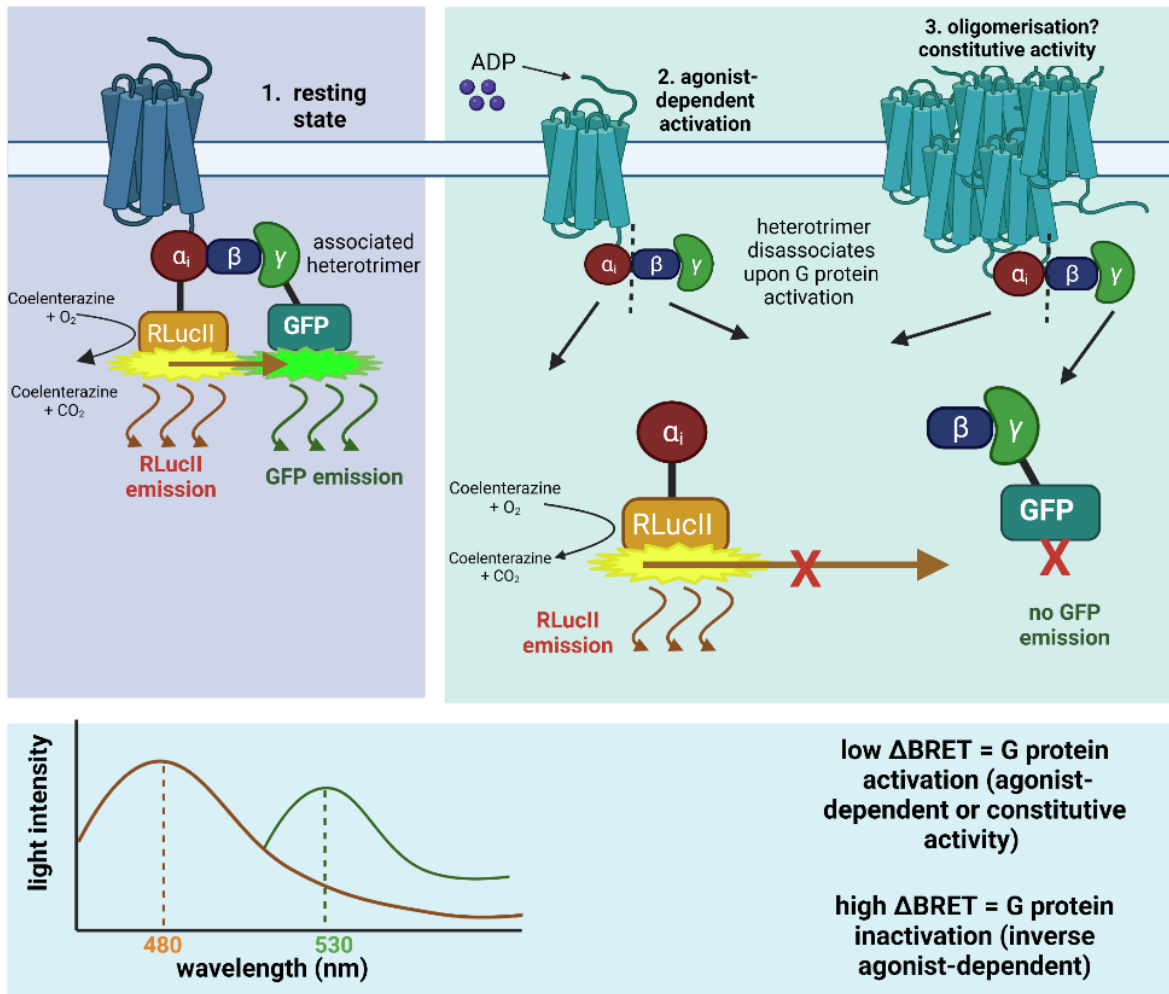
Figure 2. A schematic describing bioluminescence resonance energy transfer (BRET) assay as a measurement of G protein activation. Activation of receptor results in the disassociation of the G protein heterotrimer into the Gα subunit and Gβγ dimer, whilst inactive receptor retains G protein association. For G protein activation studies, the Gα subunit is tagged with a luciferase donor (RLucII), and the Gγ subunit is tagged with an acceptor green fluorescent protein (GFP). Co-expression of these tagged proteins allows real-time quantitative measurement of G protein interactions[84]. Upon addition of substrate coelenterazine, the RLucII donor molecule transfers energy to the acceptor molecule via dipole-dipole coupling, when the acceptor is within close proximity. This produces a fluorescent emission of a specific wavelength. Emissions from both RLucII and GFP are recorded and used to calculate the BRET ratio, a measurement of G protein activation[85]. Therefore upon G protein activation, there is little BRET signal due to distance between G protein subunits, and an increase in BRET signal is seen when the heterotrimer is associated at the inactive form of the receptor. *Created in BioRender.com*

3.1.1 Comparing P2Y12R activity to other class A GPCRs within the BRET system

Firstly, it was important to assess the activity of P2Y12R in the context of other GPCRs within the BRET system. To investigate ligand-dependent and independent activity, a BRET-based assay was employed. Transfection of RLucII-tagged $G\alpha_i$ subunits into the system would imply that only GPCRs coupled to this receptor would be measured within the BRET system. We use the P2Y1 receptor, another important purinergic receptor found on platelets involved in platelet aggregation. This a G_q-coupled GPCR whose endogenous agonist is also ADP. We therefore hypothesised that transfection of only RLucII-tagged G_i would fail to produce a response in P2Y1 receptor.

Full concentration-response curves were produced by recording the change in BRET ratio, used as a measurement of G protein activation. HEK293 cells transiently transfected with P2Y12 and P2Y1 DNA were incubated for 10 minutes with increasing concentrations of endogenous agonist ADP. Full concentration response curves are shown in *figure 3a*. Surprisingly, a P2Y1 receptor response to ADP was recorded at 1μM and 10μM of ADP. P2Y1 ADP Emax was -0.023(± 0.01) and was significantly reduced (p=0.014) in comparison to the expected [86] P2Y12 ADP Emax, -0.072(± 0.01).

 The μ opioid receptor (MOPR) is another class A GPCR that is extensively characterised GPCR within *in vitro* assays including the BRET system[87, 88]. It is another $G\alpha_i$ coupled receptor and was used as an additional control in this experiment. We hypothesised that upon activation with the highly-specific agonist DAMGO, transfected MOPR would produce full G protein activation within the BRET system. A full concentration-response curve to DAMGO is shown *figure 3b*. The DAMGO Emax for MOPR was 0.13(±0.01) as expected [69]. We also wished to investigate the constitutive activity of P2Y12R and how it relates to the degree of basal activity that has been previously recorded for the MOPR, and the apparent lack of constitutive activity in the P2Y1 receptor. Basal BRET ratios demonstrate G protein activation in the absence of ligand, and is used to quantify constitutive activity of the receptor. *Figure 3c* demonstrates the degree of basal activity of all three receptors in comparison to a control. The constitutive activity of P2Y12R was the greatest, at 0.81(±0.02) as hypothesised, whilst P2Y1 seemed to exhibit a surprisingly intermediate degree of basal activity at 0.83 (±0.03) followed by MOPR at 0.84(±0.02), as might be expected.
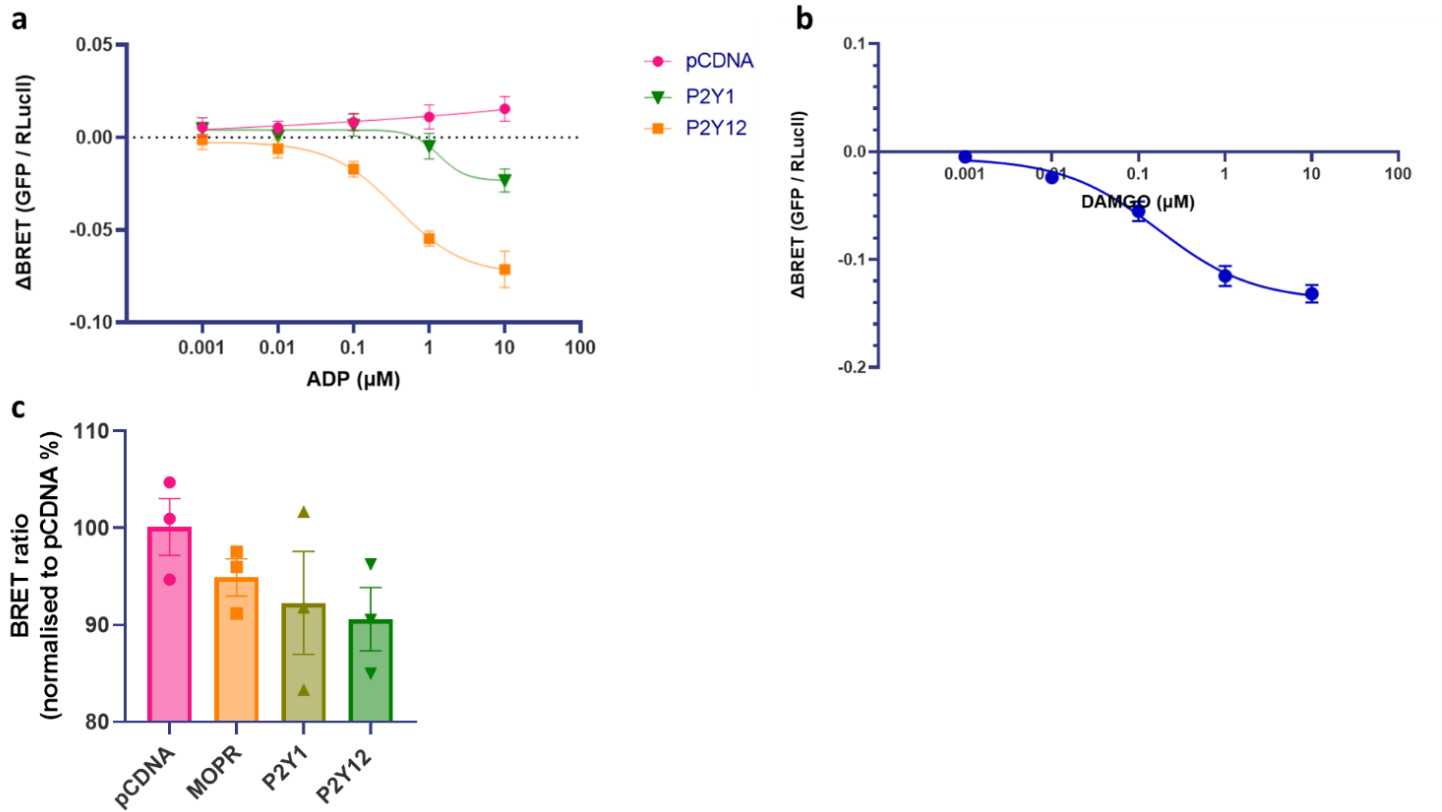
Figure 3. Ligand-dependent and constitutive activity of P2Y12, P2Y1 and μ opioid receptor in HEK293 cells. **a** Full concentration-response curves for to ADP for P2Y12 and P2Y1 receptors and control pcDNA. (N=5). **b** Full concentration-response curve to agonist DAMGO for the μ opioid receptor(N=5). **c** Basal BRET values normalised to pcDNA control for P2Y12, P2Y1 and MOPR. (N=3). Graph C was analysed using one-way ANOVA with Dunnett's post-hoc corrections for multiple comparisons. Graphs A-B represented by mean ± SEM. Graph C shows full distribution of data in box and whisker plot

3.1.2 Changes in P2Y12R expression and its effects on ligand-dependent and independent activity

The previous experiments utilised equal amounts of receptor DNA transiently transfected into the HEK293 cells to make comparable results. The next step was to focus on the P2Y12R and quantify how changes in amount of DNA transfected into these cells affects both surface expression of P2Y12R and its ligand-dependent and independent activity. *Figure 4a* utilises an ELISA technique to quantify P2Y12R surface expression with increasing amounts of transfected DNA. We see a significant increase in surface expression upon increasing amounts of DNA transfected to 2µg (p=0.011) and 5µg (p=0.001) when normalised to pcDNA control. Assessment of how changing amounts of P2Y12R transfected affects constitutive activity was then undertaken. *Figure 4b* demonstrates a step-wise increase in constitutive activity with increasing amounts of P2Y12R DNA transfected. At 0.5µg of P2Y12R DNA we see a significant increase in basal activity when compared to pcDNA control (p=0.0092), and this degree of constitutive activity increases with increasing levels of receptor expression (p=0.0001,p<0.0001 respectively). The effect of increasing P2Y12R transfection on maximal agonist and inverse agonist responses was subsequently assessed. Full concentration-response curves for the endogenous agonist ADP, and the inverse agonist ticagrelor are shown in *figure 4c* across a range of receptor concentrations. *Figure 4c* demonstrates an apparent rightward shift in ADP efficacy with increasing amounts of transfected P2Y12R DNA, and a concomitant increase in ticagrelor efficacy as demonstrated in *table 7*. Further analysis revealed no significant change in the ADP maximal response (Emax, *figure 4d*). There was however a significant decrease in ticagrelor maximal response (Imax) when comparing low (0.25µg) to high (2µg) P2Y12R receptor transfections (p=0.0076).

Table 12. ADP logEC50s and ticagrelor logIC50s for increasing amounts of P2Y12 receptor DNA transfected

	ADP LogEC50 / M	**Ticagrelor LogIC50 / M**
P2Y12 2µg	-0.69 ± (0.30)	-0.37 ± (0.24)
P2Y12 1µg	-0.30 ± (0.20)	-1.5 ± (0.85)
P2Y12 0.5µg	-0.21 ± (0.26)	-0.19 ± (0.21)
P2Y12 0.25µg	-0.056 ± (0.047)	-0.41 ± (0.28)
P2Y12 0.125µg	0.25 ± (0.13)	0.20 ± (0.32)

Data represents mean ± standard error of the mean (SEM)
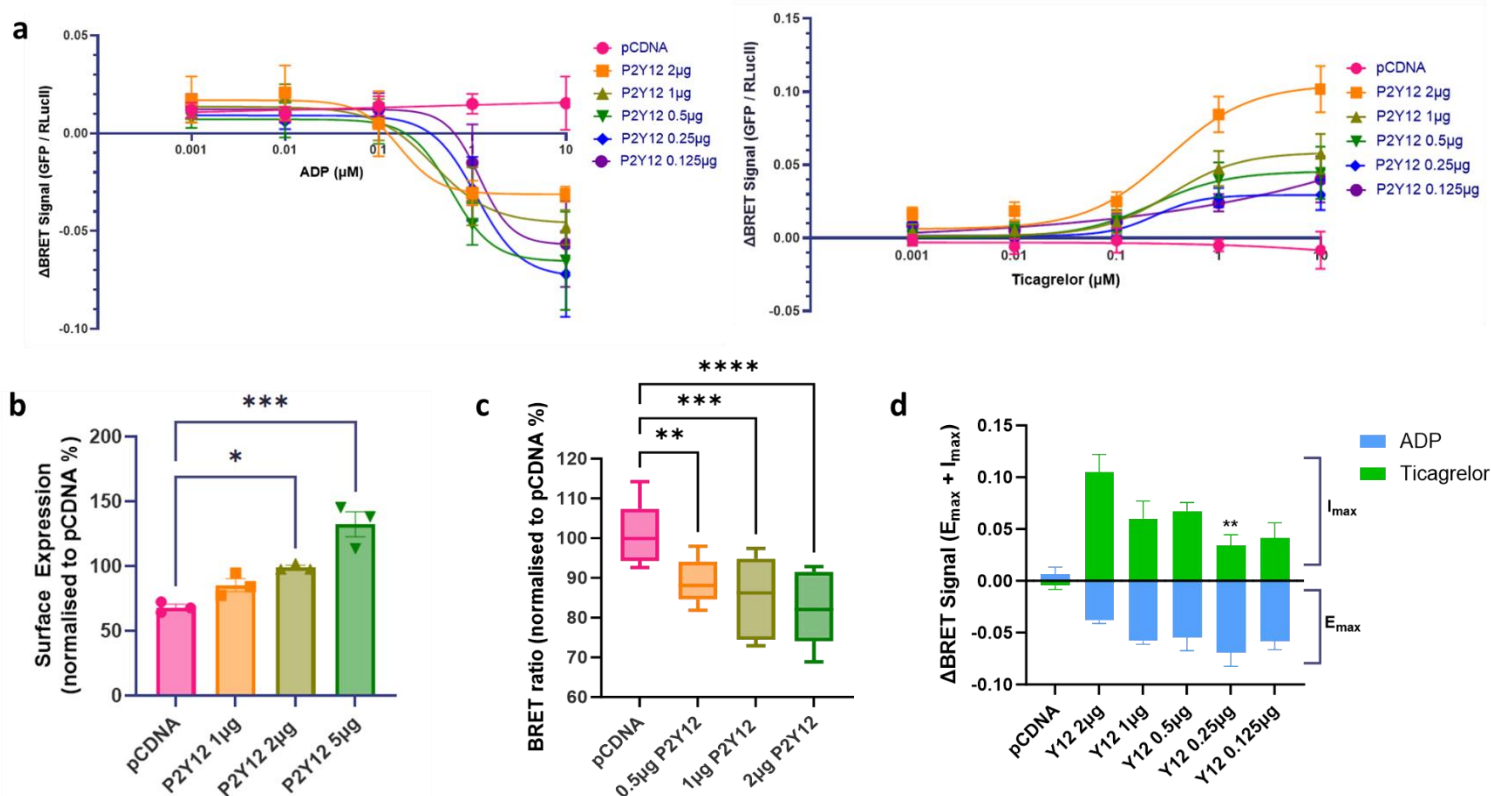
Figure 4. Effect of increasing amounts of P2Y12 receptor transfection on ligand-dependent and independent G protein activation in HEK293 cells. **a** Full concentration-response curves to ADP and ticagrelor for increasing amounts of P2Y12R transfection. (N=5). Statistical test in A-E: one-way ANOVA with Dunnett's post-hoc test for multiple comparisons. **b** Effects of increasing P2Y12 transfection amount on surface expression of P2Y12 receptor detected by ELISA in HEK293 cells. A significant increase in surface receptor expression was observed for 2µg (p<0.05) and 5µg (p<0.001) P2Y12R DNA transfected, compared to control. Values were normalised to individual Ns experimental pcDNA average. (N=3). **c** Effects of increasing P2Y12 transfection amount on constitutive P2Y12R activity. Basal BRET ratio was significant decreased for increasing amounts of P2Y12R (0.5µg,1µg,2µg) compared to control (p<0.01,p<0.001,p<0.0001 respectively). (N=6-10). **d** BRET activation window for increasing P2Y12 transfection amounts. ADP Emax and ticagrelor Imax plotted together to demonstrate the range of effect the receptor can produce. No significant increase in ADP Emax was observed for increasing P2Y12 transfection amount (N=3-4). A significant decrease in Imax was observed with 0.25µg P2Y12R compared to 2µg of P2Y12R (p<0.01). (N=3-6). Statistical test in A-E: one-way ANOVA with Dunnett's post-hoc test for multiple comparisons. Data represented in A,B,D by mean ± SEM. Graph C,D show full distribution of data in box and whisker plot. (*p<0.05, **p<0.01 ***p<0.001,****p<0.0001)

3.2: Missense mutations in P2Y12R affect ligand dependent and independent activity

3.2 Introduction

Both clinically-derived and non-clinical mutations in P2Y12R have been instrumental in identifying residues important for receptor function. Pharmacological characterisation of various missense mutations in P2Y12R have shown alterations in receptor activation, constitutive activity, and also ligand binding. In academic research this has been demonstrated through molecular modelling, such as mutational studies *in vitro* and *in silico*.

Work within the host laboratory has produced a series of mutated P2Y12R constructs [89] based on previous mutational studies. A outlined above these mutations are either derived as a result of ongoing dynamic simulations assessed P2Y12R structure-activity relationships or a result of clinically-derived mutations previously studies in platelets. A comprehensive assessment of ligand binding, receptor conformational changes using molecular dynamic simulations has been undertaken by the Mundell group. However, there is limited data on the effects of these mutations *in vitro* using the BRET system. We therefore devised a library of mutants for investigation into both ligand-dependent and independent activity. Considering the data in 3.1 where appropriate we compared the effects of changing mutant and WT expression, since the effects of changing the amount of receptor transfected for the missense P2Y12R mutations are unknown.

3.2.1 Changes in both WT and mutant Y105A, Y105C and R122C P2Y12R expression and its effects on ligand-dependent and independent activity

Initial studies focussed on the potential importance of two residues Y105 and R122. Y105 is an aromatic tyrosine residue found on TM3, identified in molecular dynamic studies playing a potentially important role in ligand/receptor interaction. Y105 was predicted from alanine scanning by Bancroft [69] to play a role in antagonist binding [90]. Intriguingly Y105C is a naturally occurring variant of this receptor, associated with abnormal platelet function (unpublished) and a patient bleeding phenotype. Another naturally occurring variant associated with abnormal P2Y12R function and platelet bleeding is R122C. R122C is part of the DRY motif outlined above, which regulates receptor activity. Initially a full concentration-response curve to ADP and ticagrelor is shown in *figure 5a* and in *figure 5b*. Surprisingly, given our previous data, there was an apparent loss of ADP response was observed with 2µg of transiently transfected WT P2Y12R, although the ADP response was conserved in mutations Y105A, Y105C and R122C with equivalent DNA transfected (*figure 5a).*

Transfection with 2μg of receptor was derived from previous ELISA-expression data. This inconsistent ADP response with the WT receptor will be discussed later. This was problematic as especially when trying to compare with mutant P2Y12R constructs. Ticagrelor continued to show an inverse agonist response to 2μg of WT P2Y12R (*figure 5b*) and this level of receptor transfectant did exhibit a significant degree of constitutive activity (*figure 5c,* p=0.0004) indicating receptor expression.

Notably, Y105A, Y105C and R122C mutants did not show a response to ticagrelor (*figure 5b*), and also exhibited a significant loss of constitutive activity (*figure 5c*, p=0.0033,p=0.014,p=0.0056 respectively). We hypothesised that the loss of ADP response to the WT receptor may be as a consequence of increased constitutive receptor activity.

Experiments were therefore subsequently repeated at 0.5μg of both WT and mutant DNA transfected. *Figure 5e and 5f* show full concentration-response curves to ADP and ticagrelor respectively for each receptor type with 0.5μg DNA transfected. A partial restoration of ADP response in WT receptor can be observed, and the concentration-response curves for the mutants in response to ADP remain relatively unchanged. We see a substantial dampening of maximal response to ticagrelor in Y105A,Y105C and R122C (*figure 5f)*, and a simultaneous decrease in maximal response by WT to ticagrelor when compared to 2μg of DNA transfected (*figure 5b)*. The effect of both P2Y12 receptor type (WT, Y105A, Y105C and R122C) and amount of receptor DNA transfected (2μg, 1μg and 0.5μg) on both ADP Emax and ticagrelor Imax was analysed using a two-way ANOVA (*data not shown*). Simple main effects analysis revealed that the receptor type had a significant effect on ADP Emax ($F_{(3, 14)} = 8.266$, p=0.0021)). For ticagrelor Imax, simple main effects analysis revealed that receptor type had a highly significant effect ($F_{(3, 20)} = 29.43$, p<0.0001). Interestingly, simple main effects analysis also revealed that the amount of DNA transfected had a significant effect on ticagrelor Imax ($F_{(2, 20)} = 7.228$, p=0.0043).

The significant constitutive activity of WT receptor in figure *5e* is conserved compared to pcDNA control (p=0.026) at 0.5μg, although it is less significant than the WT counterpart in *figure 5b*. Mutants Y105A,Y105C and R122C again do not exhibit a significant degree in constitutive activity when compared to WT receptor at 0.5μg. Taken together, it is apparent that the increase in constitutive activity of the WT receptor with increasing amounts of DNA transfected is conserved in these experiments, but there seems to be little effect on constitutive activity of the mutants with different amounts of receptor DNA.
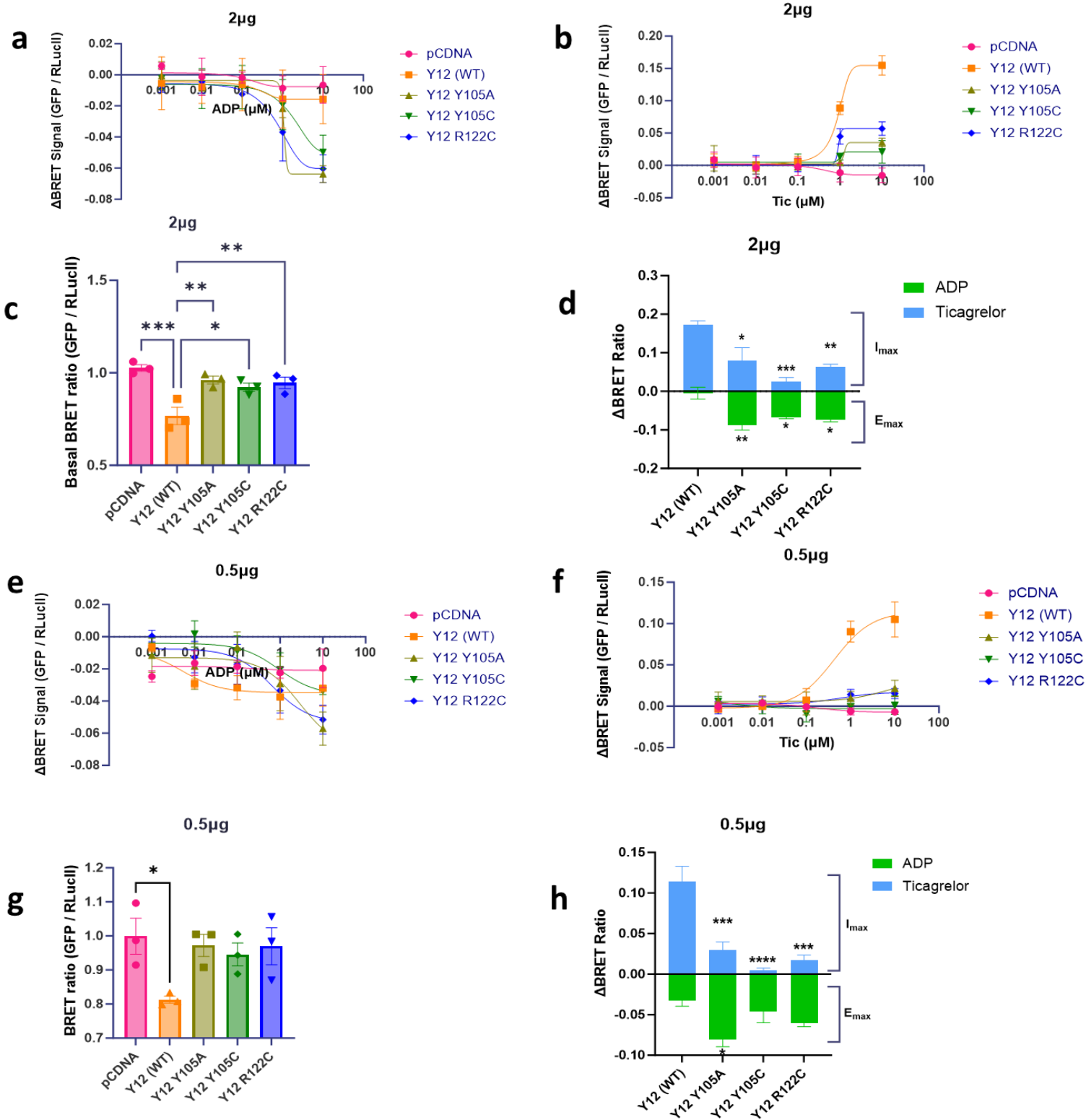
Figure 5. Effect of increasing amounts of P2Y12R transfected on the ligand-dependent and independent activity of wildtype P2Y12R, and mutants Y105A, Y105C and R122C. **a** Full concentration-response curves to ADP **b** and ticagrelor for 2μg of transfected DNA for WT and mutants Y105A,Y105C and R122C receptors. (N=3). **c** Basal BRET for 2μg of WT receptor and the Y105A,Y105C and R122C mutant receptors. Constitutive activity of WT receptor was significantly increased (p<0.001) compared to control. Y105A,Y105C and R122C mutants exhibited a significant reduction in constitutive activity compared to WT (p<0.01,p<0.05,p<0.01 respectively).**d** BRET activation window for 2μg DNA transfected for WT and mutants Y105A,Y105C and R122C receptors.

ADP Emax and ticagrelor Imax values plotted together to demonstrate the range of effect the receptor can produce. All mutants, Y105A, Y105C and R122C showed a significant increase in ADP Emax compared to WT (p<0.01,p<0.05,p<0.05 respectively). Y105A,Y105C and R122C also showed a significant reduction in ticagrelor Imax response compared to WT receptor (p<0.05,p<0.001,p<0.01 respectively). (N=3). **e** Full concentration-response curves to ADP and **f** ticagrelor for 0.5µg DNA transfected for WT and mutants Y105A,Y105C and R122C receptors. (N=3). **g** Basal BRET values were calculated for 0.5µg of WT receptor and the Y105A,Y105C and R122C mutant receptors. Basal activity of WT receptor was significantly increased (p<0.05) compared to control. Y105A,Y105C and R122C mutants did not show significant constitutive activity. **h** BRET effect window for 0.5ug of transfected WT receptor and mutants Y105A,Y105C and R122C. Y105A showed a significant increase in ADP Emax (p<0.05) compared to WT receptor. Y105C and R122C had Emax responses comparable to WT. Statistical test in C-D,G-H: one-way ANOVA corrected for Dunnett's multiple comparisons. Data represented in A-F by mean ± SEM (*p<0.05,**p<0.01***p<0.001)

3.2.2 Addressing additional variability issues of ADP response using new HEK293 cells

Given the unreliability of WT receptor construct, we tested whether there were issues with our HEK293 cells. These HEK293 cells were passage number of >20. We therefore purchased and used new HEK293 cells to assess their effects on ADP responsiveness. *Figure 6a* and *6b* show full concentration responses to ADP and ticagrelor respectively for the WT receptor in 'old' and 'new' HEK293 cells. Although non-statistical, due to low n number, there is an increase in ADP response in the new cells compared to old. A non-statistical decrease in ticagrelor response is also seen in the new cells compared to old. A variable degree of basal activity was also observed in the 'old' cells transfected with P2Y12R DNA compared to 'new' cells. The basal activity of wildtype and mutant P2Y12R constructs will be discussed later.
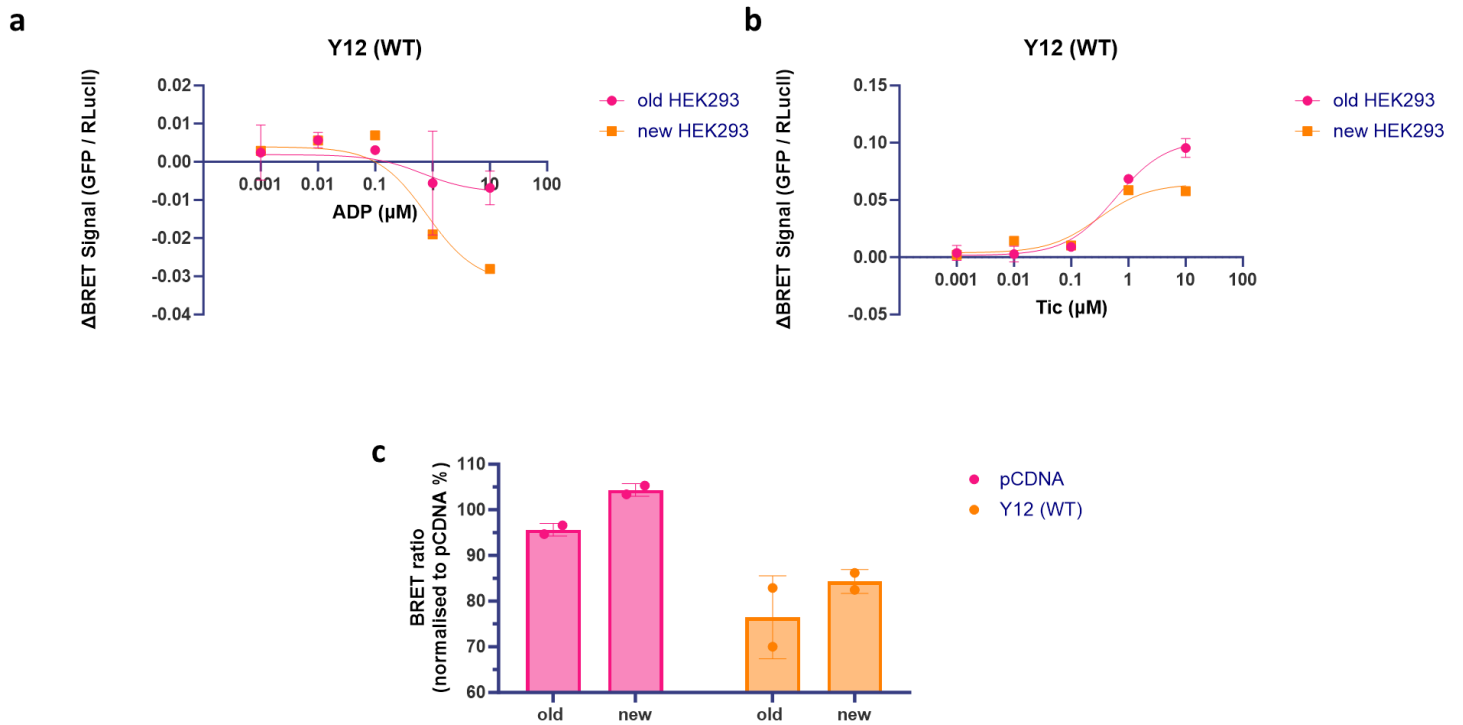
Figure 6. Exploring variability of ligand-dependent and independent activity of WT P2Y12R when transfected into different passages of HEK293 cells. Full concentration-response curves to **a** ADP and **b** ticagrelor for WT receptor transfected into 'old' and 'new' HEK293 cells. **c** Comparison of basal BRET values for WT P2Y12R in 'old' and 'new' HEK293 cells to pcDNA control. Ratios were normalised due to variability in raw experimental values. Statistical differences were not calculated due to low N numbers (N=2 for both cell types). Data represented in A-C by individual values.

3.2.3 Further investigation of ligand-dependent activity in F249W, Y209A and V234T mutant P2Y12R

Given the variation for ligand-dependent P2Y12R response were thoroughly investigated, it was decided to move forward with the 0.5µg of DNA transfected into the 'new' HEK293 cells. This allowed for comparison of each mutant and an increased confidence in the use of 0.5µg of DNA per transfection. Note that ligand-dependent activity of each P2Y12R mutant is reported first. Constitutive activity is collated and explored later in 3.2.6.

The CWxP motif is highly conserved in class A GPCRs. It is found on TM6 of P2Y12R [91] and is involved in receptor activation. In the P2Y12R, the tryptophan-249 residue of the CWxP motif is mutated to a phenylalanine, forming instead a CFxP motif. The F249W mutant was therefore generated to see if restoration of the CWxP motif would affect ligand-dependent activity. Y209 is a tyrosine residue found on TM5, and is thought to have key interactions with the tyrosine residue of the NPxxY motif, involved in receptor activation [69]. The Y209A mutation was therefore generated to see if an alanine replacement would affect interactions with NPxxY and therefore effect ligand-dependent or independent activity. V234 is a residue identified by Bancroft and is found on TM6 of the P2Y12R. The V234T mutant was therefore generated to investigate the potential role of V234 in maintaining the high degree of constitutive P2Y12R activity [69].

Figure 7a and *7b* show full concentration response curves to ADP and ticagrelor for WT and mutant receptors. All EC50 and IC50 values (*figure 7b*) of the mutants were comparable to WT. *Figure 7d* is a summary figure showing curve-fit values of both ADP Emax and ticagrelor Imax for both WT receptor and each mutant receptor. Together these values produce the BRET activation window and visually represent both changes in Emax and Imax, but also the size of the dynamic window of activation. F249W and V234T mutants had ADP Emax values comparable to WT, whilst the Y209A mutant showed a significant increase in ADP Emax (p=0.021). The ticagrelor Imax values for the F249W and V234T mutant were also comparable to WT, however the Y209A mutant showed a highly significant decrease in Imax value (p<0.0001). Together these results show no real change in ligand-dependent receptor activation for mutants F249W and V234T, whilst Y209A showed a significant increase in response to ADP accompanying a significant attenuation of response to ticagrelor. These results further supported the use of a decreased amount of transfected DNA for BRET-based assays.

a

b

c

	ADP logEC50 / M	Tic logIC50 / M
Y12 (WT)	-1.2 ± (0.56)	-0.33 ± (0.079)
Y12 F249W	0.22 ± (0.048)	-0.31 ± (0.099)
Y12 Y209A	0.27 ± (0.090)	-0.60 ± (0.13)
Y12 V234T	-0.95 ± (0.40)	-0.20 ± (0.077)

d

Figure 7. Effects of mutants F249W,Y209A and V234T on ligand-dependent activity of P2Y12R in HEK293 cells. Full concentration-response curves to **a** ADP and **b** ticagrelor for WT receptor and mutants F249W,Y209A and V234T (N=4). **c** Summary table of mean logEC50 values for ADP, and logIC50 values for ticagrelor for WT receptor and F249W,Y209A and V234T mutants. All mutant values for Emax and Imax were comparable to WT (N=4). **d** BRET activation window for WT receptor and F249W, Y209A and V234T mutants. ADP Emax and ticagrelor Imax values plotted together to demonstrate range of effect the receptor can produce. Emax was significantly increased in Y209A mutant compared to wildtype (p<0.05).(N=3-4). Imax was significant decreased in Y209A mutant compared to WT (p<0.0001). (N=3-5). Statistical test in C,D: one-way ANOVA with Dunnett's post-hoc test. Data represented in A-D by mean ± SEM (*p<0.05,****p<0.0001).

3.2.4 Characterising ligand-dependent activity of R265P and D294N

The ligand-dependent effects of the mutants D294N and R265P were then characterised. D294 is a residue found on TM7, and was used by Zhang et al [32, 33] to thermostabilise the P2Y12R. The aspartic residue mutates the NPxxY motif to a DPxxY motif in 18% of class A GPCRs. The D/NPxxY motif is widely reported in receptor activation [69] and possible receptor downregulation [92] and internalisation [93]. The D294N mutant was generated to restore the NPxxY motif seen in the majority of class A GPCRs, to assess for changes in P2Y12R activation. The R265P mutation is patient-derived mutation identified by Mundell et al. [63], and associated with a bleeding disorder and abnormal platelet function as outlined in 1.7.1.

Full concentration-response curves to ADP and ticagrelor are shown in *figure 8a* and *figure 8b.* R265P showed a significant increase in logEC50 value (*figure 8c*, p=0.022) but no significant change in logIC50. The D294N mutant logEC50 and logIC50 values were comparable to WT (*figure 8c*). The BRET activation window seen in *figure 8d* shows both the max responses to ADP and ticagrelor as well as the range of each receptor's dynamic window. R265P ADP Emax was comparable to WT, whilst D294N showed a significant increase in maximal ADP response compared to WT receptor (p=0.01). The Imax values for D294N was comparable to WT, and for R265P it was significantly diminished compared to WT receptor (p=0.0087).
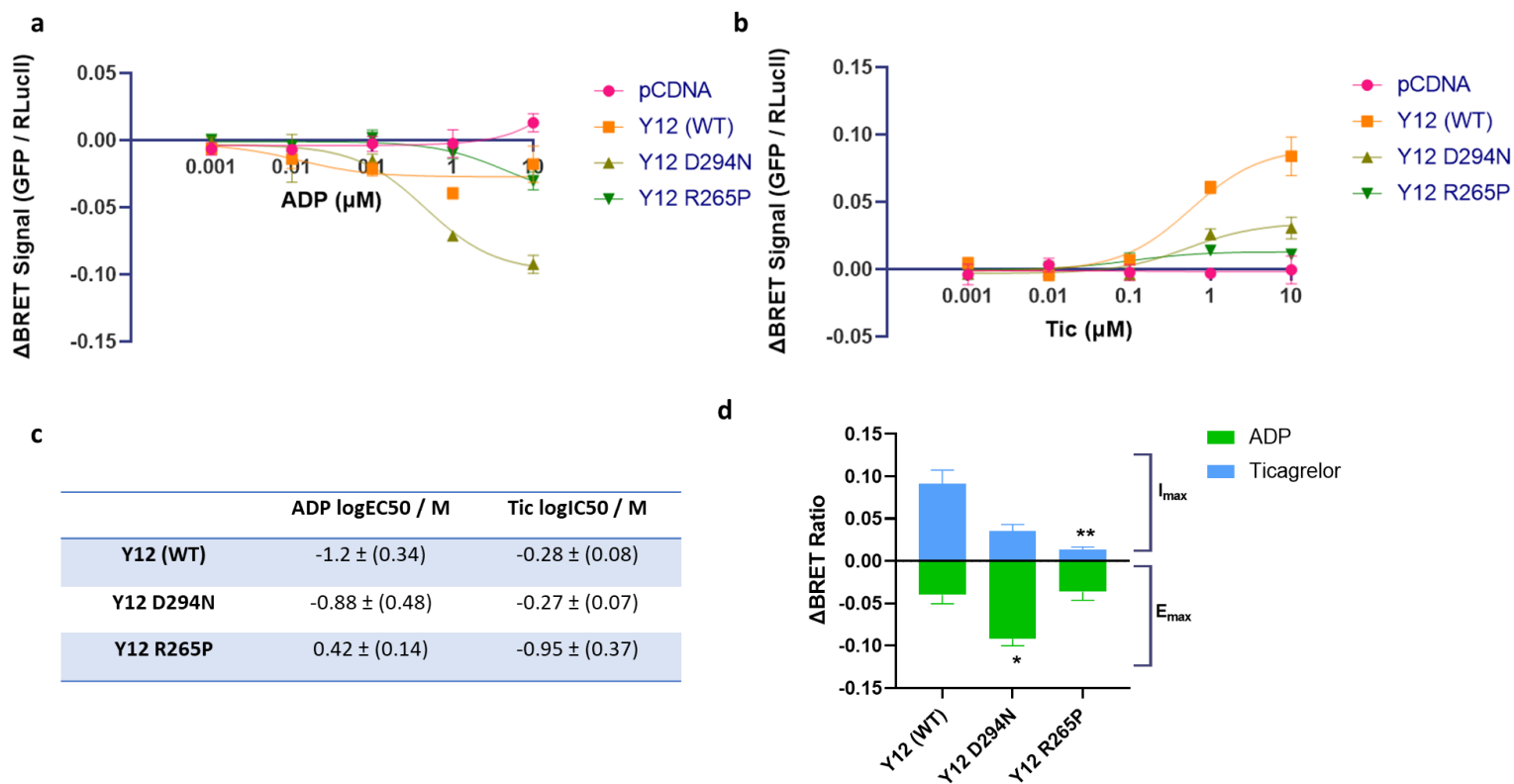
Figure 8. Effects of mutants D294N, and R265P on ligand-dependent activity of P2Y12R in HEK293 cells. Full concentration-response curves to **a** ADP and **b** ticagrelor for WT receptor and mutants D294N and R265P (N=5). **c** Summary table of mean logEC50 values for ADP, and logIC50 values for ticagrelor for WT receptor D294N and R265P mutants. R265P logEC50 value was significantly increased ($p<0.05$). Other mutant values were comparable to WT (N=5). **d** BRET activation window for WT and mutant D294N and R265P receptors. ADP Emax was significantly increased for D294N mutant compared to WT ($p<0.05$). Imax values were significant decreased for D294N and R265P compared to WT ($p<0.01$, $p<0.001$ respectively).(N=3-5). Statistical test in C,D: one-way ANOVA, or Kruskal-Wallis test where data failed normality tests, with Dunnett's correction for multiple comparisons. Data represented in A-D by mean ± SEM (*$p<0.05$,**$p<0.01$).

3.2.5 Characterising ligand-dependent activity of V238A and D70A

The final mutants to be characterised in the BRET assay were V238A and D70A.

Crystal structures of class A GPCRs have revealed a sodium binding pocket in the middle of TM7. First identified in the opioid receptor, Na^+ acts as a negative allosteric modulator of agonist binding [94]. The pocket in which Na^+ binds in class A GPCRs is coordinated by the key residues D2.5 and S3.39 [95]. Whilst this pocket is highly conserved, its location differs in δ-branched class A GPCRs, including P2Y12R. Work with PAR1 receptor, another δ class A GPCR, demonstrates a shift of this Na^+ towards the intracellular side, coordinated by $D^{2.50}$[96], also referred to as D70. Mutation of this highly conserved aspartate residue to an alanine (D70A) was therefore investigated for its potential role in agonist-dependent activity at the P2Y12R.

V238 is a residue found on TM6 that corresponds to the DRY motif of TM3, specifically the R122 residue as outlined in 3.2.1. The DRY motif is involved in receptor activation, and this residue is hypothesised to be involved in maintaining constitutive activity of the P2Y12R [42] alongside the V234 residue. V238 is a negatively charged, and so can form ionic interactions with R122 on TM3 [42]. Mutation of V238 to an alanine (V238A) was therefore investigated for its interaction with the DRY motif and its potential role in agonist-independent activity of the P2Y12R.

Figure 9a shows full concentration response curves to ADP, and *figure 9b* to ticagrelor, for WT receptor and mutants V238A and D70A. The logEC50 values for ADP and logIC50 values for ticagrelor are summarised in the table in f*igure 9c*. Both logEC50 and logIC50 values for mutants D70A and V238A were comparable to WT receptor. Both ADP Emax and ticagrelor Imax for the D70A mutant were comparable to WT (*figure 9c).* V238A mutant showed a comparable ADP Emax to WT receptor, but a significantly increased maximal ticagrelor response (*figure 9c*, p=0.0025).

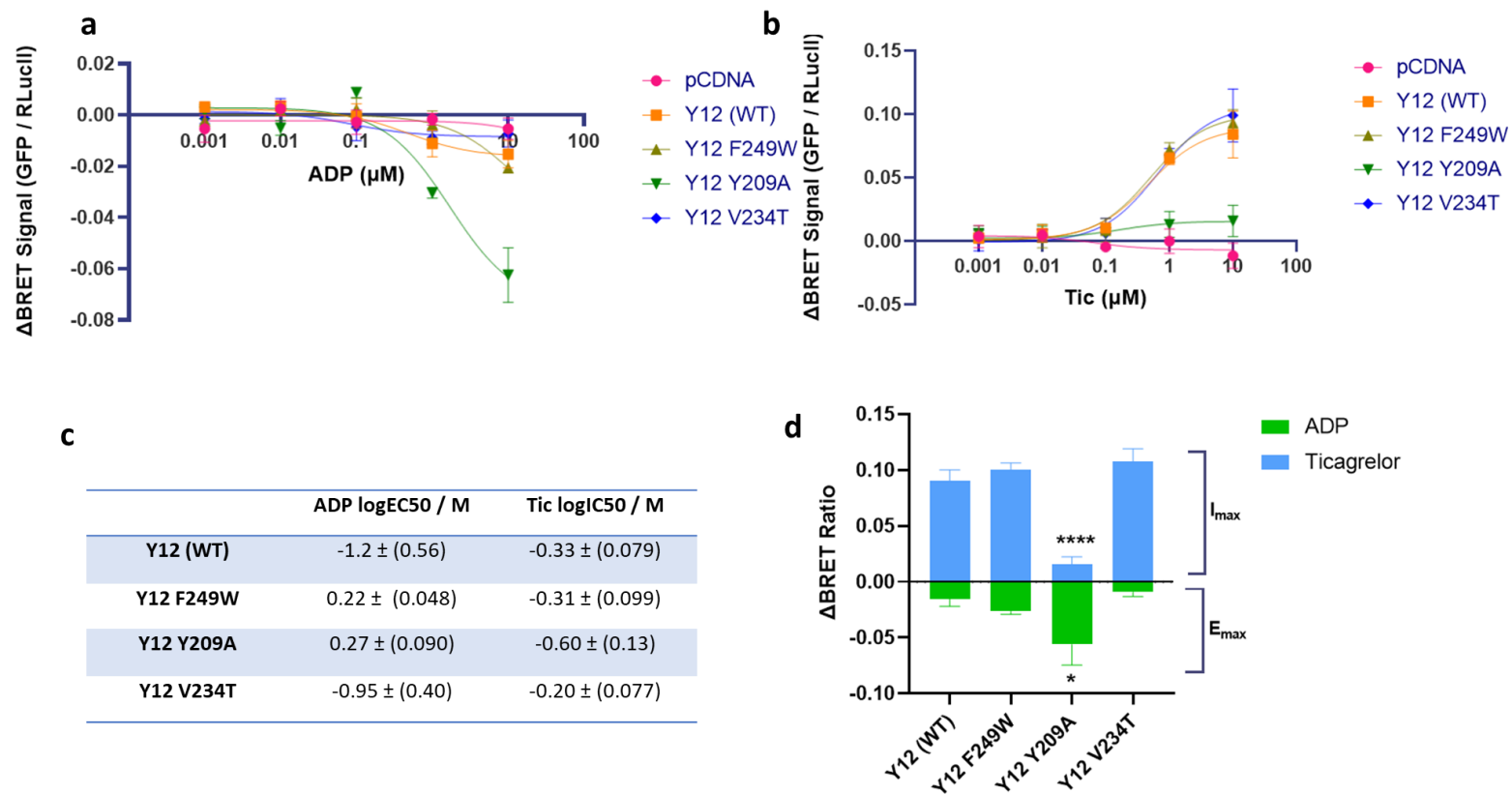|	ADP logEC50 / M	Tic logIC50 / M
Y12 (WT)	-0.10 ± (0.89)	-0.64 ± (0.19)
Y12 V238A	0.55 ± (0.62)	-0.15 ± (0.066)
Y12 D70A	-0.12 ± (0.19)	-0.40 ± (0.11)
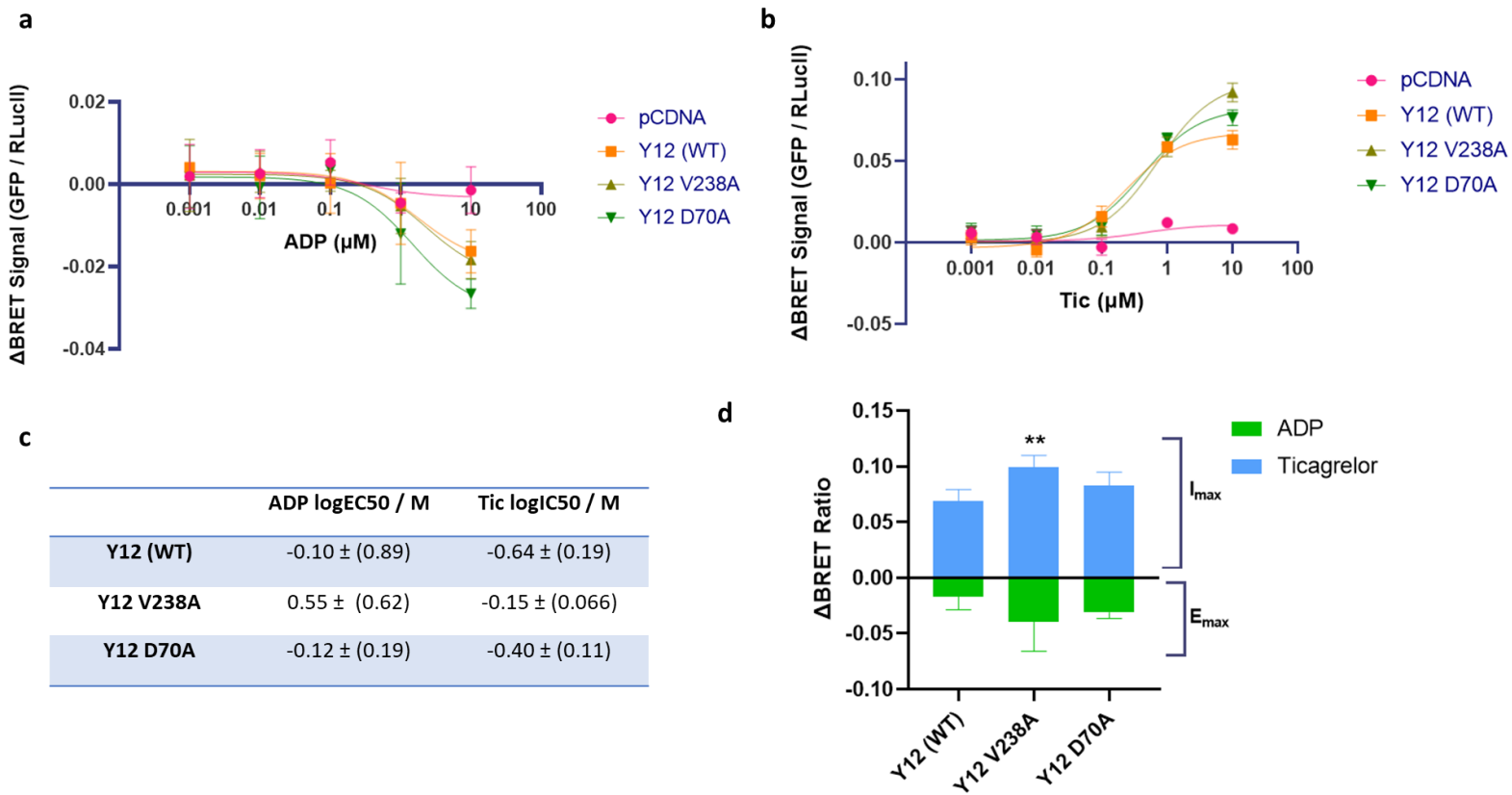
Figure 9. Effects of mutants V238A and D70A on ligand-dependent activity of P2Y12R in HEK293 cells. Full concentration-response curves to **a** ADP and **b** ticagrelor for WT receptor and mutants V238A and D70A (N=4). **c** Summary table of mean logEC50 values for ADP, and logIC50 values for ticagrelor for WT receptor V238A and D70A mutants. All mutant values were comparable to WT (N=4). **c** BRET window for WT receptor and V238A and D70A mutants. ADP Emax and ticagrelor Imax values collated to show range of effect the receptor can produce. ADP Emax values for V238A and D70A were comparable to WT. (N=4). Imax was significantly increased in V238A mutant compared to WT (p<0.01).(N=4). Statistical test in B-C: one-way ANOVA or Kruskal-Wallis test where data failed normality tests corrected for Dunnett's multiple comparisons. Data represented in A-D by mean ± SEM (**p<0.01).

3.2.6 Characterisation of constitutive activity in all investigated P2Y12R mutants

The ligand-dependent activity of each P2Y12R mutant has thus far been characterised, however it was also important to establish any effects of these mutations on agonist-independent constitutive activity. BRET ratios in the absence of ligand represent basal constitutive activity (basal BRET) are evident when compared to pcDNA control. WT P2Y12R and all the mutant P2Y12R constructs outlined above were transfected with 0.5µg receptor DNA for comparison. Each basal BRET ratio for pcDNA and mutant P2Y12R are compared to the set of WT receptor values for each experiment. *Figure 10* summarises all this data. As expected, in *figure 10a-d*, WT receptor showed a significant degree of constitutive activity compared to pcDNA control (a-d, p=0.022, p=0.26,p=0.005,p=0.034 respectively). A statistically non-significant reduction in constitutive activity was observed in mutants Y105A, Y105C and R122C *(figure 10b).* The constitutive activity of all other P2Y12R mutants was conserved and comparable to WT receptor, apart from the Y1Y209A mutant in *figure 10c*. A significant reduction, or loss of constitutive activity compared to WT receptor, was observed for the Y209A mutant (p=0.01).
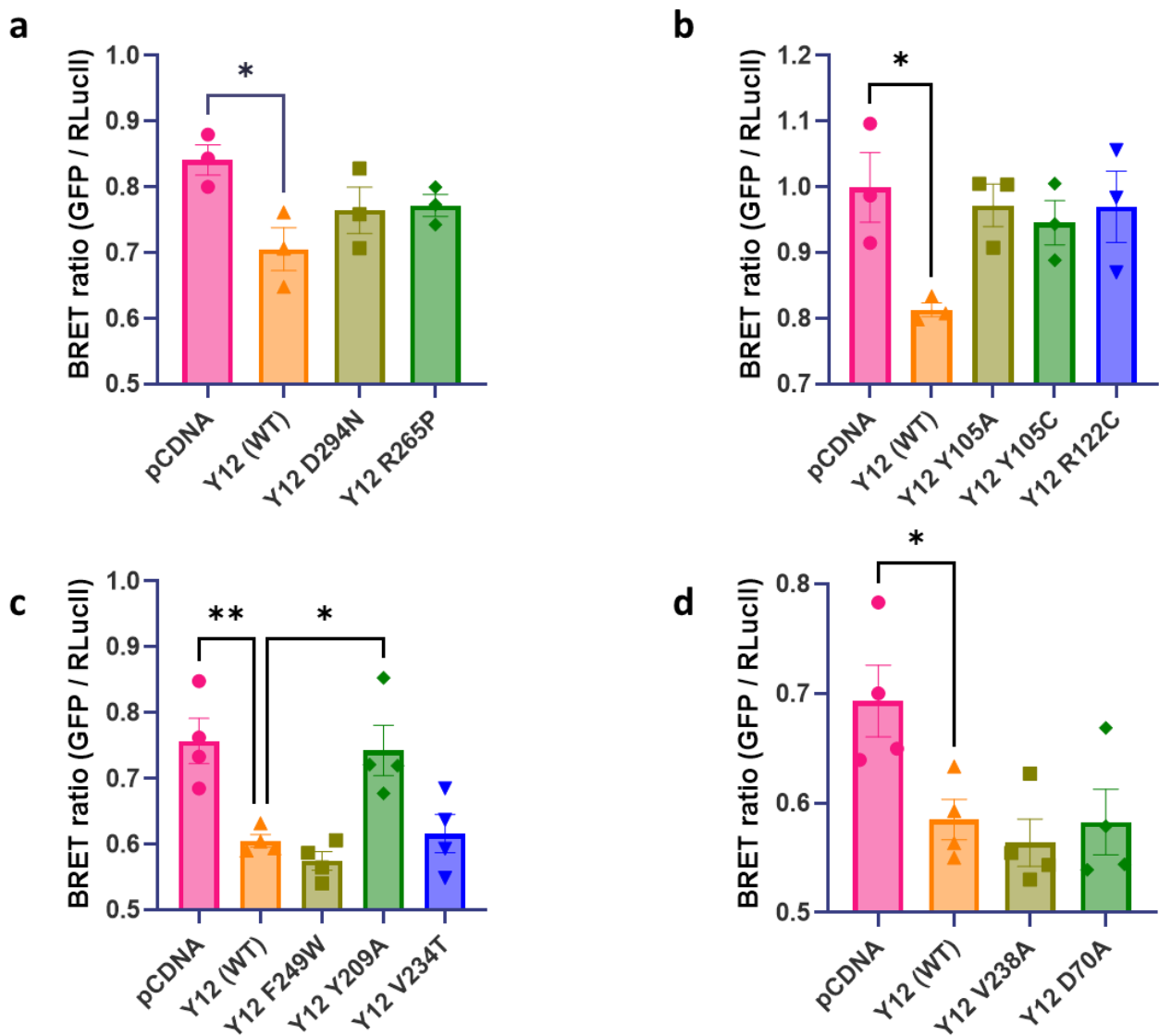
Figure 10. Constitutive activity was significantly reduced in Y209A mutant but unchanged in others in HEK293 cells. **a** Basal BRET values for WT receptor vs D294N and R265P mutants. WT receptor exhibited a significant degree of constitutive activity compared to control ($p<0.05$).Both D294N and R265P show constitutive activity comparable to WT receptor. **b** Basal BRET values for WT receptor vs Y105A, Y105C and R122C. Mutants Y105A,Y105C and R122C showed constitutive activity comparable to wildtype, which was significantly increased when compared to control ($p<0.05$). (N=3). **c** Basal BRET values for WT receptor vs F249W, Y209A and V234T mutants. WT receptor showed a significant degree of constitutive activity ($p<0.01$) compared to control.F249W and V234T mutants showed constitutive activity comparable to WT receptor, whilst Y209A showed a significant reduction ($p<0.05$) in constitutive activity compared to WT receptor. **d** Basal BRET values for WT receptor vs V238A and D70A mutants. WT receptor showed a significant degree of constitutive activity when compared to control ($p<0.05$). Mutants V238A and D70A showed constitutive activity comparable to WT receptor. All graphs were analysed using one-way ANOVA with Dunnett's corrections for multiple comparisons. All data represented by mean ± SEM (*$p<0.05$, **$p<0.01$).

3.2.7 Further pharmacological profiling of P2Y12R mutants: BRET effect window

The magnitude of effect -from full agonism to full inverse agonism- of each receptor in comparison to WT was also assessed. Similar to the previously plotted 'BRET activation windows' the difference between Emax and Imax was calculated in *Figure 11a-d*. This is termed 'BRET effect window' . The BRET effect window was conserved across 6 of the 10 investigated mutants. Perhaps as expected when evaluated with data from *figure 6c*, the BRET effect window for D294N as seen in *figure 11a* is most significantly diminished in comparison to WT (p<0.001). The Y105C and Y209A mutant in *figure 11b* and *11c* also show a significant reduction in BRET effect window (p<0.05, p<0.01 respectively) when compared to WT receptor. Interestingly, the V238A mutant in figure *11d* shows a significant increase in BRET effect window in comparison to WT receptor (p<0.05).

7 of the 10 mutants show significant changes in ADP Emax and Imax compared to WT receptor, but only 4 mutants show significant changes in BRET effect window plotted in *figure 9a-d.* As shown in the BRET activation windows for each mutant, the set point (position of no response, along the x axis) is shifted in some mutants and so the range of response of mutants will still be comparable to WT receptor. For example, an significant increase in ADP response results in an accompanying dampening of inverse agonist response, as seen in the D294N mutant. It has been postulated by the Mundell group that these shifts in the BRET effect window could be due to loss of constitutive activity for mutant receptors.

The Emax/Imax ratios calculated in *figure 11e* reveal the equilibrium of active to inactive receptors upon ligand treatment. This serves as an indirect measurement of constitutive P2Y12R activity. A greater Emax/Imax ratio is suggestive of a decrease in constitutive activity. The Emax/Imax ratio for Y105C, R122C and D294N was significantly increased compared to WT (p=0.032, p=0.047, p=0.023 respectively). Y209A showed a statistically non-significant increase in Emax/Imax ratio.
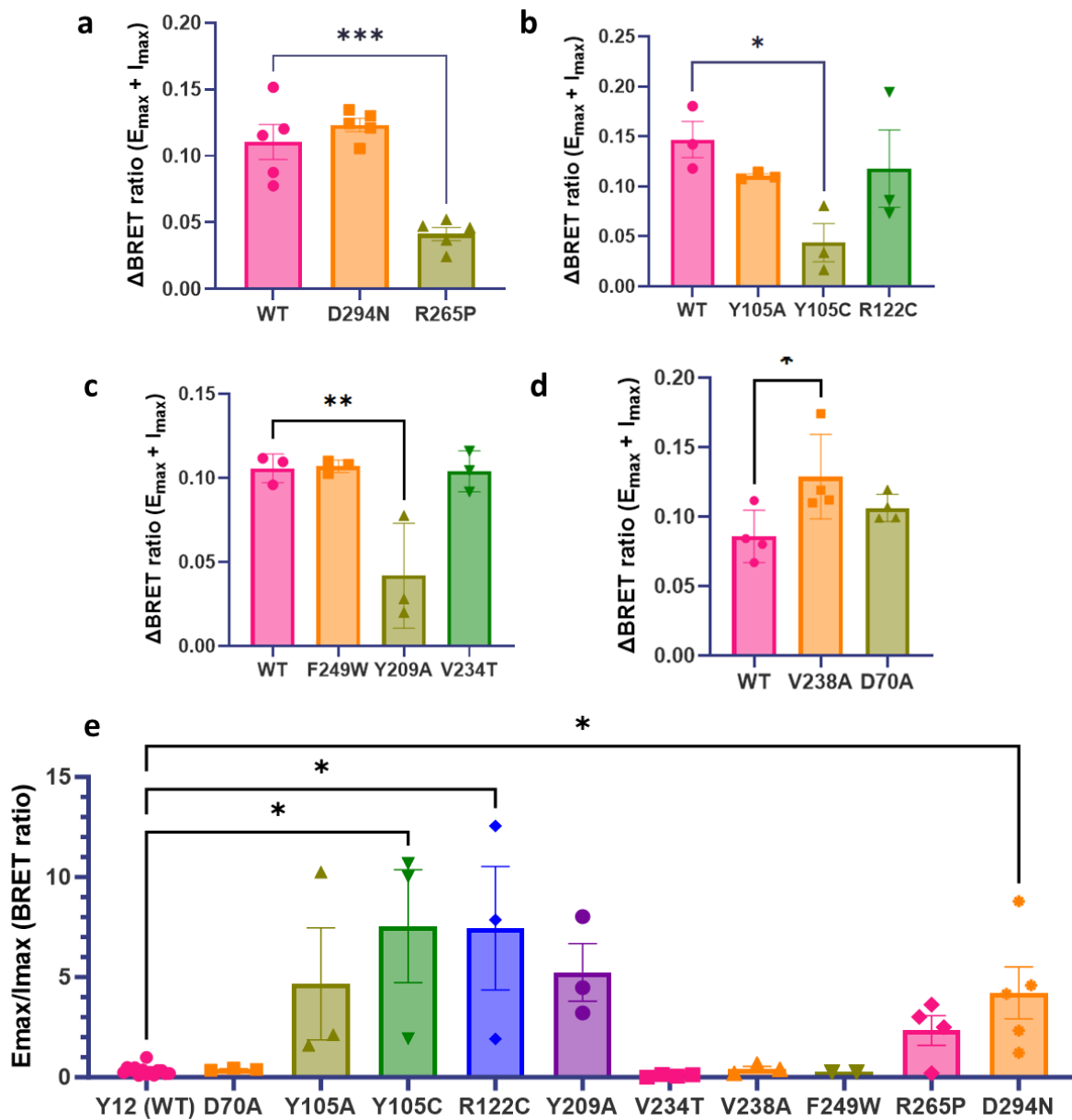
Figure 11. Effects of P2Y12 mutants on breadth of receptor dynamic window and ratio of active to inactive receptors. **a-d.** The BRET window, or breadth of effect a receptor can produce, was determined by range between Emax and Imax values. Each mutant window was compared to its own experimental WT receptor BRET window. **a** R265P mutant showed significant reduction of BRET window compared to WT receptor (p<0.001).(N=3). **b** Y105C mutant BRET window was significant decreased compared to WT (p<0.05)(N=3). **c** Y209A mutant showed significant reduction of BRET window compared to WT receptor (p<0.01).(N=3). D V248A mutant showed a significant increase in BRET window when compared to WT receptor (p<0.05). (N=4). E Ratio of active to inactive receptor found calculating Emax/Imax. Y105A,Y105C,R122C and D294N showed significant increase in Emax/Imax values compared to WT (p<0.05). (N=3-14). Graphs A-D were analysed using one-way ANOVA with Dunnett's post-hoc test for multiple comparisons. Graph E was analysed using Kruskal-Wallis nonparametric test with post-hoc multiple comparisons. All data represented by mean ± SEM (*p<0.05, **p<0.01,***p<0.001).

3.3: How do changes in membrane cholesterol levels affect P2Y12R activity and platelet aggregation?

3.3 Introduction

There are many factors within the cellular environment that may affect P2Y12R activity. It is increasingly clear that lipid raft microdomains are important for both enhancing signalling specificity and trafficking of GPCRs [72, 74]. Can lipid rafts influence the constitutive activity or ligand-dependent activity of P2Y12R? Due to the significant role of cholesterol enrichment in the formation of lipid rafts, and the proposed critical role of lipid rafts in $G\alpha_i$ signalling [81], we hypothesise that altering the cholesterol environment may affect both ligand-dependent and independent P2Y12R activity. The manipulation of membrane cholesterol levels has been reported widely, and so in our HEK293 cell system, we employed methods of cholesterol enrichment and cholesterol depletion to observe potential effects on P2Y12R activity. Incubation of cells with water-soluble cholesterol served to increase the amount of cholesterol deposited in the plasma membrane. The use of MβCD to remove cholesterol from the membrane environment is also well-established [97]. Thus, we calculated the molar ratio of MβCD : cholesterol, and the range of MβCD concentrations for our cell work, based on previous work by Pucadyil and Chattopadhyay [98] on the serotonergic receptor, and work by McGraw et al. [99] on the adenosine 2A receptor, to elicit significant removal of membrane cholesterol. Both these papers used the HEK293 cell line and so we were confident in our use of MβCD to remove cholesterol at these concentrations. Initially, we used a BRET-based approach to assess ligand dependent and independent activity of transiently transfected P2Y12R into HEK293T cells. Subsequent studies then moved into the more physiologically relevant human platelets.

We hypothesised that P2Y12R agonist-dependent activity will be increased with cholesterol enrichment. Incubation with cholesterol may introduce more cholesterol-enriched microdomains of the plasma membrane, promoting further enrichment of the P2Y12R into lipid rafts to enhance ligand-dependent and -independent activity. We also hypothesised that depletion of membrane cholesterol by MβCD may reduce the agonist-dependent and -independent P2Y12R activity. A reduction in intrinsic $G\alpha_i$ activity was observed by Ropero et al. [100] upon cholesterol depletion, and reduction of downstream signaling of the adenosine 2A receptor by McGraw et al. [99] further supports this hypothesis.

Previous work by Quinton et al. [81] have shown that platelet aggregation is reduced upon cholesterol depletion in platelets, which can be restored by cholesterol repletion. There however is little work on cholesterol enrichment and its effects on platelet aggregation. Thus, we aim to

characterise the effect of enriching cholesterol on platelet aggregation. We hypothesise that an increase in platelet aggregation will be observed. However, we are cautious of the global effects that an increase in cholesterol may have on whole-platelet function. Therefore, lower concentrations of cholesterol than used in HEK293 cells will also be assayed here. A 5mM final concentration of MβCD was chosen to supplement our BRET data and also the accompanying the work done by Quinton et al. We hypothesise that cholesterol depletion in platelets will support previous findings, resulting in a decrease following treatment with MβCD. Removing cholesterol from the platelet plasma membrane may also have global effects on platelet functionality and thus lower concentrations of MβCD than in HEK293 cells were also used.

3.3.1 Manipulation of cholesterol environment and its effects on P2Y12R activity

Initial studies were undertaken in P2Y12R-transfected HEK293T cells treated with either 0.732mM water-soluble cholesterol are (termed as 'cholesterol-enriched'), or 5mM MβCD (termed as 'cholesterol-depleted'). 'Untreated' cells were used as a control in these assays. Full concentration-response curves to ADP *(figure 12a)* and ticagrelor *(figure 12b)* are shown, using 2μg P2Y12R for untreated, cholesterol enriched and cholesterol depleted cells. Untreated P2Y12R produced the greatest response to ADP followed by cholesterol enriched P2Y12R. Cholesterol depleted P2Y12R showed little ADP response. Cholesterol enriched P2Y12R showed a substantial increase in response to ticagrelor compared to untreated P2Y12R, and again cholesterol depleted P2Y12R had a reduced response to ticagrelor.

Both cholesterol-depleted and cholesterol-enriched P2Y12R like the WT showed significant constitutive activity compared to untreated pcDNA control (p=0.035, p=0.0021 respectively). On this occasion, the untreated P2Y12R did demonstrate significantly increased constitutive activity. The BRET activation window in *figure 12d* shows a significant attenuation of ADP max response in the cholesterol-depleted P2Y12R cells in comparison to untreated P2Y12R cells (p=0.014). The cholesterol-enriched P2Y12R had an ADP Emax value comparable to untreated P2Y12R. Ticagrelor Imax values for cholesterol-enriched and depleted P2Y12R were comparable to untreated P2Y12R. Taken together these results showed an apparent effect of cholesterol treatment on both the constitutive activity of P2Y12R and ADP-dependent P2Y12R activity.
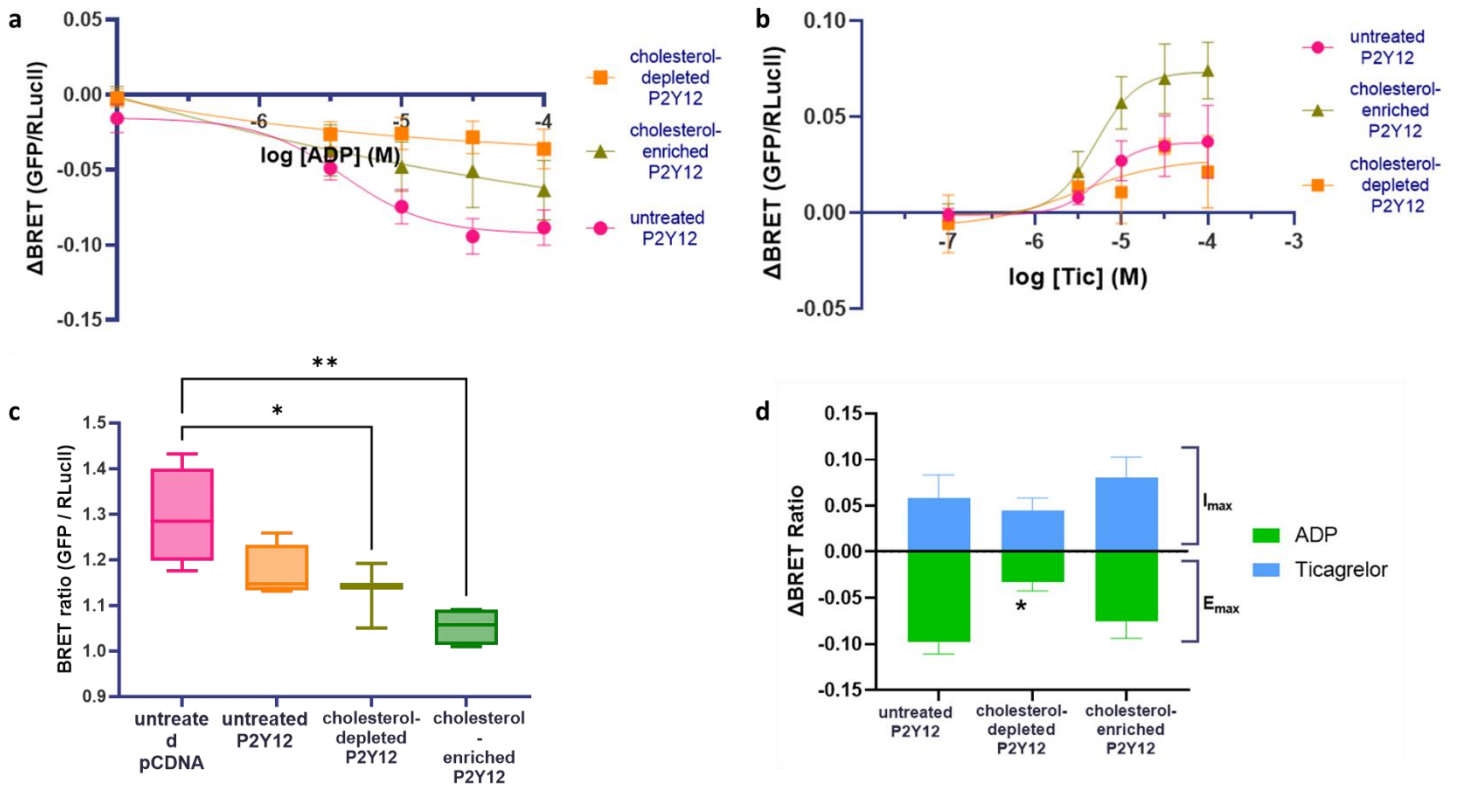
Figure 12. Effects of manipulating cholesterol environment on P2Y12 activity in HEK293T cells.
Concentration-response curves to **a** ADP and **b** ticagrelor for P2Y12 in high cholesterol environment, cholesterol-depleted environment and untreated environment (N=5). **c** Basal BRET values show a significant increase in constitutive activity for both cholesterol depleted and cholesterol-enriched environments for P2Y12 ($p < 0.05$, $p < 0.01$ respectively) compared to control. (N=3-4). **d** BRET activation window for untreated P2Y12 compared to a cholesterol depleted or enriched environment. ADP Emax and ticagrelor Imax values plotted together to demonstrate breadth of receptor activation. Emax was significant reduced ($p < 0.05$) in the cholesterol-depleted cells compared to untreated P2Y12.(N=4-5). Imax values for both changed cholesterol environments were comparable to untreated P2Y12 (N=4-5). Statistical test in C,D: one-way ANOVA with Dunnett's post-hoc test. All data represented by mean ± SEM (*$p < 0.05$,**$p < 0.01$)

3.3.2 Effects of increasing environmental cholesterol on platelet aggregation in response to agonist

Based on the significant findings from the BRET assays in the HEK293T system , we subsequently used more physiologically relevant assays based in human platelet work. Light-transmission aggregometry (LTA), a gold-standard technique for platelet aggregation, was employed to measure the real-time platelet response to agonists. Similar to the HEK293T system work, platelet rich plasma (PRP) was treated with water-soluble cholesterol to determine the effects of increasing environmental cholesterol on whole-platelet response, or treated with vehicle. The maximal concentration of cholesterol used was the same as that used in the cell line work, 0.732mM, followed by decreasing concentrations (0.366mM and 0.183mM). *Figure 13a*-c show representative LTA traces of platelet aggregation in response to increasing concentrations of ADP. 2.5uM ADP *(figure 13a)* and 5µM ADP *(figure 13b)* produced a sub-maximal platelet response in untreated platelets, whilst 10µM ADP *(figure 13c)* produced a full aggregation response. Perhaps surprisingly, a decrease in ADP-mediated platelet aggregation was found with increasing concentrations of cholesterol at both concentrations of ADP.

There was minimal platelet aggregation when platelets were treated with high cholesterol concentration (0.732mM). Whilst there was some platelet aggregation following treatment with 0.366mM and 0.183mM cholesterol treatment, there was a step-wise reduction in platelet aggregation with increasing concentrations of cholesterol. 5µM ADP produced a similar step-wise decrease in platelet aggregation with increasing concentrations of cholesterol treatment. 2.5µM ADP showed minimal platelet aggregation at all cholesterol concentrations. Quantification of this apparent trend was determined using area under the curve as a measurement of aggregation, collated in *figure 13d* across cholesterol treatments and ADP concentrations. There were no observed significant effects of cholesterol treatment or ADP concentration on platelet aggregation.
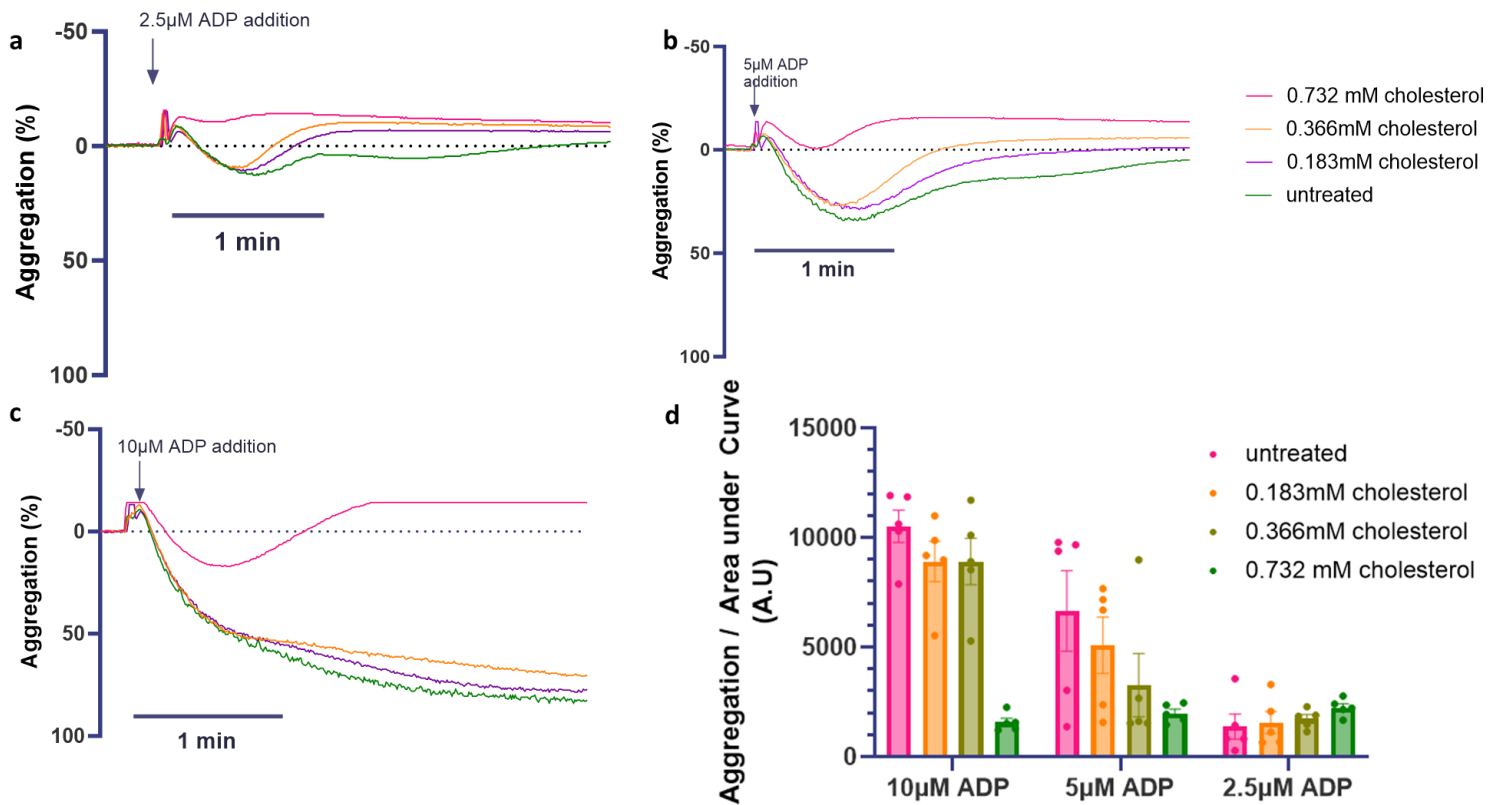
Figure 13. Effects of increasing environmental cholesterol on platelet aggregation in response to agonist ADP. **a** Representative light transmission aggregometry (LTA) trace showing platelet aggregation in response to 2.5µM ADP in untreated platelets with increasing concentrations of cholesterol. Scale bar indicates 1 minute. (N=1). **b** LTA trace showing platelet aggregation in response to 5µM ADP in untreated platelets, and platelets treated with increasing concentrations of cholesterol. Scale bar indicates 1 minute. (N=1). **c** Representative LTA trace showing platelet aggregation in response to maximal 10µM ADP in untreated and cholesterol treated platelets. Scale bar indicates 1 minute. (N=1). **d** Summary graph showing aggregation quantified by area under the curve derived from LTA traces .for untreated platelets, and platelets treated with increasing cholesterol concentrations, in the presence of maximal and submaximal concentrations of ADP. (N=3-5). At each ADP concentration, there were no observed significant effects of cholesterol treatment on ADP-mediated platelet aggregation. One-way ANOVAs per ADP concentration were performed due to failure of Shapiro-Wilk's (SW) test for normality for a two-way ANOVA. Where one-way ANOVAs failed SW test for normality, a Kruskal-Wallis nonparametric test was performed. Both parametric and non-parametric tests were corrected using Dunnett's multiple comparisons. Graph C represented by mean ± SEM.

This series of experiments was then repeated with the agonist U46619, a synthetic analogue of prostaglandin 2 that acts at the thromboxane A2 (TP) receptor. The TP receptor is involved in platelet shape change and aggregation, and was employed in these assays to see whether the effects of cholesterol enrichment was specific to ADP and P2Y12R responses. As shown in *figure 14*, TP receptor-mediated platelet aggregation was similarly diminished by cholesterol enrichment to ADP-mediated aggregation. Representative LTA traces for 5µM (*figure 14a)*, and 10µM (*figure 13b)* U46619 show maximal platelet aggregation upon stimulation with agonist. Again there was a step-wise pattern of decreased platelet aggregation with increasing in cholesterol concentrations. Quantification of aggregation across cholesterol treatments and U46619 concentrations in *figure 14c* supported this observation. A two-way ANOVA revealed that cholesterol concentration had a significant effect on platelet aggregation (p=0.0018). All together these results indicate a global effect of enriching membrane cholesterol attenuating platelet response to ADP and U46619 agonist.
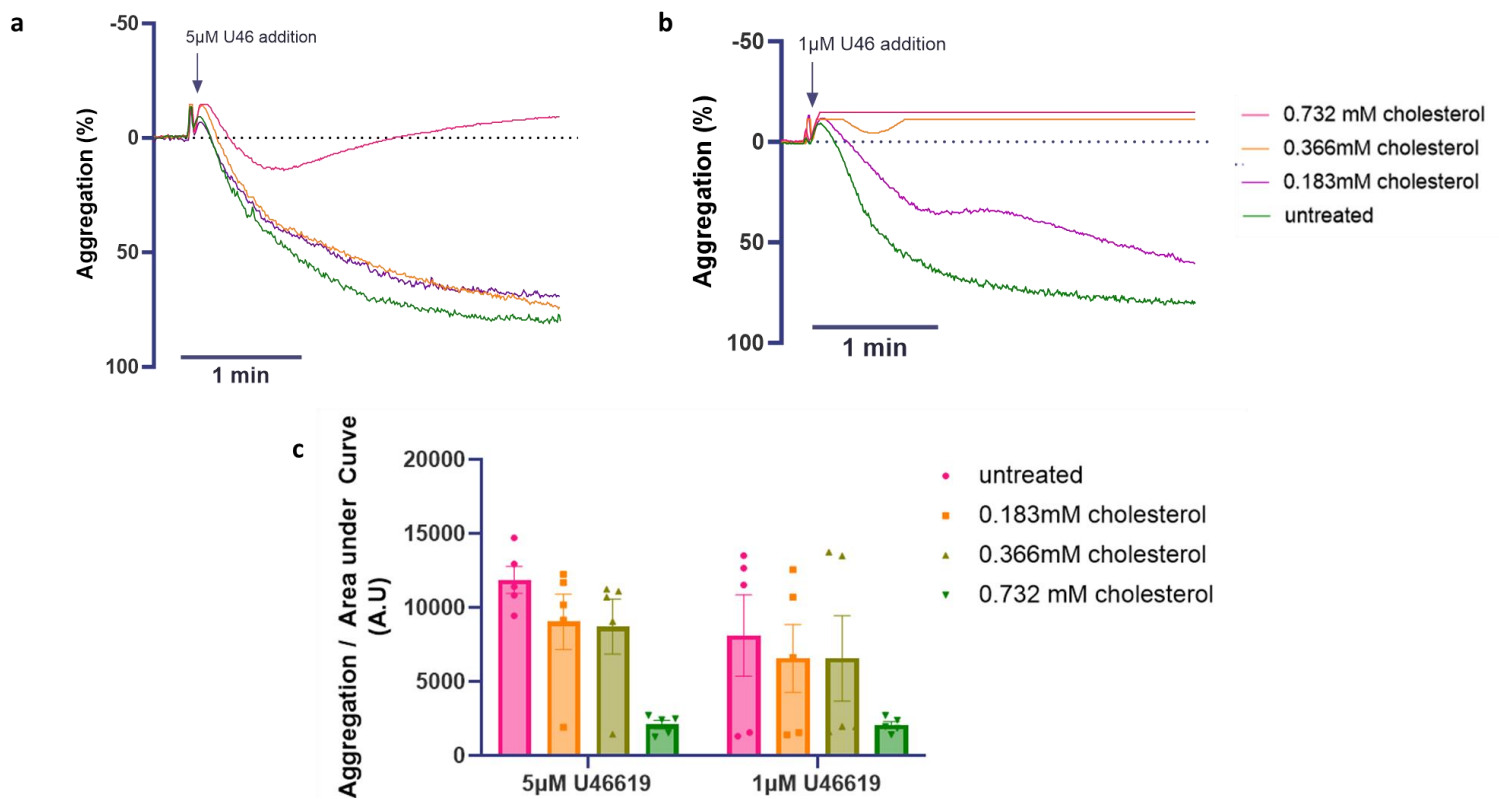
Figure 14. Effects of increasing environment cholesterol on platelet aggregation in response to agonist U46619. **a** Representative LTA trace showing platelet aggregation in response to maximal 5µM U46619 untreated platelets and platelets treated with increasing concentrations of cholesterol. Scale bar indicates 1 minute. (N=1). **b** Representative LTA trace showing platelet aggregation in response to 1µM U46619 in untreated and cholesterol treated. Scale bar indicates 1 minute. (N=1). **c** Summary graph showing area under the curve used to quantify platelet aggregation, derived from LTA traces for untreated platelets, and platelets treated with increasing cholesterol concentrations, in the presence of maximal and submaximal concentrations of U46619. (N=5). A significant reduction in platelet aggregation was observed with 0.732mM cholesterol treated platelets when compared to untreated platelets, when stimulated with 5µM U46619 (p<0.01).(N=5). Platelet aggregation was not significantly diminished in any cholesterol-enriched platelets when compared to untreated platelets when stimulated with 1µM U46619. (N=5). One-way ANOVAs per U46619 concentration were performed due to failure of Shapiro-Wilk's (SW) test for normality for a two-way ANOVA. Where one-way ANOVAs failed SW test for normality, a Kruskal-Wallis nonparametric test was performed. Both parametric and non-parametric tests were corrected using Dunnett's multiple comparisons Graph C represented by mean ± SEM.

3.3.2 Effects of depleting environmental cholesterol on platelet aggregation in response to agonist

Following an assessment of the effects of cholesterol enrichment on platelet aggregation, the effects of cholesterol depletion in platelets was undertaken. Similar to the water soluble cholesterol treatment, these assays used a concentration of 5mM MβCD alongside 1.5mM and 0.5mM MβCD. Both ADP and U46619 ligands were used to elicit platelet aggregation through distinct pathways. *Figure 14b* shows a representative LTA trace for ADP-mediated platelet aggregation upon addition of 2.5µM ADP, which failed to initiate platelet aggregation. Once again, 5µM ADP produced sub-maximal platelet aggregation in untreated platelets (*figure 15b*). *Figure 14c* shows a representative LTA trace upon addition of 10µM ADP, producing a maximal platelet aggregation response in untreated platelets. Interestingly, although perhaps more expected, high concentrations of MβCD resulted in ablation of platelet aggregation, or disaggregation of any platelets similar to the high 0.732mM cholesterol treatment. Quantification of aggregation across MβCD treatments and ADP concentrations in *figure 15c* supported this observation. A two-way ANOVA revealed both a significant effect of MβCD concentration ($p=0.0065$) and of ADP concentration ($p<0.0001$) on platelet aggregation. The interaction between these variables was also deemed significant ($F_{(6, 24)} = 3.089$, $p=0.0219$)).

Figure 15. Effects of increasing MβCD concentration to deplete environment cholesterol on platelet aggregation in response to endogenous against ADP **a** Representative LTA trace showing platelet aggregation in response to 2.5µM ADP for untreated platelets and platelets depleted of cholesterol by increasing concentrations of methyl-β-cyclodextrin (MβCD). Scale bar indicates 1 minute. (N=1). **b** Representative LTA trace showing platelet aggregation in response to submaximal 5µM ADP in untreated and MβCD-treated platelets. Scale bar indicates 1 minute. (N=1). **c** Representative LTA trace showing platelet aggregation in response to submaximal 10µM ADP in untreated and MβCD-treated platelets over a 200 second time course. (N=1). **d** Summary graph showing aggregation quantified by area under the curve derived from LTA traces for untreated platelets, and platelets treated with increasing MβCD concentrations, in the presence of maximal and submaximal concentrations of ADP. (N=3). The effect of ADP concentration and MβCD concentration on platelet aggregation was analysed using a two-way ANOVA. A significant effect of both ADP concentration ($p < 0.0001$) and MβCD concentration ($p < 0.01$) on platelet aggregation was determined using simple effects analysis. Interaction between these variables was also significant ($F_{(6, 24)} = 3.089$, $p < 0.05$).(N=3). Tukey's correction for multiple comparisons also found a significant effects between untreated platelets and 10µM and 5µM ADP concentration. Graph C represented by mean ± SEM

Addition of 5µM U46619 resulted in maximal platelet aggregation response, as shown in the representative LTA trace in *figure 16a,* which was conserved across all blood donors. 2.5µM U46619, as shown in the representative LTA trace in *figure 16b* had varying effects across donors, predominantly producing maximal platelet aggregation response. Treatment with 5mM MβCD ablated U46619-stimulated platelet aggregation. Quantification of platelet aggregation across MβCD treatments and U46619 concentration is shown in *figure 16c*. Treatment with 5mM MβCD significantly reduced platelet aggregation upon addition of 5µM U46619 ($p<0.001$) compared to untreated platelets. 1.5mM MβCD and 5mM MβCD-treated platelets showed a significant decrease in aggregation compared to untreated platelets, when stimulated with 2.5µM U46619 (($p=0.008$,$p=0.0017$ respectively).

Together these results tell a similar story to that of the cholesterol-enriched platelets. At the top concentration of MβCD, taken from work in the HEK293T system there was a complete block of platelet aggregation at all agonist concentrations. A step-wise reduction in platelet aggregation was then observed for intermediate MβCD concentrations compared to untreated platelets. The effect of both MβCD treatment and ligand concentration and its interaction were highly significant for ADP-mediated aggregation, and significant effects of MβCD treatment were also observed for U46619-mediated platelet aggregation.

-

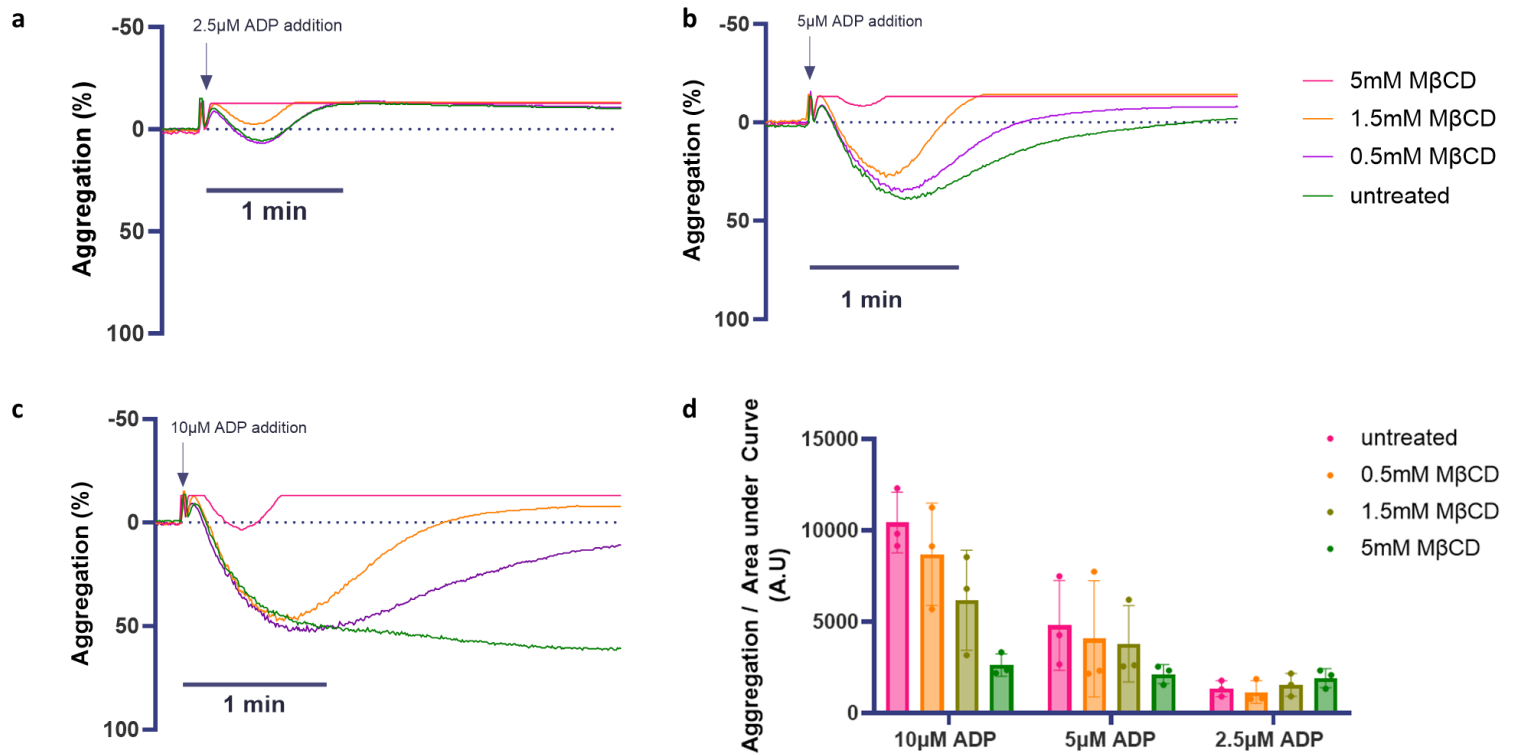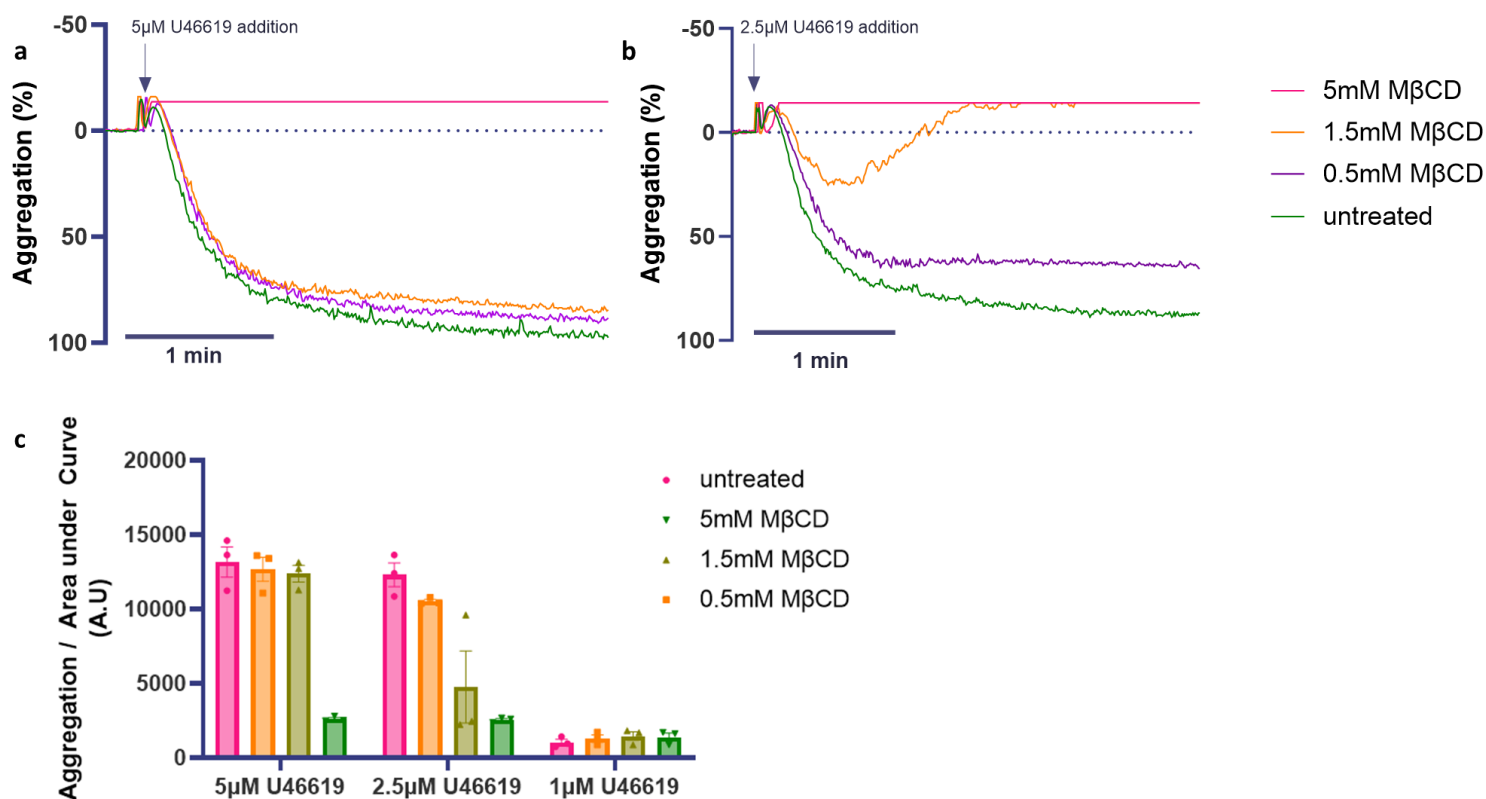*Figure 16. Effects of increasing MβCD concentration to deplete environment cholesterol on platelet aggregation in response to U46619* **a** Representative LTA trace showing platelet aggregation in response to 5μM U46619 for untreated platelets and platelets depleted of cholesterol by increasing concentrations of MβCD. Scale bar indicates 1 minute. (N=1). **b** Representative LTA trace showing platelet aggregation in response to 1μM U46619 in untreated platelets and platelets treated with increasing concentrations of MβCD. Scale bar indicates 1 minute. (N=1). **C** Summary graph showing area under the curve derived from LTA traces quantifies platelet aggregation, for untreated platelets, and platelets treated with increasing MβCD concentrations, in the presence of maximal and submaximal concentrations of U46619. (N=3) Platelets treated with 5mM MβCD showed a highly significant reduction in platelet aggregation compared to untreated platelets, when stimulated with 5μM U46619 (p<0.0001). (N=3). Platelets treated with either 1.5mM MβCD and 5mM MβCD shows a significant reduction in platelet aggregation compared to untreated platelets, when stimulated with 2.5μM U46619 (both p<0.01) (N=3). One-way ANOVAs per U46619 concentration were performed due to failure of Shapiro-Wilk's (SW) test for normality for a two-way ANOVA. Where one-way ANOVAs failed SW test for normality, a Kruskal-Wallis nonparametric test was performed. Both parametric and non-parametric tests were corrected using Dunnett's multiple comparisons. Graph C represented by mean ± SEM.

3.3.3 Effects of depleting cholesterol on ADP's ability to inhibit phospho-VASP production in platelets

Given the apparent global effects on platelet function and observed aggregation response, P2Y12R signalling was subsequently assessed in platelets using flow cytometry. We therefore employed flow cytometry to assess the effect of cholesterol depletion on effectors downstream of P2Y12R, to see if cholesterol depletion specifically targeted P2Y12R signalling. Although not proximal to the P2Y12R, a phosphor-vasodilator-stimulated phosphoprotein (pVASP) assay was employed. As outlined in *figure 1,* signalling through $G\alpha_i$ subunit decreases cAMP levels, resulting in a reduction of pVASP. In this assay PGE1-stimulated PKA-dependent phosphorylation of VASP is attenuated by signalling through $G\alpha_i$. Therefore ADP-mediated effects through P2Y12R activation result in a significant decrease in pVASP accumulation in platelets.

As shown in *figure 17a* and *figure 17b*, there were, surprisingly given previous data [81], no significant effects of depleting membrane cholesterol on P2Y12R's ability to inhibit PGE1-stimulated phospho-VASP production.
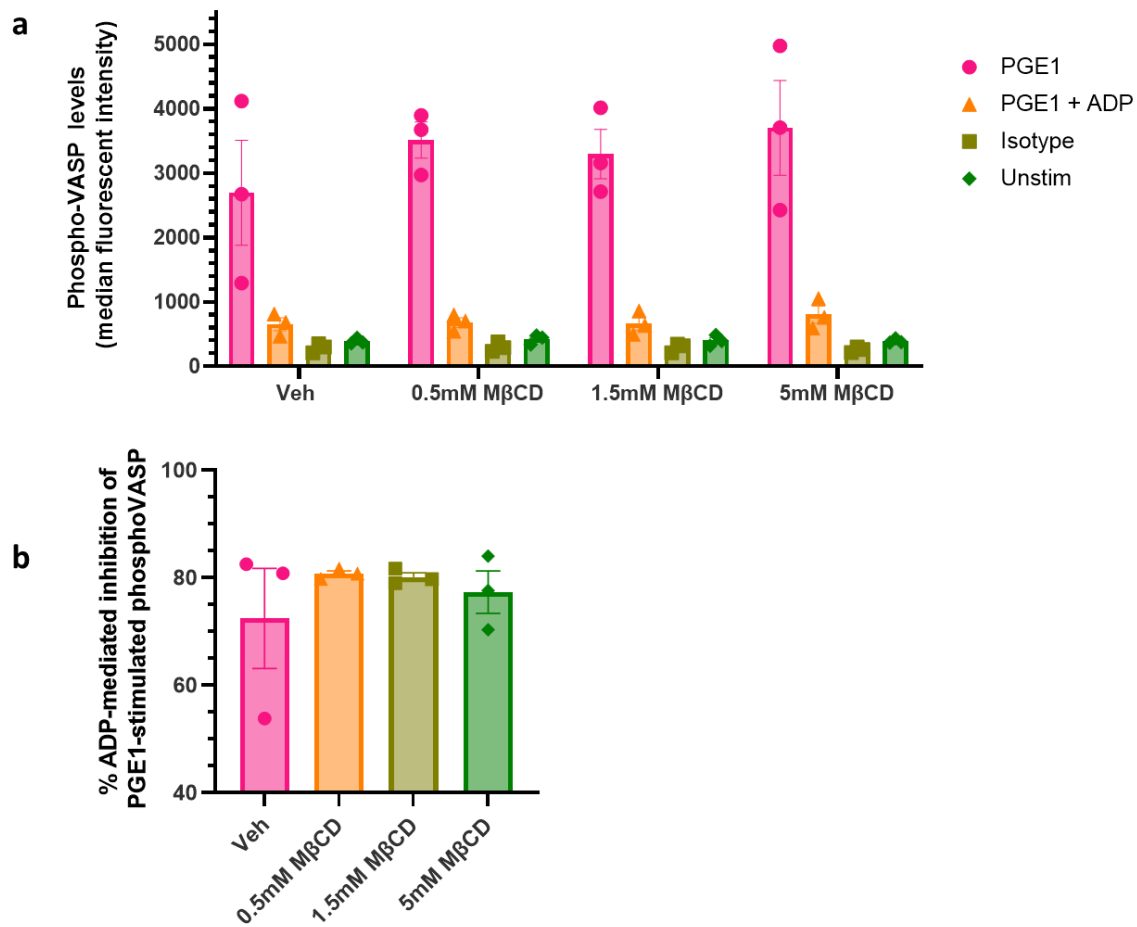
Figure 17. Effects of increasing MβCD concentration to deplete environmental cholesterol on ADP-mediated inhibition of PGE1-stimulated phospho-VASP in platelets. **a** Graph showing levels of phospho-vasodilator-stimulated phosphoprotein (phospho-VASP) in response to prostaglandin E1 (PGE1) only, in response to PGE1 + 10μM ADP, and in non-stimulated platelets. Each ligand treatment was then tested in increasing concentrations of MβCD to assess effect of MβCD treatment on ADP's ability to inhibit phospho-VASP levels. (N=3) **b** There was no significant effect of increasing MβCD concentration on ADP's ability to inhibit PGE1-stimulated production of phospho-VASP when compared to vehicle control platelets. (N=3). Failed normality tests prevented statistical analysis of graph A. Graph B was analysed using one-way ANOVA corrected for Dunnett's multiple comparisons. Both graphs represented by mean ± SEM.

Chapter 4: Discussions

ACS arises from a reduction in blood flow to the heart, leading to severe cardiovascular events including myocardial infarction. Platelets play a key role in ACS following atherosclerotic plaque rupture, contributing to arterial occlusions. Anti-platelet therapies targeting the platelet P2Y12 receptor exhibits constitutive activity, and anti-P2Y12R therapies such as ticagrelor and cangrelor, are inverse agonists that require further investigation. This thesis continues to explore the molecular pharmacology of P2Y12R in light of these relatively recent findings.

4.1 Effects of changing receptor expression

As outlined in the introduction, recent studies have suggested that patient pathology [52, 53] and age [54] affects P2Y12R surface expression in human platelets. A distinctive platelet phenotype is associated with aging, including an increased basal tone, platelet hyperreactivity and increased surface density of P2Y12R [54]. A reported increase in P2Y12R surface expression has also been noted in patients with ACS [52] or Type2-DM [53]. Given this background, we investigated whether increasing P2Y12R surface expression affected agonist-independent receptor activity.

The first aim of this thesis was to explore how changes in receptor expression can influence the degree of basal activity, and in turn how this may affect the ligand-dependent activity of P2Y12R. By employing both *in vitro* BRET and ELISA assays, we have investigated the effects of changing receptor expression in the HEK293 cell system.

4.1.1 Evaluating the increase in ligand-independent P2Y12R activity with increasing DNA transfection amount

We hypothesised that an increase in the amount of P2Y12R DNA transfected would result in an increase in surface expression of P2Y12R which we demonstrated by making use of a FLAG-tag epitope on the receptor. Interestingly, a significant increase in P2Y12R constitutive activity was observed with increasing receptor DNA transfection. So what could be the molecular mechanism underlying this? Potentially an increase in receptor surface expression may result in the formation of more higher order oligomers that help shift the activation equilibrium to R*.

Originally GPCRs were thought to be monomeric receptors, however recent evidence catalysed by the development of FRET/BRET techniques have demonstrated the ability of GPCRs to also exist as dimers and higher-order oligomers [101]. Although these techniques have been instrumental in demonstrating formation of multimeric receptor complexes, such as the formation of dopamine 2

receptor oligomers at physiological expression levels [102], quantification of these complex sizes, and how they may move within the plasma membrane cannot be demonstrated by these methods.

Due to the shortcomings of BRET/FRET techniques, the GPCR field has begun to employ the use of total internal reflection fluorescence (TIRF) microscopy to assess receptor organisation at the cell surface [103]. β_1 and β_2 adrenoreceptors, also class A GPCRs increase the proportion of dimers and oligomers vs monomers, with increasing receptor density [104]. Importantly the formation of dimers and oligomers was also observed at densities comparable to native tissue expression. The formation of homodimers has also been shown to be essential for P2Y12R function [63, 105]. Therefore, the formation of P2Y12R oligomers, particularly at high expression levels as demonstrated in this thesis, is not unreasonable. Whether or not oligomeric P2Y12R assembly will increase its constitutive activity remains unresolved, however the increase in G protein activation observed in stabilised oligomers of the platelet activating factor receptor (PAFR) may predict an increase in ligand-dependent P2Y12R activity [106].

Given these findings with other GPCRs, further research examining whether increased expression of P2Y12R results in receptor clustering that promotes constitutive activity of P2Y12R is certainly merited. Potentially employing the use of TIRF microscopy would be insightful [103, 107], to track the levels of monomers and dimeric/oligomeric formation of P2Y12R with increasing DNA transfection amounts in HEK293 cells.

4.1.2 Constitutive P2Y12R activity influences ligand-dependent receptor responses

Using the BRET assay, the effects of increasing transfected P2Y12R DNA was assessed on receptor agonism and inverse agonism. As briefly introduced within the results section, it is believed that the proportion of constitutively active receptors within a population will substantially impact the degree of both agonism, and inverse agonism. This is in concordance with the two-state model of receptor activation [108]. A greater proportion of basally active receptors could 'mask' agonism and decrease agonist efficacy, whilst increasing the negative intrinsic efficacy of an inverse agonist. Newman-Tancredi et al. in 2000 [109] demonstrated that increasing the stoichiometric ratio of receptor: G protein (R:G), resulted in increased receptor expression of serotonergic (5-HT$_{1B}$) receptors. This was observed with an accompanying increase in constitutive activity for membranes with a higher R:G ratio than a lower ratio. The inverse agonist methiothepin in this study had a significant increase in high-affinity binding to these basally active receptors, with the paper concluding that the efficacy of inverse agonists was significantly increased with associated increase in constitutive receptor activation. This body of work corroborates with the results in this thesis. There is a significant

69

increase in constitutive activity with increased receptor DNA transfection, and an accompanying increase in ticagrelor Imax. Notably there was also a decrease in maximal ADP responses with increasing DNA transfection, potentially as a consequence of increased levels of receptor in an active conformation prior to agonist binding. Together these results help to better characterise the effects of increasing the amount of P2Y12R DNA into the HEK293 cell line, and the effects on surface receptor expression, constitutive receptor activity and the resultant effects on agonism and inverse agonism.

Increased platelet P2Y12R surface expression has been observed in patients with ACS [52] and Type2-DM [53], which may potentiate agonist-independent receptor activity as outlined in 4.1.1. It is therefore a reasonable assumption that this increase in P2Y12R constitutive activity may influence the platelet hyperreactivity seen in patients with ACS and Type2-DM. This in turn may alter the patient response to P2Y12R-specific therapies, such as increasing the degree inverse agonism produced by ticagrelor.

4.2 Investigating the loss of ADP response in P2Y12R expressing cells – limitations and effects of receptor expression

As outlined in the results chapter, during the course of this body of work there was an ongoing issue of loss of ADP response in wildtype P2Y12R expressing cells. The problem was extensively troubleshooted by: using cells at a low passage that were already within the Mundell lab; comparison of different RLucII-tagged Gαi DNA constructs to see if it was a loss of RLucII emission within the assay; comparison of FLAG-tagged vs HA-tagged P2Y12R DNA to assess whether the tag was affecting receptor expression or function; and different wildtype P2Y12R constructs. All results from these optimisation assays proved inconclusive, with an evident inconsistent ADP response. Initially a 2ug of receptor DNA transfection was chosen as the optimal amount due to it producing the most reliable surface receptor expression in preliminary ELISA assays. Initially this provided a satisfactory ADP response in our BRET assay system. However as the project progressed this ADP response was lost. This was particularly troublesome as ultimately we intended to assess ADP responses across a selection of P2Y12R variants.

An explanation for loss of ADP response could perhaps lie in a change in transfection efficiency and protein expression in the HEK293 cell line. The HEK293 cells used in initial studies were cell passage >20. Potentially age-dependent changes in cell physiology may have upregulated transfection efficiency, gene transcription/translation or many other factors that ultimately result in different and potentially inconsistent receptor expression and function [110]. We hypothesised that, for reasons

that were beyond the scope and timeline of this research, that P2Y12R translation and expression may have been significantly upregulated. This in turn would lead to a significant increase in the degree of WT constitutive activity, which would 'mask' agonism as previously discussed in respect to the two-state model of receptor activation, and may also explain the significant increase in inverse agonism by ticagrelor

A loss of ADP response occurred in the WT P2Y12R expressing cells alongside the mutants Y105A, Y105C and R122C when they were first investigated. To explore whether this loss of ADP response also occurred in the mutant P2Y12R, we looked at the constitutive activity of each amount of DNA transfected for both wildtype receptor and the respective mutants, outlined in *figure 5*. 2µg of WT P2Y12R DNA transfection led to a highly significant degree of constitutive activity, which decreased with 0.5µg of DNA (p=0.0004, p=0.026 respectively). The constitutive activity of the mutants Y105A, Y105C and R122C were not significantly affected by amount of DNA transfected. Together, these results would suggest that there was an issue pertaining only to WT P2Y12R, where a substantial increase in P2Y12R basal activity may have 'masked' ADP response.

We noted therefore that less and less receptor cDNA was needed to produce measurable ADP responses. We therefore purchased and compared new HEK293 cells with low passage (1-10) termed 'newHEK293' compared to the cells used within the lab, termed 'old HEK293' (passage >20). 'New HEK293' cells showed a reassuring increase in ADP response and accompanying reduction in Ticagrelor Imax. A significant increase in ADP Emax in WT receptor was observed, conversely accompanied by small decreases in Emax with P2Y12R mutants. Decrease in ticagrelor Imax values were also observed. There was also an apparent decrease in WT P2Y12R constitutive activity in the 'new' cells compared to 'old'. This would help to explain the increase in ADP response and decrease in ticagrelor response, due to a reduced population of basally active receptor. Taking the results of all of these comparative studies together, we were more confident in comparing the pharmacological parameters of mutant P2Y12R to the wildtype P2Y12 in following assays.

It is important to note that we were unable to produce ELISA studies for the P2Y12R mutants due to time constraints. A comprehensive assessment of all mutant P2Y12R surface expression is required for future studies.

4.3 Assessing ligand-dependent and independent activity of P2Y12R mutants

4.3.1 R122: the DRY motif

Arginine-122 (R122) is a residue of particular interest as it forms part of the DRY motif. In other class A GPCRs, an 'ionic lock' is formed between the DRY motif and helix VI. Helix VI is also free to move outward upon agonist to allow for G protein binding and further receptor activation [111] important

for G protein activation. However in P2Y12R, the R122 residue is shifted by a half α-helical turn within helix VI, and so it is found at the same level as the hydrophobic V238 residue. The polar interactions usually formed between the DRY motif and helix VI are lost, and has therefore been postulated to be partly responsible for high basal P2Y12R activity [33]. Mutation of the R122 to a cysteine residue was thereby predicted to potentially affect constitutive activity of P2Y12R.

A patient study by Patel et al. [64] investigated the R122C mutation of P2Y12R. Defects in P2Y12R downstream signaling, receptor trafficking and a significant reduction in surface receptor expression in platelets in a patient presenting with a history of lifelong bleeding problems were described. A particularly interesting finding from this paper was that forskolin-mediated activity of adenylyl cyclase was still decreased with R122C mutation, despite the lack of ADP-stimulated response. This suggests that the R122C mutation conserves basal activity comparable to WT receptor. The results of this thesis support this finding, as the R122C mutation ultimately exhibited a degree of constitutive activity comparable to WT receptor. Whilst this perhaps was not expected in terms of the proposed role derived from the crystal structure of P2Y12, it does support the findings of real-world, clinical data. This work would also explain how the V234T mutation tested also showed no significant effects on P2Y12R constitutive activity. If the proposed R122C mutation has no real effect, then its complementary residue on TM6, V234 will have a limited effect when mutated to a threonine either.

The ligand-dependent behaviour of R122C was then assessed. As part of the patient study by Patel [64] transfection of 1321N1 cells with R122C P2Y12R resulted in a significant attenuation of ADP's ability to undergo agonist-stimulated surface receptor loss in an ELISA assay, and impairment of ADP-mediated aggregation in platelet work. Our work demonstrates a significant reduction in maximal ADP response which corroborates this patient study. As Patel et al., first suggested, the mutation of the arginine residue to a cysteine could possibly introduce disulphide bridges with other residues within P2Y12 structure, or with other cytosolic factors that may impact P2Y12R function. Ligand binding of R122C however was not affected [64], and thus it is evident that further study is required. Maximal inverse agonism by ticagrelor is not affected by the R122C mutation in this thesis, which may be expected as constitutive activity of this mutant remains unchanged.

4.3.3 V234 and V238: interactions with the DRY motif

Both V234 and V238 are found within TM6 of P2Y12R, involved in receptor activation [42]. Both residues were hypothesised to be important in regulating the constitutive activity of P2Y12R. The V234T mutation showed comparable ligand-dependent and -independent P2Y12R activity to WT receptor. This indicates that V234 is not important in receptor activation.

The V238 residue was identified as the corresponding residue to R122 of the DRY motif on TM3, and was mutated to an alanine to assess the role of the receptor in P2Y12R constitutive activity. Perhaps unexpectedly, V238A demonstrated constitutive activity comparable to WT receptor. A significant increase in ticagrelor responsiveness and substantial increase in ADP response contributed to a significant increase in the BRET activation window compared to WT P2Y12R. This is the first mutant identified in the Mundell group to demonstrate greater ligand-dependent activity compared to WT receptor. It is unclear how changes to TM6 resulted in this increase in BRET effect window, and therefore further pharmacological investigation, and dynamic modelling simulation is required.

4.3.4 Y105

Y105 is a residue identified by Bancroft found on TM3 that may play a role in ligand/receptor interaction. This thesis investigates Y105A, a residue identified through alanine scanning [69] and the patient-derived Y105C (unpublished).

The Y105A mutation exhibited a significant decrease in constitutive activity compared to P2Y12R through a significant increase in the Emax/Imax ratio. The work of this thesis does not support this, as no significant decrease in constitutive activity was observed in the absence of ligand in BRET-based assays. However, there are two things of note here that may help explain this discrepancy. Visual assessment of the BRET ratio graphs show a very similar BRET ratio of both Y105A and Y105C compared to the pcDNA control, and the p values for both are close to significance (p=0.058, p=0.061 respectively), and so an increase in N number would help clarify the real effect of Y105 mutations. The calculation of Emax/Imax is distinct from *in vitro* observations, and so there may also be incongruity there.

The Y105A was predicted from alanine scanning [69] to only affect antagonist binding. Our results support this, as both the Y105 and Y105C mutants showed a highly significant reduction of ticagrelor Imax. Surprisingly, Bancroft also found a significant increase in EC50 value for the Y105A mutant, and this increase in agonist response was unexpected. We observed a supporting significant increase in ADP Emax for the Y105A mutant. The limitations of alanine scanning have been considered by Bancroft. Namely, its ability to only predict ligand binding, and thus any ligand efficacies affected by changes in constitutive activity could not be predicted. However, our results have shown no significant reduction in P2Y12R basal activity, and so the loss increase of ADP response does not seem to lie in an accompanying loss of constitutive activity.

The Y105C mutant was investigated as is has been associated with abnormal platelet function in a patient with a bleeding phenotype (unpublished). The BRET effect window was significantly reduced

compared to WT P2Y12R, which is unsurprising considering the complete loss of ticagrelor response. The Y105C mutant had a significant increase in Emax/Imax ratio similar to Y105A, which would indicate a higher proportion of basally active receptors. However, this ratio is also most likely influenced by the abolishment of the ticagrelor response. This global reduction in P2Y12R functionality may contribute to the abnormal platelet response seen in the patient data. Possible explanations for this reduced functionality include defects in receptor trafficking, ligand binding, similar possibly to the R265P mutation [63].

To note, as discussed previously, the conclusion that Y105 mutations do not have reduced constitutive activity is not entirely assured, due to p values that are close to significance and a seemingly conflicting reduction in Emax/Imax ratio for Y105A as calculated by Bancroft. It is clear that further investigation into ADP-mediated effects on Y105 mutations is required.

4.3.5 D70

The D70A P2Y12R mutant was postulated to coordinate the allosteric Na^+ binding pocket located in TM7 [95]. Na^+ acts as a negative allosteric modulator of agonist activity, and so D70A was hypothesised to alter ligand-dependent activity of the P2Y12R. Perhaps surprisingly, there were no significant effects on either ADP or ticagrelor responses in D70A. Constitutive activity of D70A was comparable to WT. These results would suggest there is no significant role of D70 in ligand-dependent activity. However, this thesis is the first to characterise the D70A mutant in P2Y12R and so it is important to further investigate the activity of this mutant.

4.3.6 R265

The R265P mutant is of particular interest as it is clinically-derived [63]. It is located at the extracellular loop 3 (EL3) and is expected to detrimentally affect both receptor signaling and ligand binding, which will be further discussed later. This thesis is the first to assess the constitutive activity of R256P mutation, and results indicate that the R265 residue does not have any involvement in maintaining P2Y12R constitutive activity.

The ADP response of the R265P mutation was comparable to wildtype, which conflicts with work done previously [64] that showed a reduction in ADP-mediated surface receptor loss, and substantial signaling defects within platelet studies. This paper also examined molecular dynamic simulations, providing structural explanations for this attenuation of ADP response. Patel et al. describe the loss of a hydrogen bond within extracellular loop 3 which both destabilises helix VI, affecting receptor signalling. A real possibility in terms of the discrepancy of our work compared to this, is the ongoing issue with the ADP response in our wildtype P2Y12R. If our ADP response is diminished in the wildtype, which it may be, we would therefore be unable to detect a significant loss of ADP response

with the R265P mutation. Thus, the data in this thesis should be treated with caution with respects to comparing wildtype and mutant ADP responses. A significant reduction in ticagrelor Imax was also observed for the R265P mutant. As found by Mundell et al. [63], the R265P mutation may contribute to a disruption in the ligand binding pocket of P2Y12R, and therefore a possible explanation is that ticagrelor is unable to bind effectively to the receptor to induce a maximal ticagrelor response. This could be further explored by using a radioligand binding assessment for ticagrelor, such as that described by Giezen et al. [112].

4.3.7 F249: the CWxP motif

The F249W mutation is a part of the conserved CWxP motif of class A GPCRs, found on TM6. Here the tryptophan (W) residue is mutated to a phenylalanine (F) in the P2Y12R. The tryptophan residue has been investigated in the MOPR, finding it produces rotameric changes, acting as a 'hinge' that facilitates GPCR activation [91]. Upon receptor activation a cavity produced on its intracellular side allows for the interaction of the receptor with G proteins and other cytoplasmic downstream effectors. In P2Y12R, the CF(W)xP motif therefore does not contain this tryptophan residue, and so it is unknown if these effects are lost with the phenylalanine mutation. Thus, the F249W mutation was generated to see if restoration of the CWxP motif would produce any ligand-dependent or independent effects that may reflect the receptor activation of other class A GPCRs that exhibit reduced basal activity. Our data suggests that constitutive activity is not affected by changes to the CWxP motif.

Similar to the constitutive activity, the back-mutation of the CFxP motif to the CWxP motif appears to have no effect on either ADP or ticagrelor responses compared to wildtype P2Y12R. Together these results indicate that the CWxP motif does not play an integral role in P2Y12R activation as compared to other class A GPCRs, such as MOPR.

4.3.8 D294 and Y209: the D/NPxxY motif

The results from mutations in D/NPxxY motif were of particular interest in this body of work, based on predictions from Bancroft's work and this thesis' findings from constitutive activity assays. Found on TM7, the NPxxY motif is thought to be important in receptor activation, stabilising the active form of the receptor [113]. The mutation of aspartic acid (D) to asparagine (N), D/NPxxY, is thought to change the dynamics of the neighbouring proline kink. This may subsequently alter the interaction of the NPxxY motif with TM7 seen in the majority of class A GPCRs, and thus affect receptor activation.

The D294N mutant was inserted into the DPxxY motif by Zhang et al. [32, 33] in the crystallised P2Y12R structure to improve the protein yield of the receptor, producing a NPxxY motif.. The study found no significant change in ligand binding upon P2Y12R mutation. Bancroft [69] first suggested

that the DPxxY motif may affect the constitutive activity of P2Y12R, which this thesis has investigated. Our results suggest that there is no significant change in constitutive activity with the D294N mutation. This supports work by Bancroft [69] who also found no shift in the Emax/Imax ratio as a measurement of constitutive activity. The use of D294N as a thermostabilising mutant by Zhang et al. and work by Bancroft showing a reduction in the dynamic nature of P2Y12R, may suggest that it is the activity of other residues within, and interacting, with the NPxxY motif that govern constitutive activity.

Looking at D294N together with Y209A helps to understand the intricate nature of agonist-dependent receptor activation and constitutive activity. A DPxxY motif, although found in the minority of class A GPCRs, is still found in 18% and may therefore produce milder effects than changes in highly conserved residues in P2Y12R. Y209 is a highly conserved residue across all class A GPCRS, and is found on TM5. Although it is not strictly part of the NPxxY motif, has been shown to form a salt bridge with the Y residue of the NPxxY motif, stabilising the active receptor conformation [69]. We hypothesise that the mutation of the tyrosine (Y) to the non-polar alanine (A) could prevent formation of this salt bridge and result in the loss of constitutive P2Y12R activity. The Y209A mutant is the only variant in this thesis that does show a significant loss of constitutive activity when compared to the WT receptor. This work also supports the Emax/Imax calculation in Bancroft's work that suggests constitutive activity is lost. This work further consolidates the utmost importance of the Y209 residue in governing constitutive activity.

Dynamic modelling simulations by Bancroft [69] found binding of inverse agonist to P2Y12R to cause the intracellular end of TM7 to shift outwards, favouring the inactive state of the NPxxY motif. Bancroft also found that the receptor dynamics for the D294N were more rigid, and produced a higher energy barrier between the inactive and active form of the receptor. Whilst this was an effect insufficient to significantly reduce constitutive activity, it did produce a ligand-dependent effect. D294N produced a significantly increased maximal ADP response. The same effect was also observed in the Y209A mutant, which was accompanied by a hugely significant decrease in ticagrelor Imax. This is encouraging, as the significant loss of constitutive activity at Y209A is accompanied by both an increase in ADP response and a loss of ticagrelor response, conducive to a receptor population that is preferentially stabilised in an inactive conformation, resulting in a significantly reduced proportion of basally-active receptors. These results together highlight that the D/NPxxY motif helps to govern ligand-dependent receptor dynamics, and disruption of highly conserved residues that interact with this motif are critical in governing P2Y12R constitutive activity.

4.4 The BRET Effect Window

The BRET effect window, as first introduced in the results chapter, is a direct measurement of the breadth of receptor activation from full agonism to full inverse agonism. This measurement, alongside constitutive receptor activity, is a helpful insight into receptor function.

A significant decrease in BRET effect window was observed in the Y105C, from which the virtual loss of ticagrelor response seems to be predominantly responsible. The set point of this window is relatively unchanged as constitutive activity was comparable to WT receptor and so was ADP response. Together, these results show that Y105 may affect ticagrelor binding to the receptor as suggested previously in this discussion chapter.

R265P mutant also demonstrated a significant decrease in the BRET effect window, led predominantly again by virtual loss of ticagrelor response with no change in constitutive activity. The ligand binding pocket of P2Y12R is thought to be disrupted with this mutation, and therefore again it is likely that the E265P mutation prevents ticagrelor binding to the activated receptor.

Y209A also demonstrated a decreased BRET effect window. This change in window however may be due to the loss of constitutive P2Y12R activity. The increased ADP response, enhanced by the smaller proportion of basally active receptors, was insufficient to combat the highly significant reduction in response to ticagrelor. Imax of ticagrelor was sufficiently reduced.

4.4.1 Emax/Imax Ratios

As outlined in 3.2.7, the Emax/Imax ratio reveals the dynamic equilibrium of active to inactive receptors for each P2Y12R mutant. This can be used as an indirect measurement of constitutive activity as first shown by Bancroft [69]. A significant increase was observed in Emax/Imax ratio for Y105A, Y105C, R122C and D294N indicating that conformational equilibrium of these receptor is shifted to R. Encouragingly, the basal BRET ratios outlined in *figure 10a-b* for these mutants also reveal (although non-significant) a supporting reduction in constitutive activity. These mutants were further assessed and found that the degree of basal BRET was not significantly different from pcDNA control (data not shown) which indicates a lack of agonist-independent receptor activity. Taken together these findings provide a comprehensive characterisation of mutant P2Y12R constitutive activity.

Y209A Emax/Imax ratio was substantially increased compared to WT, which is in agreement with findings from Bancroft [69]. The basal BRET values in *figure 10c* further support that Y209A mutant shows a significant lack of constitutive activity, favouring the R conformation.

Surprisingly, this thesis finds a significant increase in Emax/Imax for D294N, whereas Bancroft does not. This discrepancy may be explained by a substantial, but not significant reduction in constitutive activity in the D294N mutant (*figure 10a*), or perhaps this level of constitutive receptor activity comparable to WT level was an artefact of D294N overexpression. It is also important to note that the Emax/Imax ratios could well be inaccurate, as the Emax value of the WT P2Y12R is calculated using a possibly inconsistent ADP response, and thus may not accurately reflect the equilibrium between active and inactive P2Y12R.

The Emax/Imax ratio is an insightful measurement of the receptor conformational equilibrium used alongside basal BRET values to characterise P2Y12R constitutive activity. However, as work in this thesis has shown these parameters can at times, be at odds with associated findings. This ultimately highlights the delicate nature of receptor expression influencing both ligand-dependent and -independent receptor activity.

4.5 Effect of manipulating environment cholesterol on P2Y12R in HEK293T cells

Lipid rafts and membrane microdomains are speculated to play a significant role in GPCR signalling. This research aims to build on results from the Quinton et al. [81] who showed that disruption of lipid rafts attenuate P2Y12R activity in platelets. The use of both water-soluble cholesterol and MβCD to manipulate the cholesterol content of the plasma membrane is a well-established technique in many cell lines, including HEK293 cells. Following papers that have depleted cholesterol from HEK293 cells in research of both P2Y12R [81] and other GPCR [98, 99] pharmacology as guidance, we depleted cholesterol from the membrane using 5mM MβCD and enhanced cholesterol levels using 0.732mM of cholesterol. Quantification of this change in membrane cholesterol could not be assayed due to time restrictions, and the limitations of this will be discussed later on. Employing the BRET system again to measure G protein activation, manipulation of membrane cholesterol produced insightful results.

4.5.1 Effects of depleting cholesterol by MβCD treatment on P2Y12R activity

Cholesterol depletion across GPCRs [98, 99] generally results in an attenuation of downstream signalling, and data in this thesis supports this. Full concentration-response curves to ADP and ticagrelor for cholesterol-depleted P2Y12R show a clear loss of both agonism and inverse agonism. This is reflected in the significant loss of maximal ADP response. Ticagrelor activity is not significantly diminished. The BRET activation window is substantially smaller than that of both untreated and cholesterol-enriched cells. This would suggest that treatment with MβCD has resulted in a global reduction of P2Y12R functionality. As cholesterol is such an essential constituent of the plasma

membrane, it is perhaps not surprising that significant removal results in attenuation of receptor function. Depletion of cholesterol *in* vitro significantly increases mechanical stress and membrane tension, affecting both whole-cell and receptor functionality [114]. It is also important to set this cholesterol depletion in a clinical context. Significant cholesterol reduction often results in human disease states. For example, mutations in the NPC1/NPC2 gene results in a disease named Niemann-Pick disease type C [115]. Defective lipid trafficking reduces cholesterol accumulation at the plasma membrane, resulting in progressive neurodegeneration [116].

Perhaps surprisingly, we still see a significant degree of P2Y12R constitutive activity that is greater than that in untreated P2Y12R. An explanation for this could be that while MβCD has depleted cholesterol, lipid rafts are still able to form with any remaining cholesterol. Conversely, a study by Villar et al. in 2016 [72] looking at constitutively-active dopamine receptors described that, in its basal state the receptors were not predominantly localised to lipid rafts. This may indicate that lipid rafts are not essential for basal receptor activity. This does not seem likely however, due to the extensive evidence showing the important role of lipid rafts in the mechanism of activated GPCRs uncoupling from G proteins to enhance receptor signalling [74, 117].

4.5.2 Effects of enriching cholesterol on P2Y12R activity

This body of work focuses on the enrichment of plasma cholesterol, rather than the replenishment of cholesterol upon depletion which has been described in various GPCR studies [98, 99]. This was due to both time constraints for completion of this work, and also to investigate how non-physiological levels of cholesterol may affect P2Y12R activity. Increased cholesterol can be observed in diseases states, and considering the pivotal role of cholesterol in cardiovascular disease [118, 119], it seemed pertinent to investigate an 'enrichment' of plasma membrane cholesterol. Considering the full concentration-response curves to ADP and ticagrelor, it appears that enriching cholesterol causes a slight reduction in agonist response and a substantial increase in inverse agonism of P2Y12R. This can be in part explained by the significant increase in constitutive activity observed with cholesterol-enriched P2Y12R. This an encouraging find as it both explains the shift in ligand-dependent effects to favour inverse agonism, and consolidates the importance of lipid rafts in G protein activity for P2Y12R. An increase in cholesterol-rich microdomains may have resulted in a greater movement of P2Y12R into lipid rafts, enhancing its constitutive activity. The role of cholesterol in the GPCR assembly has also been investigated. A paper by Kwon et al. [120] found that cholesterol was essential for the formation of β_2-AR dimers. Interestingly, this paper also revealed that the dimerisation of β_2-AR governs its constitutive activity and subsequent degree of inverse agonism. This highlights the potential importance of cholesterol in both regulation of both ligand-dependent and -independent receptor activity, alongside receptor dimerisation.

A recent review by Paukner et al. (2022) [118]describes a significant increase in plasma cholesterol levels in industrialised countries. Whilst genetics and environmental factors both contribute to the complex nature of plasma cholesterol regulation, it is speculated that an increase in cholesterol can contribute to cardiovascular diseases such as atherosclerosis. We hypothesis that increased constitutive P2Y12R activity, as seen in cholesterol enriched cells, may help to contribute to progression of cardiovascular diseases. Increased P2Y12R activity on the platelet surface could result in platelet hyperreactivity, enhancing the progression of diseases associated with dysregulated platelet aggregation such as the atherosclerosis and coronary arterial disease (CAD). An upregulation of basal P2Y12R tone may contribute to patient platelet pathology. This concept is a foundational basis for the work in this thesis, as the delicate nature of P2Y12R constitutive activity may prove to be an underlying factor in the progression of cardiovascular diseases.

4.6 Effect of manipulating environment cholesterol on platelet aggregation

Following our cell-based work on changes in plasma cholesterol, work then moved into the more physiologically relevant systems of platelets. Similar to Quinton et al. [81] ADP-induced aggregation of platelets was measured upon cholesterol depletion. We also examined if cholesterol enrichment affected platelet response. We were curious to see whether we could replicate results in the cell work with the more physiologically relevant platelet response.

4.6.1 Effects of depleting cholesterol by MβCD treatment on ADP and U46619-mediated platelet aggregation

Guided by the Quinton paper [81] and results of the BRET experiments, a maximal concentration of 5mM MβCD was used, followed by decreasing concentrations to see if an intermediate change in aggregation response could be observed. 5mM MβCD consistently reversed or completely inhibited both ADP-mediated and U46619-mediated platelet aggregation. These findings support our hypothesis, in that depletion of cholesterol can detrimentally affect P2Y12R function and result in an attenuation of ADP-mediated platelet aggregation. A step-wise increase in platelet aggregation with decreasing MβCD treatment was noted. As this observed effect was seen with both P2Y12R-mediated and TP receptor-mediated aggregation, the effects of MβCD treatment could potentially be due to a global effect on platelet function which will require further investigation. Our results are obviously complicated by the fact that downstream P2Y12R signalling significantly contributed to the complex feed-forward mechanism of platelet aggregation including that following TP receptor activation [121].

Although LTA provides a powerful real-time measurement of platelet aggregation, it is limited to quantification of whole-platelet responses. Thus, we employed flow cytometry to assess the effect of

cholesterol depletion on downstream P2Y12R signalling, to see if cholesterol depletion specifically targeted P2Y12R signalling. If cholesterol depletion resulted in a decrease in P2Y12R response to ADP, we would expect to see a decrease in the inhibition of pVASP production. Our results found no definitive change in ADP-mediated inhibition of pVASP production. This would suggest that a much more global effect on platelet functionality by cholesterol depletion is affecting the platelet's ability to aggregate upon agonist-dependent activation. The unaltered inhibition of pVASP production after MβCD treatment may also be explained by the blood preparation used in this assay. The Quinton paper for example, used washed platelets for experimentation [81], whereas the pVASP assay used whole blood. There may be confounding interactions of MβCD with other blood components, or a possible dilution of MβCD concentration when using whole blood compared to isolated, washed platelets. Therefore the effect of MβCD on platelets may be lost in these experiments. Therefore, this assay in the future should be repeated using washed platelets.

4.6.2 Effects of enriching cholesterol on ADP and U46619-mediated platelet aggregation

Once again we utilised the water-soluble cholesterol concentration from our cell work as the maximal concentration (0.732mM) used to explore how enriching plasma membrane cholesterol would affect platelet aggregation, using light transmission aggregometry. Unexpectedly, cholesterol enrichment followed the same pattern as MβCD treatment, showing a step-wise reduction in platelet aggregation with increasing cholesterol concentrations, resulting in a complete reversal or inhibition of platelet aggregation at maximal cholesterol concentration. These effects were seen with both ADP and U46619-mediated platelet aggregation. This implies again that treating platelets with cholesterol results in a global effect on platelet function. This result was unexpected, particularly as previous studies have been able to see an enhancement of ADP response in platelets upon cholesterol loading, described by Shattil et al. [122]. It is possible that our method of cholesterol enrichment was contributing to attenuation of platelet function. For example, Calkin et al. in 2009 [123] loaded washed platelets with cholesterol (at a higher concentration than used in this work) rather than PRP, for use in LTA assays. They described a significant increase in ADP response as expected. Therefore it would be pertinent to repeat this experiment again with washed platelets using methodology similar to Calkin et al. Alternatively, the Shattil paper utilised liposomes to deliver cholesterol to the platelets, resulting in similar findings to the Calkin paper. The unsuitableness of our methodology is also highlighted by the issues encountered with repeating cholesterol enrichment in platelets for calcium studies (data not shown). Due to both time constraints and unwanted platelet pre-activation upon cholesterol treatment, we were unable to examine how cholesterol enrichment influenced

calcium levels in the platelets. It is evident there were substantial flaws in our own methodology which can be improved for future experimentation.

In order to explain why our results produced opposing results, the global effects of cholesterol manipulation must be considered. Increasing the cholesterol content of the plasma membrane results in membrane rigidity [124], and has been shown to inhibit lipid raft formation [125]. Downstream consequences of this include attenuation of receptor signalling, trafficking and changes in interactions with other membrane proteins [123, 125, 126]. It is abundantly clear that the fields of membrane lipid composition and their indirect and direct interactions with surface receptors on platelets is a complex field. This work has also highlighted the complex and delicate nature of cholesterol homeostasis, and how important the regulation of cholesterol is for receptor activity.

An alternative explanation to the dramatic loss of platelet aggregation upon both MβCD and cholesterol treatment is platelet death. Due to the apparent shape change on the LTA traces and initial aggregation, this seems unlikely. Upon inspection, assayed platelets maintained their characteristic 'swirliness'. However, to ensure this is not the case, a platelet viability assay at all MβCD and cholesterol treatments should be utilised [127].

Although the work in the BRET system with cholesterol was encouraging, it highlights the all-too-common difficulty in translating *in vitro* cell line work into more physiologically relevant, *ex vivo* work, such as that in platelets.

4.7 Limitations and Future Investigations

4.7.1 Wildtype and mutant P2Y12R: receptor expression and organisation

Due to time constraints, there are several limitations with regards to both the HEK293 and platelet assays undertaken in this thesis. In order to substantiate findings from this work, mutant P2Y12R surface expression in HEK293 cells needs to be completed. Whilst surface expression ELISAs were planned for this thesis, ongoing issues in host lab with failure to detect the FLAG-tag on transfected P2Y12R made it impossible to assess any surface expression with reproducible confidence. Although some of these mutants, such as R265P [63] R122C [64] have been determined within the Mundell group to express similarly to wildtype P2Y12R, these mutants have not. Therefore, any ligand-dependent effects may be unknowingly influenced by changes in surface receptor expression. This is particularly pertinent given that changes in WT P2Y12R expression influenced agonist-dependent and -independent activity. In the future, the use of other tagged constructs, such as SNAP or CLIP tags could be could be utilised in the Mundell group [128]. There are numerous advantages to

generating new SNAP and CLIP-tagged receptors, such as their use in TIRF microscopy and FRET imaging [129, 130]. These methods would allow for real-time observation of GPCR dimer and oligomer formation, and has been used in live cells such as Asher et al. in 2021 [107]. These techniques could be used in the future to supplement results of this work showing how receptor expression increases with an increase in P2Y12R transfection. It could also be used to see how changes in this expression and receptor clustering may be influenced by manipulation of plasma membrane cholesterol levels.

4.7.2 Ligand dependent P2Y12R mutant effects

The effect of each mutant on ligand-dependent activity have been discussed, however this thesis is limited to discussing efficacy, and not ligand binding. Whilst it is building on molecular dynamic simulations as produced by Bancroft [69], there has been no minimal *in vitro* characterisation of these novel mutants. For example, the loss of ticagrelor response in the Y105C and Y209A mutants may be due to the inability of ticagrelor to bind to the receptor. Therefore in the future, ligand binding should be assessed using radioligand binding assays [64, 131]. Unfortunately there are no commercially available P2Y12R radioligands at present. Generation of new P2Y12R constructs, as outlined above, may also help to restore a more robust, consistent ADP response in HEK293 cells. This would give a more solid foundation for comparisons of WT receptor to mutations. This issue was highlighted by the discrepancy between constitutive activity measured by BRET ratio vs the Emax/Imax ratio. Whilst the BRET ratio is a much more direct measurement, it would be encouraging if this raw data matched the Emax/Imax calculations upon use of new tagged-backgrounds for P2Y12R constructs.

4.7.2 Validating cholesterol levels

Another limitation of this work is the lack of measurement of plasma membrane cholesterol levels. To support these findings of this thesis in the future, it is vital to employ techniques to validate whether methods of cholesterol manipulation actually result in changes in membrane cholesterol, both HEK293 and platelet plasma membranes. Quantifying how much plasma cholesterol has increased or decreased would be particularly insightful, as this could be further translated to known disease states. This would help to set this thesis' findings in a relevant clinical context, the ultimate goal of bench-based research. Quantification of membrane cholesterol can be assessed in many ways, such as Western blotting [81] or by sucrose gradient flotation centrifugation as described by Yao et al. [132].

4.8 Concluding Remarks

Whilst there are limitations to the methodology, and validation assays are certainly required to substantiate these findings, a range of interesting results have been described in this thesis. A large part of this work pertains to characterisation of P2Y12R mutants *in vitro*, and has opened up some interesting avenues of research into the unique structure and constitutive activity of P2Y12R. The Y209 residue has been identified as being important for ligand-independent P2Y12R activity, alongside Y105, D294 and R265 residues demonstrating significant changes in ligand-dependent activity. Manipulation of the cholesterol environment and the subsequent effect on P2Y12R and platelet responses have produced both encouraging and surprising results. These findings have both supported work by others and asked further questions regarding P2Y12R and external factors influencing its activity in HEK293 cells and in *ex vivo* platelet work.

This work has also demonstrated an increase in P2Y12R constitutive activity with increasing P2Y12R expression. Our findings ask whether the reported upregulation of P2Y12R surface expression on ACS patient platelets thereby increases agonist-independent P2Y12R activity. Consequently, does this significantly contribute to platelet hyperreactivity as observed in these patients?

An emerging question is whether the use of inverse agonists such as ticagrelor in disease treatment improves patient outcomes over classical antagonists, and more broadly whether inverse agonists should be a focus for drug discovery and development. The high degree of agonist-independent P2Y12R signalling as described here presents a sound argument for inverse agonism as a viable therapeutic strategy in the treatment of ACS.

This work helps further our molecular understanding of ligand-dependent and -independent activity of the platelet P2Y12 receptor, which can be translated into therapeutic benefit in the future.

References

1. Koupenova, M., et al., *Thrombosis and platelets: an update.* European Heart Journal, 2016. **38**(11): p. 785-791.
2. Varga-Szabo, D., I. Pleines, and B. Nieswandt, *Cell Adhesion Mechanisms in Platelets.* Arteriosclerosis, Thrombosis, and Vascular Biology, 2008. **28**(3): p. 403-412.
3. Rendu, F. and B. Brohard-Bohn, *The platelet release reaction: granules' constituents, secretion and functions.* Platelets, 2001. **12**(5): p. 261-273.
4. Jackson, S.P., *The growing complexity of platelet aggregation.* Blood, 2007. **109**(12): p. 5087-5095.
5. Offermanns, S., *Activation of Platelet Function Through G Protein–Coupled Receptors.* Circulation Research, 2006. **99**(12): p. 1293-1304.
6. Cattaneo, M., et al., *Released adenosine diphosphate stabilizes thrombin-induced human platelet aggregates.* Blood, 1990. **75**(5): p. 1081-6.
7. Yuan, S., et al., *The Molecular Mechanism of P2Y1 Receptor Activation.* Angewandte Chemie International Edition, 2016. **55**(35): p. 10331-10335.
8. Hu, G.-M., T.-L. Mai, and C.-M. Chen, *Visualizing the GPCR Network: Classification and Evolution.* Scientific Reports, 2017. **7**(1): p. 15495.
9. Léon, C., et al., *Defective platelet aggregation and increased resistance to thrombosis in purinergic P2Y1 receptor–null mice.* The Journal of Clinical Investigation, 1999. **104**(12): p. 1731-1737.
10. Foster, C.J., et al., *Molecular identification and characterization of the platelet ADP receptor targeted by thienopyridine antithrombotic drugs.* The Journal of Clinical Investigation, 2001. **107**(12): p. 1591-1598.
11. André, P., et al., *P2Y12 regulates platelet adhesion/activation, thrombus growth, and thrombus stability in injured arteries.* The Journal of Clinical Investigation, 2003. **112**(3): p. 398-406.
12. Leunissen, T.C., et al., *The effect of P2Y12 inhibition on platelet activation assessed with aggregation- and flow cytometry-based assays.* Platelets, 2017. **28**(6): p. 567-575.
13. Cattaneo, M., *P2Y12 receptors: structure and function.* Journal of Thrombosis and Haemostasis, 2015. **13**(S1): p. S10-S16.
14. Huang, J., et al., *Platelet integrin αIIbβ3: signal transduction, regulation, and its therapeutic targeting.* Journal of Hematology & Oncology, 2019. **12**(1): p. 26.
15. Pei, L.-l., et al., *Dual antiplatelet therapy reduced stroke risk in transient ischemic attack with positive diffusion weighted imaging.* Scientific Reports, 2020. **10**(1): p. 19132.
16. Kang, J., et al., *Dual antiplatelet therapy de-escalation in acute coronary syndrome: an individual patient meta-analysis.* European Heart Journal, 2023. **44**(15): p. 1360-1370.
17. Maffrand, J.-P., *The story of clopidogrel and its predecessor, ticlopidine: Could these major antiplatelet and antithrombotic drugs be discovered and developed today?* Comptes Rendus Chimie, 2012. **15**(8): p. 737-743.
18. Hollopeter, G., et al., *Identification of the platelet ADP receptor targeted by antithrombotic drugs.* Nature, 2001. **409**(6817): p. 202-207.
19. Farid, N.A., A. Kurihara, and S.A. Wrighton, *Metabolism and disposition of the thienopyridine antiplatelet drugs ticlopidine, clopidogrel, and prasugrel in humans.* J Clin Pharmacol, 2010. **50**(2): p. 126-42.
20. Bouman, H.J., et al., *Paraoxonase-1 is a major determinant of clopidogrel efficacy.* Nature Medicine, 2011. **17**(1): p. 110-116.
21. Quinn, M.J. and D.J. Fitzgerald, *Ticlopidine and Clopidogrel.* Circulation, 1999. **100**(15): p. 1667-1672.
22. Husted, S., *New developments in oral antiplatelet therapy.* European Heart Journal Supplements, 2007. **9**(suppl_D): p. D20-D27.
23. Gurbel, P.A. and U.S. Tantry, *Clopidogrel resistance?* Thromb Res, 2007. **120**(3): p. 311-21.

24.   Wiviott, S.D., et al., *Prasugrel versus clopidogrel in patients with acute coronary syndromes.* N Engl J Med, 2007. **357**(20): p. 2001-15.

25.   Sinha, N., *Ticagrelor: molecular discovery to clinical evidence: Ticagrelor: a novel antiplatelet agent.* Indian Heart Journal, 2012. **64**(5): p. 497-502.

26.   Springthorpe, B., et al., *From ATP to AZD6140: The discovery of an orally active reversible P2Y12 receptor antagonist for the prevention of thrombosis.* Bioorganic & Medicinal Chemistry Letters, 2007. **17**(21): p. 6013-6018.

27.   Navarese, E.P., et al., *A critical overview on ticagrelor in acute coronary syndromes.* QJM: An International Journal of Medicine, 2012. **106**(2): p. 105-115.

28.   Schüpke, S., et al., *Ticagrelor or Prasugrel in Patients with Acute Coronary Syndromes.* New England Journal of Medicine, 2019. **381**(16): p. 1524-1534.

29.   Husted, S. and J.J.J. Van Giezen, *Ticagrelor: The First Reversibly Binding Oral P2Y12 Receptor Antagonist.* Cardiovascular Therapeutics, 2009. **27**(4): p. 259-274.

30.   Storey, R.F., et al., *Inhibition of platelet aggregation by AZD6140, a reversible oral P2Y12 receptor antagonist, compared with clopidogrel in patients with acute coronary syndromes.* J Am Coll Cardiol, 2007. **50**(19): p. 1852-6.

31.   James, S.K., et al., *Ticagrelor versus clopidogrel in patients with acute coronary syndromes intended for non-invasive management: substudy from prospective randomised PLATelet inhibition and patient Outcomes (PLATO) trial.* Bmj, 2011. **342**: p. d3527.

32.   Zhang, J., et al., *Agonist-bound structure of the human P2Y12 receptor.* Nature, 2014. **509**(7498): p. 119-122.

33.   Zhang, K., et al., *Structure of the human P2Y12 receptor in complex with an antithrombotic drug.* Nature, 2014. **509**(7498): p. 115-118.

34.   Costa, T. and A. Herz, *Antagonists with negative intrinsic activity at delta opioid receptors coupled to GTP-binding proteins.* Proc Natl Acad Sci U S A, 1989. **86**(19): p. 7321-5.

35.   Kenakin, T., *Agonist-receptor efficacy. I: Mechanisms of efficacy and receptor promiscuity.* Trends Pharmacol Sci, 1995. **16**(6): p. 188-92.

36.   Cerione, R.A., et al., *The mammalian beta 2-adrenergic receptor: reconstitution of functional interactions between pure receptor and pure stimulatory nucleotide binding protein of the adenylate cyclase system.* Biochemistry, 1984. **23**(20): p. 4519-25.

37.   Parfitt, A.M., et al., *Hypercalcemia due to constitutive activity of the parathyroid hormone (PTH)/PTH-related peptide receptor: comparison with primary hyperparathyroidism.* J Clin Endocrinol Metab, 1996. **81**(10): p. 3584-8.

38.   Watkins, L.R. and C. Orlandi, *In vitro profiling of orphan G protein coupled receptor (GPCR) constitutive activity.* British Journal of Pharmacology, 2021. **178**(15): p. 2963-2975.

39.   Hauser, A.S., et al., *GPCR activation mechanisms across classes and macro/microscales.* Nature Structural & Molecular Biology, 2021. **28**(11): p. 879-888.

40.   Chalmers, D.T. and D.P. Behan, *The use of constitutively active GPCRs in drug discovery and functional genomics.* Nature Reviews Drug Discovery, 2002. **1**(8): p. 599-608.

41.   Aungraheeta, R., et al., *Inverse agonism at the P2Y12 receptor and ENT1 transporter blockade contribute to platelet inhibition by ticagrelor.* Blood, 2016. **128**(23): p. 2717-2728.

42.   Garcia, C., et al., *Deciphering biased inverse agonism of cangrelor and ticagrelor at P2Y12 receptor.* Cellular and Molecular Life Sciences, 2019. **76**(3): p. 561-576.

43.   Fredriksson, R., et al., *The G-protein-coupled receptors in the human genome form five main families. Phylogenetic analysis, paralogon groups, and fingerprints.* Mol Pharmacol, 2003. **63**(6): p. 1256-72.

44.   Picard, L.P., A.M. Schonegge, and M. Bouvier, *Structural Insight into G Protein-Coupled Receptor Signaling Efficacy and Bias between Gs and β-Arrestin.* ACS Pharmacol Transl Sci, 2019. **2**(3): p. 148-154.

45.   Rasmussen, S.G., et al., *Crystal structure of the β2 adrenergic receptor-Gs protein complex.* Nature, 2011. **477**(7366): p. 549-55.

46. Sansom, M.S. and H. Weinstein, *Hinges, swivels and switches: the role of prolines in signalling via transmembrane alpha-helices.* Trends Pharmacol Sci, 2000. **21**(11): p. 445-51.

47. Agasid, M.T., et al., *The Effects of Sodium Ions on Ligand Binding and Conformational States of G Protein-Coupled Receptors—Insights from Mass Spectrometry.* Journal of the American Chemical Society, 2021. **143**(11): p. 4085-4089.

48. Palczewski, K., et al., *Crystal structure of rhodopsin: A G protein-coupled receptor.* Science, 2000. **289**(5480): p. 739-45.

49. Park, J.H., et al., *Crystal structure of the ligand-free G-protein-coupled receptor opsin.* Nature, 2008. **454**(7201): p. 183-7.

50. Chidiac, P., et al., *Inverse agonist activity of beta-adrenergic antagonists.* Mol Pharmacol, 1994. **45**(3): p. 490-9.

51. Pozvek, G., et al., *Structure/function relationships of calcitonin analogues as agonists, antagonists, or inverse agonists in a constitutively activated receptor cell system.* Mol Pharmacol, 1997. **51**(4): p. 658-65.

52. Szelenberger, R., et al., *Dysregulation in the Expression of Platelet Surface Receptors in Acute Coronary Syndrome Patients-Emphasis on P2Y12.* Biology (Basel), 2022. **11**(5).

53. Hu, L., et al., *Platelets Express Activated P2Y(12) Receptor in Patients With Diabetes Mellitus.* Circulation, 2017. **136**(9): p. 817-833.

54. Gnanenthiran, S.R., et al., *Identification of a Distinct Platelet Phenotype in the Elderly: ADP Hypersensitivity Coexists With Platelet PAR (Protease-Activated Receptor)-1 and PAR-4-Mediated Thrombin Resistance.* Arterioscler Thromb Vasc Biol, 2022. **42**(8): p. 960-972.

55. Silvain, J., et al., *High on-thienopyridine platelet reactivity in elderly coronary patients: the SENIOR-PLATELET study.* Eur Heart J, 2012. **33**(10): p. 1241-9.

56. De Rosa, R., et al., *High on-treatment platelet reactivity and outcome in elderly with non ST-segment elevation acute coronary syndrome - Insight from the GEPRESS study.* Int J Cardiol, 2018. **259**: p. 20-25.

57. Greasley, P.J. and J.C. Clapham, *Inverse agonism or neutral antagonism at G-protein coupled receptors: a medicinal chemistry challenge worth pursuing?* Eur J Pharmacol, 2006. **553**(1-3): p. 1-9.

58. Yang, Y., et al., *Ticagrelor Is Superior to Clopidogrel in Inhibiting Platelet Reactivity in Patients With Minor Stroke or TIA.* Frontiers in Neurology, 2020. **11**.

59. Wallentin, L., et al., *Ticagrelor versus Clopidogrel in Patients with Acute Coronary Syndromes.* New England Journal of Medicine, 2009. **361**(11): p. 1045-1057.

60. Cattaneo, M., et al., *Identification of a New Congenital Defect of Platelet Function Characterized by Severe Impairment of Platelet Responses to Adenosine Diphosphate.* Blood, 1992. **80**(11): p. 2787-2796.

61. Cattaneo, M., *The platelet P2Y12 receptor for adenosine diphosphate: congenital and drug-induced defects.* Blood, 2011. **117**(7): p. 2102-2112.

62. Remijn, J.A., et al., *Novel molecular defect in the platelet ADP receptor P2Y12 of a patient with haemorrhagic diathesis.* 2007. **45**(2): p. 187-189.

63. Mundell, S.J., et al., *Receptor homodimerization plays a critical role in a novel dominant negative P2RY12 variant identified in a family with severe bleeding.* Journal of Thrombosis and Haemostasis, 2018. **16**(1): p. 44-53.

64. Patel, Y.M., et al., *A novel mutation in the P2Y12 receptor and a function-reducing polymorphism in protease-activated receptor 1 in a patient with chronic bleeding.* Journal of Thrombosis and Haemostasis, 2014. **12**(5): p. 716-725.

65. Hoffmann, K., et al., *Involvement of basic amino acid residues in transmembrane regions 6 and 7 in agonist and antagonist recognition of the human platelet P2Y12-receptor.* Biochemical Pharmacology, 2008. **76**(10): p. 1201-1213.

66. Mao, Y., et al., *Mutational analysis of residues important for ligand interaction with the human P2Y(12) receptor.* Eur J Pharmacol, 2010. **644**(1-3): p. 10-6.

67.   Alfonso-Prieto, M., L. Navarini, and P. Carloni, *Understanding Ligand Binding to G-Protein Coupled Receptors Using Multiscale Simulations.* Front Mol Biosci, 2019. **6**: p. 29.

68.   Grouleff, J., et al., *The influence of cholesterol on membrane protein structure, function, and dynamics studied by molecular dynamics simulations.* Biochimica et Biophysica Acta (BBA) - Biomembranes, 2015. **1848**(9): p. 1783-1795.

69.   Bancroft, S., *Defining the molecular mechanisms of constitutive activity and inverse agonism at the P2Y12 G-protein coupled receptor*, in *School of Physiology, Pharmacology & Neuroscience* 2023 University of Bristol. p. 224.

70.   Cattaneo, M., et al., *Molecular bases of defective signal transduction in the platelet P2Y12 receptor of a patient with congenital bleeding.* Proceedings of the National Academy of Sciences of the United States of America, 2003. **100**(4): p. 1978-1983.

71.   Karnovsky, M.J., et al., *LIPID DOMAINS IN MEMBRANES*.* Annals of the New York Academy of Sciences, 1982. **401**(1): p. 61-74.

72.   Villar, V.A., et al., *Localization and signaling of GPCRs in lipid rafts.* Methods Cell Biol, 2016. **132**: p. 3-23.

73.   Sezgin, E., et al., *The mystery of membrane organization: composition, regulation and roles of lipid rafts.* Nature Reviews Molecular Cell Biology, 2017. **18**(6): p. 361-374.

74.   Barnett-Norris, J., D. Lynch, and P.H. Reggio, *Lipids, lipid rafts and caveolae: Their importance for GPCR signaling and their centrality to the endocannabinoid system.* Life Sciences, 2005. **77**(14): p. 1625-1639.

75.   and, D.A.B. and E. London, *FUNCTIONS OF LIPID RAFTS IN BIOLOGICAL MEMBRANES.* Annual Review of Cell and Developmental Biology, 1998. **14**(1): p. 111-136.

76.   Pike, L.J., *Lipid rafts: bringing order to chaos.* J Lipid Res, 2003. **44**(4): p. 655-67.

77.   Kumar, R., et al., *The differential role of the lipid raft-associated protein flotillin 2 for progression of myeloid leukemia.* Blood Adv, 2022. **6**(12): p. 3611-3624.

78.   Simons, K. and E. Ikonen, *Functional rafts in cell membranes.* Nature, 1997. **387**(6633): p. 569-572.

79.   Canobbio, I., C. Balduini, and M. Torti, *Signalling through the platelet glycoprotein Ib-V-IX complex.* Cell Signal, 2004. **16**(12): p. 1329-44.

80.   Baglia, F.A., et al., *The Glycoprotein Ib-IX-V Complex Mediates Localization of Factor XI to Lipid Rafts on the Platelet Membrane*.* Journal of Biological Chemistry, 2003. **278**(24): p. 21744-21750.

81.   Quinton, T.M., et al., *Lipid rafts are required in Gαi signaling downstream of the P2Y12 receptor during ADP-mediated platelet activation.* Journal of Thrombosis and Haemostasis, 2005. **3**(5): p. 1036-1041.

82.   Savi, P., et al., *The active metabolite of Clopidogrel disrupts P2Y12 receptor oligomers and partitions them out of lipid rafts.* Proceedings of the National Academy of Sciences, 2006. **103**(29): p. 11069-11074.

83.   Rabani, V., et al., *Impact of ticagrelor on P2Y1 and P2Y12 localization and on cholesterol levels in platelet plasma membrane.* Platelets, 2018. **29**(7): p. 709-715.

84.   Marullo, S. and M. Bouvier, *Resonance energy transfer approaches in molecular pharmacology and beyond.* Trends Pharmacol Sci, 2007. **28**(8): p. 362-5.

85.   Parichatikanond, W., et al., *BRET-based assay to specifically monitor β(2)AR/GRK2 interaction and β-arrestin2 conformational change upon βAR stimulation.* Methods Cell Biol, 2021. **166**: p. 67-81.

86.   Khalil, J., et al., *Ticagrelor inverse agonist activity at the P2Y12 receptor is non-reversible versus its endogenous agonist ADP.* British Journal of Pharmacology. **n/a**(n/a).

87.   Hill, R., et al., *The novel μ-opioid receptor agonist PZM21 depresses respiration and induces tolerance to antinociception.* British Journal of Pharmacology, 2018. **175**(13): p. 2653-2661.

88.   Malcolm, N.J., et al., *Mu-opioid receptor selective superagonists produce prolonged respiratory depression.* iScience, 2023. **26**(7): p. 107121.

89. Cunningham, Margaret R., Shaista P. Nisar, and Stuart J. Mundell, *Molecular mechanisms of platelet P2Y12 receptor regulation.* Biochemical Society Transactions, 2013. **41**(1): p. 225-230.

90. Schmidt, P., et al., *Identification of determinants required for agonistic and inverse agonistic ligand properties at the ADP receptor P2Y12.* Mol Pharmacol, 2013. **83**(1): p. 256-66.

91. Zhang, X.C., Y. Zhou, and C. Cao, *Proton transfer during class-A GPCR activation: do the CWxP motif and the membrane potential act in concert?* Biophysics Reports, 2018. **4**(3): p. 115-122.

92. Bouley, R., et al., *Functional role of the NPxxY motif in internalization of the type 2 vasopressin receptor in LLC-PK1 cells.* American Journal of Physiology-Cell Physiology, 2003. **285**(4): p. C750-C762.

93. Bouley, R., et al., *Functional role of the NPxxY motif in internalization of the type 2 vasopressin receptor in LLC-PK1 cells.* Am J Physiol Cell Physiol, 2003. **285**(4): p. C750-62.

94. Pert, C.B., G. Pasternak, and S.H. Snyder, *Opiate agonists and antagonists discriminated by receptor binding in brain.* Science, 1973. **182**(4119): p. 1359-61.

95. Katritch, V., et al., *Allosteric sodium in class A GPCR signaling.* Trends in Biochemical Sciences, 2014. **39**(5): p. 233-244.

96. Zhang, C., et al., *High-resolution crystal structure of human protease-activated receptor 1.* Nature, 2012. **492**(7429): p. 387-92.

97. Zidovetzki, R. and I. Levitan, *Use of cyclodextrins to manipulate plasma membrane cholesterol content: evidence, misconceptions and control strategies.* Biochim Biophys Acta, 2007. **1768**(6): p. 1311-24.

98. Pucadyil, T.J. and A. Chattopadhyay, *Cholesterol depletion induces dynamic confinement of the G-protein coupled serotonin1A receptor in the plasma membrane of living cells.* Biochimica et Biophysica Acta (BBA) - Biomembranes, 2007. **1768**(3): p. 655-668.

99. McGraw, C., et al., *Membrane cholesterol depletion reduces downstream signaling activity of the adenosine A(2A) receptor.* Biochim Biophys Acta Biomembr, 2019. **1861**(4): p. 760-767.

100. Ropero, S., et al., *Cholesterol cell content modulates GTPase activity of G proteins in GH4C1 cell membranes.* Cell Signal, 2003. **15**(1): p. 131-8.

101. Ferré, S., et al., *G protein-coupled receptor oligomerization revisited: functional and pharmacological perspectives.* Pharmacol Rev, 2014. **66**(2): p. 413-34.

102. Guo, W., et al., *Dopamine D2 receptors form higher order oligomers at physiological expression levels.* Embo j, 2008. **27**(17): p. 2293-304.

103. Hern, J.A., et al., *Formation and dissociation of M1 muscarinic receptor dimers seen by total internal reflection fluorescence imaging of single molecules.* Proc Natl Acad Sci U S A, 2010. **107**(6): p. 2693-8.

104. Calebiro, D., et al., *Single-molecule analysis of fluorescently labeled G-protein-coupled receptors reveals complexes with distinct dynamics and organization.* Proc Natl Acad Sci U S A, 2013. **110**(2): p. 743-8.

105. Guo, X., et al., *G protein-coupled purinergic P2Y receptor oligomerization: Pharmacological changes and dynamic regulation.* Biochemical Pharmacology, 2021. **192**: p. 114689.

106. Liu, J., et al., *Biased signaling due to oligomerization of the G protein-coupled platelet-activating factor receptor.* Nat Commun, 2022. **13**(1): p. 6365.

107. Asher, W.B., et al., *Single-molecule FRET imaging of GPCR dimers in living cells.* Nature Methods, 2021. **18**(4): p. 397-405.

108. Leff, P., *The two-state model of receptor activation.* Trends in Pharmacological Sciences, 1995. **16**(3): p. 89-97.

109. Newman-Tancredi, A., et al., *Inverse agonism and constitutive activity as functional correlates of serotonin h5-HT(1B) receptor/G-protein stoichiometry.* Mol Pharmacol, 2000. **58**(5): p. 1042-9.

110. de los Milagros Bassani Molinas, M., et al., *Optimizing the transient transfection process of HEK-293 suspension cells for protein production by nucleotide ratio monitoring.* Cytotechnology, 2014. **66**(3): p. 493-514.

111. Oldham, W.M. and H.E. Hamm, *Heterotrimeric G protein activation by G-protein-coupled receptors.* Nature Reviews Molecular Cell Biology, 2008. **9**(1): p. 60-71.

112. van Giezen, J.J.J., et al., *Comparison of ticagrelor and thienopyridine P2Y12 binding characteristics and antithrombotic and bleeding effects in rat and dog models of thrombosis/hemostasis.* Thrombosis Research, 2009. **124**(5): p. 565-571.

113. Konvicka, K., et al., *A Proposed Structure for Transmembrane Segment 7 of G Protein-Coupled Receptors Incorporating an Asn-Pro/Asp-Pro Motif.* Biophysical Journal, 1998. **75**(2): p. 601-611.

114. Biswas, A., et al., *Cholesterol Depletion by MβCD Enhances Cell Membrane Tension and Its Variations-Reducing Integrity.* Biophysical Journal, 2019. **116**(8): p. 1456-1468.

115. Wojtanik, K.M. and L. Liscum, *The transport of low density lipoprotein-derived cholesterol to the plasma membrane is defective in NPC1 cells.* J Biol Chem, 2003. **278**(17): p. 14850-6.

116. Berry-Kravis, E., *Niemann-Pick Disease, Type C: Diagnosis, Management and Disease-Targeted Therapies in Development.* Semin Pediatr Neurol, 2021. **37**: p. 100879.

117. Dawaliby, R., et al., *Allosteric regulation of G protein–coupled receptor activity by phospholipids.* Nature Chemical Biology, 2016. **12**(1): p. 35-39.

118. Paukner, K., I. Králová Lesná, and R. Poledne, *Cholesterol in the Cell Membrane-An Emerging Player in Atherogenesis.* Int J Mol Sci, 2022. **23**(1).

119. Benito-Vicente, A., et al., *Familial Hypercholesterolemia: The Most Frequent Cholesterol Metabolism Disorder Caused Disease.* Int J Mol Sci, 2018. **19**(11).

120. Kwon, Y., et al., *Dimerization of β(2)-adrenergic receptor is responsible for the constitutive activity subjected to inverse agonism.* Cell Chem Biol, 2022. **29**(10): p. 1532-1540.e5.

121. SHANKAR, H., et al., *P2Y12 receptor-mediated potentiation of thrombin-induced thromboxane A2 generation in platelets occurs through regulation of Erk1/2 activation.* Journal of Thrombosis and Haemostasis, 2006. **4**(3): p. 638-647.

122. Shattil, S.J., et al., *Platelet hypersensitivity induced by cholesterol incorporation.* J Clin Invest, 1975. **55**(3): p. 636-43.

123. Calkin, A.C., et al., *Reconstituted High-Density Lipoprotein Attenuates Platelet Function in Individuals With Type 2 Diabetes Mellitus by Promoting Cholesterol Efflux.* Circulation, 2009. **120**(21): p. 2095-2104.

124. Lingwood, D. and K. Simons, *Lipid rafts as a membrane-organizing principle.* Science, 2010. **327**(5961): p. 46-50.

125. Nguyen, D.H., J.C. Espinoza, and D.D. Taub, *Cellular cholesterol enrichment impairs T cell activation and chemotaxis.* Mechanisms of Ageing and Development, 2004. **125**(9): p. 641-650.

126. Schoenwaelder, S., et al., *Identification of a Unique Co-operative Phosphoinositide 3-Kinase Signaling Mechanism Regulating Integrin αIIbβ3 Adhesive Function in Platelets.* Journal of Biological Chemistry, 2007. **282**: p. 28648-28658.

127. Hu, L.-L., et al., *Functional role and molecular mechanisms underlying prohibitin 2 in platelet mitophagy and activation.* Mol Med Rep, 2021. **23**(5): p. 384.

128. Hoehnel, S. and M.P. Lutolf, *Capturing Cell-Cell Interactions via SNAP-tag and CLIP-tag Technology.* Bioconjug Chem, 2015. **26**(8): p. 1678-86.

129. Tyagi, S., et al., *Continuous throughput and long-term observation of single-molecule FRET without immobilization.* Nature Methods, 2014. **11**(3): p. 297-300.

130. Shrestha, D., et al., *Understanding FRET as a research tool for cellular studies.* Int J Mol Sci, 2015. **16**(4): p. 6718-56.

131. JJ, V.A.N.G., et al., *Ticagrelor binds to human P2Y(12) independently from ADP but antagonizes ADP-induced receptor signaling and platelet aggregation.* J Thromb Haemost, 2009. **7**(9): p. 1556-65.
132. Yao, Y., et al., *The differential protein and lipid compositions of noncaveolar lipid microdomains and caveolae.* Cell Research, 2009. **19**(4): p. 497-506.